THE BLOOM'S SYNDROME DNA HELICASE COMPLEX: IDENTIFICATION AND CHARACTERIZATION OF ACTIVITIES CONSERVED IN THE ORTHOLOGOUS COMPLEX FROM *SACCHAROMYCES CEREVISIAE*

by

CHI-FU CHEN

A Dissertation submitted to the

Graduate School-New Brunswick

Rutgers, The State University of New Jersey

and

The Graduate School of Biomedical Sciences

University of Medicine and Dentistry of New Jersey

in partial fulfillment of the requirements

for the degree of

Doctor of Philosophy

Graduate Program in Biochemistry

written under the direction of

Dr. Steven J. Brill

and approved by

_____

_____

_____

_____

New Brunswick, New Jersey

May, 2010

ABSTRACT OF THE DISSERTATION

The Bloom's syndrome DNA helicase complex: identification and characterization of activities conserved in the orthologous complex from *Saccharomyces cerevisiae*

by CHI-FU CHEN

Dissertation Director:

Dr. Steven J. Brill

Bloom's Syndrome (BS) is a rare human disease characterized by genome instability and cancer predispostion. The gene mutated in BS, *BLM*, encodes a member of the RecQ family of DNA helicases. This family consists of five human paralogs that play crucial roles in guarding against DNA rearrangements. All BLM orthologs, including budding yeast Sgs1, bind stably to a protein complex composed of DNA topoisomerase 3α (Top3) and the OB-fold protein Rmi1. Although the BLM/Sgs1 complex is known to suppress homologous recombination, it's mechanism of action is unknown.

I found that a stable Top3-Rmi1 complex can be isolated from yeast cells overexpressing these two subunits and it shows increased superhelical relaxation activity compared to Top3 alone. The Rmi1 subunit also stimulates Top3 activity in reconstitution experiments. In both cases, elevated temperatures are required for optimal

relaxation unless the substrate contains a ssDNA bubble. Interestingly, Rmi1 binds only weakly to ssDNA on its own, but it stimulates the ssDNA binding activity of Top3 five-fold. Top3 and Rmi1 also cooperate to bind the Sgs1 N-terminus and promote its interaction with single-strand (ss) DNA.

In addition to the highly-conserved DNA helicase domain, all BLM/Sgs1 orthologs contain a large (652 aa) N-terminal domain that has no known catalytic activity. To determine the function of the N-terminal domain, I assayed truncated Sgs1 proteins for ssDNA binding activity. I identified a sub-domain of the Sgs1 N-terminus (SE, aa #103-322) that displays *in vitro* ssDNA binding, ssDNA annealing and strand exchange (SE) activities. These activities are conserved in the human and *Drosophila* orthologs. Strand exchange between duplex DNA and homologous ssDNA requires no cofactors and is inhibited by a single mismatched base-pair. The SE domain of Sgs1 is required *in vivo* for the suppression of hyper-recombination, suppression of synthetic-lethality and heteroduplex rejection. The *top3*Δ slow-growth phenotype is also SE-dependent. Surprisingly, the highly divergent SE domain from human BLM functions in yeast. Thus, SE activity is a new molecular function of BLM/Sgs1 that is conserved in other recombinases. The data suggest that at least one role of SE is to mediate the strand-passage events catalyzed by Top3-Rmi1.

Acknowledgements

I would like to express my sincere gratitude to my advisor, Dr. Steven Brill, for his patience, encouragement and inspiration. His guidance helped me in all the time of research. This thesis would not have been possible unless his help.

I would like to thank my thesis committee: Dr. Marc Gartenberg, Dr. Mark Brenneman and Dr. Nancy Walworth, for their encouragement and insightful comments.

I am grateful to my current and former lab members for their continued support. Janet Mullen is especially thanked for helping me with lab things and general advice.

Finally, I am forever indebted to my parents and Leah for their understanding, encouragement and endless patience.

Table of Contents

List of tables

List of Figures

Chapter I

Introduction

Helicases

Helicases are specialized molecular motors that couple the nucleoside triphosphate (NTP) hydrolysis to the unwinding of double-strand (ds) DNA and RNA. Helicase protein was first discovered in *Escherichia coli* in 1976 (Abdel-Monem, Durwald et al. 1976). They are vital components of nearly every cellular nucleic acid metabolic process including DNA replication, DNA repair, transcription, translation, ribosome synthesis, RNA maturation, RNA splicing, and nuclear export (Singleton, Dillingham et al. 2007).

Translocation rates of helicases vary from a few to several thousand base pairs per second and are controlled in a number of ways such as interaction with accessory factors. Helicases are categorized by their conserved helicase motifs and by their direction of translocation along nucleic acid. They are believed to fall into six superfamilies based on primary sequence analysis (Koonin and Gorbalenya 1992). Recently, several nucleic acid motors were defined as Superfamily 6 (SF6), which are members of the AAA^+ (ATPase Associated with various cellular Activities). Different helicase families share similar three-dimensional folds (RecA-like fold) (Bird et al., 1998). All of these proteins bind ATP and all of them possess the classic Walker A (phosphate-binding loop, or p-loop) and Walker B (Mg^{2+}-binding aspartic acid) motifs (Walker, Saraste et al. 1982).

Superfamilies 1 and 2 (SF1 and SF2) (table 1) are the two largest groups and they contain a total of seven characteristic motifs (I, Ia, II, III, IV, V and VI). These two superfamilies contain a large numbers of DNA and RNA helicases from archaea, eubacteria, eukaryotes and viruses, and unwind nucleic acids in either the $5' \rightarrow 3'$ or $3' \rightarrow 5'$

direction. SF1 and SF2 helicases are involved in DNA recombination, replication and initiation of translation (Singleton and Wigley 2002).

A third superfamily (SF3), which includes small putative helicase domains of ~100 amino acid residues that were originally identified in the genomes of small DNA and RNA viruses, has only three conserved motifs, including the two classical ATP-binding motifs. The first crystal structures of SF3 helicases have been determined and reveal a closer structural relationship to AAA+ proteins than to RecA. SF3 helicases participates in replication initiation by distorting DNA structure before replication forks can be assembled. At these forks, the SF3 helicases act as replicative helicases (Hickman and Dyda 2005).

A fourth superfamily consists of helicases that are related in sequence to the *Escherichia coli* DnaB protein (Caruthers and McKay 2002). These proteins have five motifs, unwind DNA in the 5′ to 3′ direction and form hexameric ring structures (Ilyina, Gorbalenya et al. 1992).

The Rho transcription termination factor was classified as a superfamily 5 member with sequence similar to the β subunit of proton-translocating ATPase (Gogol, Seifried et al. 1991). Berger's lab determined the structure of Rho, a hexameric RNA/DNA helicase, revealing that single-stranded RNA bound to the motor domains of the protein (Skordalakes and Berger 2003). They demonstrated that RNA directly communicates with the ATPase active site of Rho's motor domains and provide a molecular rationale for the behavior of numerous ATPase- and translocation-defective mutants.

Table 1. Characteristics of Selected Helicases

Superfamily	Proteins (Direction)	Conserved Motifs
SF1	RecB (3′→5′), RecD(5′→3′), UrvD(3′→5′), Srs2(3′→5′), Fbh1(3′→5′), Pif1(5′→3′), Rrm3(5′→3′)	7
SF2	RecQ(3′→5′), Sgs1(3′→5′), BLM(3′→5′), WRN(3′→5′), RecQ1(3′→5′), RecQ5(3′→5′), RecQ4(3′→5′), Mer3(3′→5′), PriA(3′→5′), RecG(3′→5′)	7
SF3	BPV E1	3
SF4	T7 gp4D	5
SF5	Rho	-
SF6	MCM, RuvB	-

RecQ family

The first RecQ helicase was identified over 20 years ago in *Escherichia coli* by screening for mutants resistant to thymineless-death (Nakayama, Nakayama et al. 1984). RecQ family members are identified in prokaryotes and eukaryotes. The eukaryotic branch of this family is significant because it includes three human disease proteins, which are associated with cancer predisposition, premature ageing and developmental abnormalities, in addition to the yeast homologues Sgs1 and Rqh1 from *S. cerevisiae* and *S. pombe*, respectively. Mutations in *WRN* and *BLM* result in Bloom's (BS) and Werner's syndromes (WS), respectively, and *RECQ4* is associated with three distinct disorders: Rothmund-Thomson (RTS), RAPADILINO and Baller-Gerold syndromes. WS is characterized by several main clinical features including numerous features of premature ageing such as graying and thinning of hair, loss of subcutaneous fat, wrinkling of skin, cataracts, osteoporosis, type II diabetes, lamb atrophy, atherosclerosis and also some features not seen in normal ageing like short stature, leg ulceration and soft-tissue calcification. The mains clinical features of BS includes proportional dwarfism, sun-induced erythaema (particular on the face), type II diabetes, narrow face and prominent ears, male infertility, female subfertility and frequent infections (Hickson 2003). People with RTS, also known as poikiloderma congenitale, display growth deficiency, photosensitivity with poikilodermatous skin changes, early greying and hair loss. Apart from RTS, *RECQ4* mutations were detected in Finnish patients with an autosomal recessive disorder RAPADILINO syndrome (radial hypoplasia/aplasia, patellae hypoplasia/aplasia and cleft or highly arched palate, diarrhoea and dislocated joints, little size and limb malformation, nose slender and normal intelligence) (Siitonen, Kopra et al.

2003). Although many features of the two genetic disorders overlap, poikiloderma, a hallmark of RTS, has been described as being generally absent from RAPADILINO syndrome. *RECQL4* mutations have also been identified in a subgroup of patients with Baller–Gerold syndrome, a rare autosomal recessive condition with radial aplasia/hypoplasia and craniosynostosis (Van Maldergem, Siitonen et al. 2006). In addition to WRN, BLM and RECQ4, the two other human RecQ helicases are RECQ1 and RECQ5, which are not yet genetically linked to a disease. Mutations in *RECQ1* or *RECQ5* might also cause a hereditary chromosomal instability disorder or individual cancer predisposition (Wu and Brosh ; Chu and Hickson 2009).

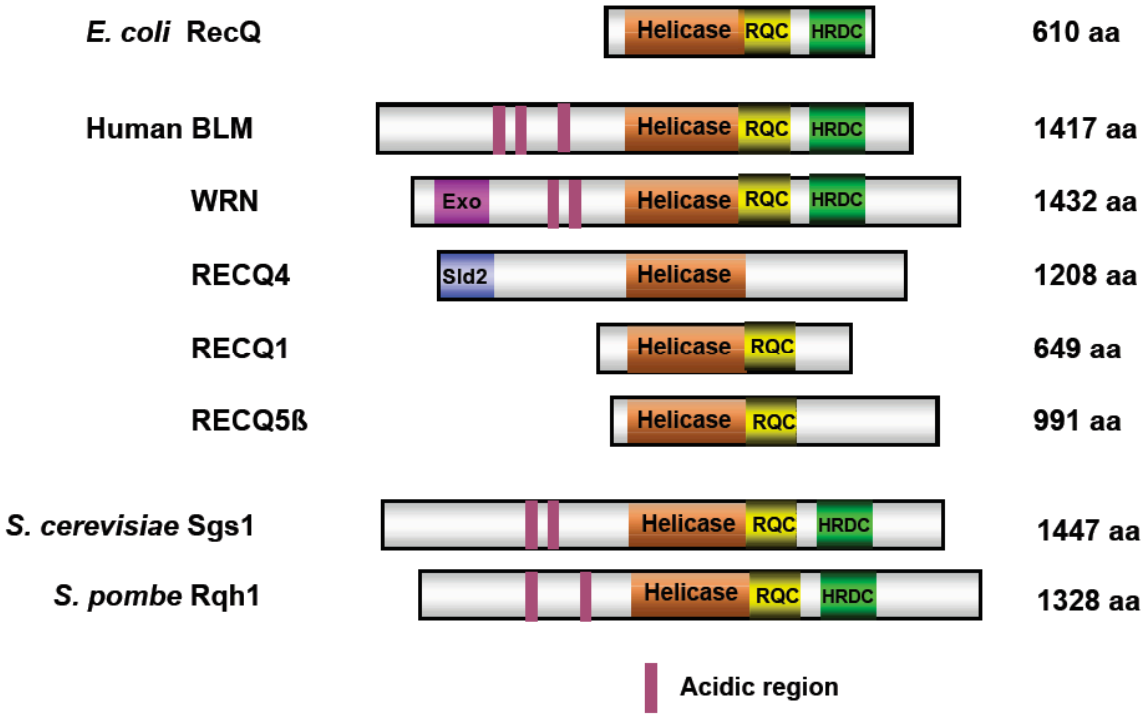

Figure 1. The RecQ helicase family

RecQ helicases in human (BLM, WRN, RecQ4, RecQ1 and RecQ5β), budding yeast (Sgs1) and fission yeast (Rqh1) are aligned by the conserved helicase domain, RecQ C-terminal (RQC) and Helicase and RNase D C-terminal domain (HRDC). The sizes of proteins are shown on the right.

Structural domains of RecQ helicases

Three conserved sequence element are commonly found in RecQ helicases including Helicase, RecQ-C-terminal (RQC) and Helicase-and-RNaseD-like-C-terminal (HRDC) domains (Fig.1). All RecQ proteins have a conserved helicase domain and the RQC and HRDC domains are found in most RecQ helicases but missing in a small subset of family members (e.g. human RecQ1 and RecQ5β lack HRDC domain and RecQ4 lacks RQC and HRDC domains). In addition to these elements, eukaryotic RecQ proteins often have N- or C-terminal extensions that confer additional enzymatic activities such as the exonuclease domain in WRN. Limited proteolysis studies of *E.coli* RecQ demonstrated that RecQ protein is composed of two structural domains (Bernstein and Keck 2003). The first domain includes the Helicase and RQC elements, which combine to form the RecQ 'catalytic core' having ATPase and helicase activities (Fig. 2). The HRDC domain forms the second structural domain in *E.coli* RecQ and it is important for structure specific DNA binding (Fig. 2).

RecQ helicase motifs- Helicases catalyze the separation of ds (double-stranded) DNA through the binding and hydrolysis of NTP. The unwinding activities of helicases are co-ordinated by seven sequence motifs (Bernstein and Keck 2003) that are hallmarks of both SF1 and SF2 helicases. The RecQ family (SF2) contains these seven motifs plus an motif 0 that is N-terminal to motif I (Fig2) (Bernstein, Zittel et al. 2003). A mutation of motif 0 in this region of Sgs1 leads to a hyper-recombination phenotype and sensitivity to DNA damage (Onoda, Seki et al. 2000). A mutation of the conserved motif 0 glutamine to arginine is sufficient to cause BS and abolishes its ATPase and DNA-unwinding activities (Bahr, De Graeve et al. 1998; German, Sanz et al. 2007). A solution structure of

E. coli RecQ provided the evidence that motif 0 contributes to the adenine-binding pocket (Bernstein, Zittel et al. 2003). Motif I in the RecQ family appears to contact the phosphate and metal (Bernstein, Zittel et al. 2003). The mutations of the invariant phosphate-binding lysine residue in motif I of the human RecQ helicases WRN (Brosh, Orren et al. 1999), BLM (Neff, Ellis et al. 1999), RECQ1 (Sharma, Sommers et al. 2005) and RECQ5b (Garcia, Liu et al. 2004), and the yeast Sgs1 helicase (Lu, Mullen et al. 1996) seriously impair or abolish their ATPase and DNA-unwinding activities, suggesting a functionally conserved role of this motif. Motif II in RecQ proteins represents the Walker B motif (Bennett and Keck 2004) and is implicated in NTP hydrolysis. *E. coli* RecQ contains a conserved aromatic-rich loop in its helicase domain between motifs II and III that maps to a similar tertiary position as found in the SF1 helicases (Zittel and Keck 2005). The conserved aromatic-rich loop in motif III of SF1 helicases mediates both ATP and ss (single-stranded) DNA binding (Korolev, Hsieh et al. 1997; Velankar, Soultanas et al. 1999). Mutational analysis of the RecQ aromatic-rich loop provided evidence that this region is critical for coupling ATPase and DNA binding and unwinding activities (Zittel and Keck 2005).

RQC- The RQC motif residing the C-terminal conserved helicase domain is found in the vast majority of RecQ helicases, with the exception of RECQ1, RECQ4 and RECQ5β (Fig. 1). The RQC region was first determined to contain a Zn^{2+}-binding domain and a winged helix domain from the crystal structure of *E. coli* RecQ (Fig. 2) (Bernstein, Zittel et al. 2003). Mutations in *E. coli* RecQ within the Zn^{2+}-binding domain severely impaired its DNA binding (Liu, Rigolet et al. 2004). Modeling studies suggested a Zn^{2+}-binding domain in the BLM RQC region and mutational analyses implicate its role in DNA

binding and protein conformation (Guo, Rigolet et al. 2005). A structure of a recombinant human WRN protein fragment indicated that the WRN RQC region also forms a $Zn2^{+}$-binding domain and winged helix domain (Hu, Feng et al. 2005). Furthermore the WRN RQC has been shown to bind DNA (von Kobbe, Thoma et al. 2003; Lee, Kusumoto et al. 2005) and other proteins (Lee, Harrigan et al. 2005).

HRDC- In addition to the catalytic core, a conserved 80-amino-acid motif designated HRDC found in a number of DNA-metabolizing proteins is present in most RecQ family members (Fig. 1). Indeed, the HRDC domain of Sgs1 (Liu, Macias et al. 1999) and *E. coli* RecQ (Bernstein and Keck 2005) has been shown to bind ssDNA *in vitro*, suggesting an auxiliary function in substrate recognition. In WRN, the HRDC, RQC and exonuclease motifs confer a DNA substrate-binding specificity (von Kobbe, Thoma et al. 2003). The radioresistant bacterium *Deinococcus radiodurans* RecQ helicase has three HRDC domains at its C-terminus that are involved in DNA binding and regulatory functions of the helicase (Killoran and Keck 2006).

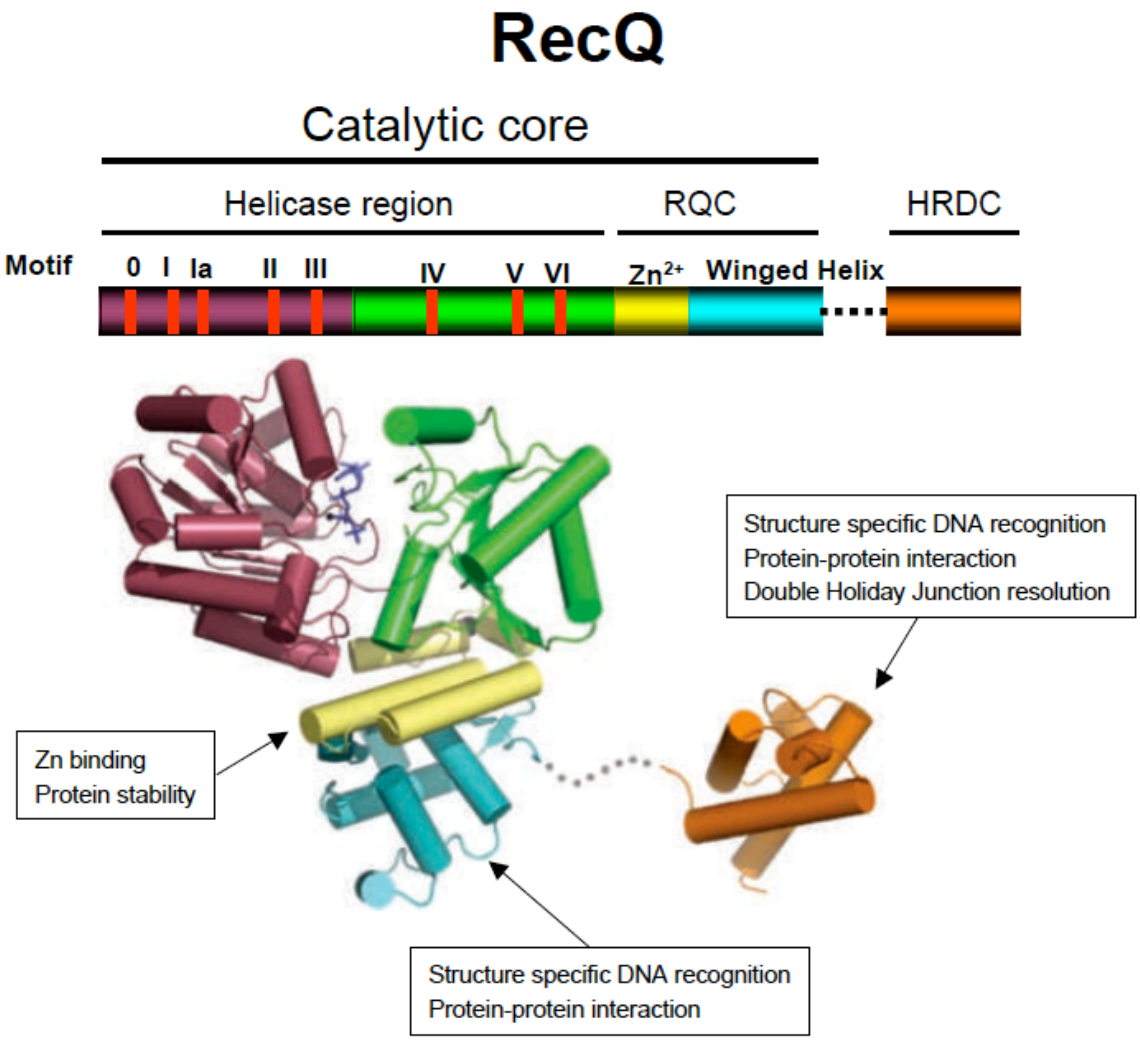

Figure 2. Structural and functional RecQ in *Escherichia coli*

Schematic diagram at the top shows conserved regions in *E. coli* RecQ. Helicase region is shown in purple and green, and contains seven motifs (red, conserved in SF1 and SF2), which are responsible for ATPase and DNA binding/unwinding function. C-terminal helicase domain (RQC) is shown in yellow (Zn-binding) and blue (Wingedhelix). The second conserved domain in RecQ is Helicase and RNase D C-terminal (HRDC) domain shown in orange.

WRN and its homologues contain three motifs near the N-terminus that share identity with the exonuclease domain of *E. coli* pol (DNA polymerase) I and RNaseD (Moser, Oshima et al. 1999). The conserved exonuclease motifs in WRN are found in three human DNA polymerases that contain proofreading exonuclease domains and two exonucleases that are proposed to have auxiliary proofreading functions. Some of the RecQ homologues have strongly acidic regions in the N-terminal region before the helicase domain (Figure 1). WRN has a highly acidic 27-amino-acid direct repeat located in the N-terminus between the exonuclease and helicase domains. This acidic repeat in WRN has been implicated in transcriptional activation (Balajee, Machwe et al. 1999) and the physical interaction with replication protein A (RPA) (Doherty, Sommers et al. 2005).

Consistent with the presence of the conserved Walker A and B motifs (ATPase motifs I and II), all characterized RecQ helicases exhibit ATPase activity that is dependent on a bivalent cation (generally Mg^{2+}). ssDNA stimulating ATP hydrolysis by RecQ helicases is greater degree compared with dsDNA effector (Cejka and Kowalczykowski ; Brosh, Orren et al. 1999; Orren, Brosh et al. 1999; Cui, Arosio et al. 2004; Macris, Krejci et al. 2006). Generally, longer ssDNA molecules are significantly more effective in stimulating ATP hydrolysis by RecQ helicases than ssDNA, suggesting that RecQ helicases may have the ability to translocate processively along long stretches of ssDNA without additional binding steps. All RecQ helicases that have been shown to unwind dsDNA in the 3′ to 5′ direction with respect to the ssDNA flanking the duplex. In general, the deoxy or ribodeoxy form of ATP is the preferred nucleotide as the energy source for DNA unwinding by RecQ helicases. *E. coli* RecQ helicase activity is sensitive to the ratio of Mg^{2+} to ATP with an optimal ratio of 0.8 and a free Mg^{2+} concentration of

50 μM (Harmon and Kowalczykowski 2001). In addition, *E. coli* RecQ helicase activity displayed a sigmoidal dependence on ATP concentration (Harmon and Kowalczykowski 2001). Like *E. coli* RecQ, human RECQ1 helicase activity is significantly inhibited at Mg^{2+}/ATP ratios greater than 1 (Sharma, Sommers et al. 2005).

SGS1

The RecQ orthologue of *S. cerevisiae* was identified by three different groups using different approaches, but in all cases the approaches involved topoisomerase genes. *SGS1* was isolated in a screen for suppressors of the *top3* slow growth phenotype (Gangloff, McDonald et al. 1994). Watt et al. identified the same gene in a yeast two-hybrid screen for interaction partners of topoisomerase II (Watt, Louis et al. 1995). Lu et al. isolated the *SGS1* gene based on its genetic interaction with mutations affecting topoisomerase I (Lu, Mullen et al. 1996). Sgs1 is 1447 amino acids in length and predicted molecular mass is 164 kDa. In 1998, as expression and purification of full-length Sgs1 have proved unsuccessful, enzymatic analyses of a C- and N-terminally truncated protein designated $Sgs1_{400–1268}$ was characterized. The enzymatic properties of this recombinant protein resemble those of the RecQ helicases generally. The recombinant $Sgs1_{400–1268}$ protein has been shown to bind specifically to the single-stranded–double-stranded junction of DNA substrates, and this binding requires a 3′ overhanging DNA tail of at least 3-4 nt. The recombinant $Sgs1_{400–1268}$ protein makes specific contacts within the first 4 nt of a ssDNA region, and can also distinguish between 3′→5′ and 5′→3′ backbones (Bennett, Sharp et al. 1998). Sgs1 helicase is also able to unwind RNA/DNA hybrid molecules. In 2010, full-length Sgs1 was purified and shows a remarkably active helicase that acts on broad range of DNA molecules, making it an appropriate helicase in the resection stage of recombination (Cejka and Kowalczykowski). The marked differences between $Sgs1_{400–1268}$ and full-length Sgs1 suggest that the N and C-terminal regions contain auxiliary DNA binding domains that enable Sgs1 to bind and unwind a wider spectrum of DNA substrates. For example,

structural studies showed that the HRDC domain, which resides on C-terminal helicase domain, resembles the auxiliary helicase domains of bacterial DNA helicases and suggested that it might interact with DNA and is dispensable for Blm in dissolution of double holiday junctions (dHJ) reaction (Wu, Chan et al. 2005).

The intracellular level of Sgs1 shows cell-cycle-dependent changes. It is very low in the M and G_1 phases, peaks in S phase and decreases again in G_2. Similarly, Sgs1 is almost undetectable in cells during M and G_1, but forms nuclear foci in S-phase cells, which partially co-localize with Rad53 and the origin recognition complex found within replication foci. These foci are then lost when the cells traverse G_2. Sinclair et al. also reported a significant enrichment of Sgs1 in the nucleolus (Sinclair, Mills et al. 1997). *sgs1* mutants show an approximate 40% decrease in average lifespan and a greater than 50% decrease in maximum lifespan compared with wild-type cells (Sinclair, Mills et al. 1997; Mankouri and Morgan 2001). Detailed lifespan analyses revealed two classes of senescent cells. Some of the *sgs1* cells stop dividing early, and accumulate as large budded cells, which is a characteristic of G_2-arrested cells. In contrast, those cells that cease cell division at later times are similar to senescent wild-type cells in being bud-free (G_1 cells). The G_2 arrest was reported to be an age-independent stochastic event, while the second class of cells arresting in G_1 was suggested to represent prematurely aged cells. The lifespan of *sgs1* cells that escape the stochastic G_2 arrest can be extended by mutations in other genes that also extend the lifespan of wild-type cells, such as a *fob1* mutation or the overexpression of Sir2. The stochastic G_2 arrest was shown to be dependent, at least partially, on *RAD9* and therefore on the DNA damage checkpoint;

however, deletion of *RAD9* cannot restore a normal lifespan in *sgs1* cells (McVey, Kaeberlein et al. 2001).

S. cerevisiae cells that lack either the telomerase RNA component, *TLC1*, or *EST1*/*EST2*, which encode subunits of telomerase, are defective in the major pathway for the maintenance of telomeres. These mutants senesce much more rapidly than do wild-type cells. Some cells can escape this premature senescence and maintain their telomeres in the absence of telomerase. These cells may employ recombination-mediated pathway to maintain teloneres, termed alternative lengthening of telomeres (ALT). *S. cerevisiae* overcomes telomere crisis by utilizing one of two Rad52-dependent recombination-mediated pathways, termed Types I and II. The emergence of type I survivors require Rad52 and Rad51, while the type II survivors require functional Rad52 and Rad50. The type II survivors grow faster and generally predominate in surviving clones (Lundblad 2002). *sgs1* mutants do not show differences in telomere length from wild-type cells (Watt, Hickson et al. 1996), indicating that increased telomere erosion cannot be the overriding reason for their reduced lifespan. However, *sgs1 tlc1* and *sgs1 est2* double mutants show an increased rate of telomere shortening compared with *tlc1* single mutants, and also a higher proportion of cells arrest in G_2/M. Both of these double mutants generate survivors with similar efficiency to *tlc1* or *est2* mutants, although only after a protracted delay. The emergence of type II survivors, however, is blocked by an *sgs1* mutation, indicating that Sgs1 is involved in the generation of type II survivors together with Rad50. Reintroduction of Sgs1 into established type I survivors is not apparently sufficient to induce the cells to convert into a type II phenotype. These data suggest that Sgs1 is not required for the maintenance of the characteristic chromosomal

end structure, but may be required for the transition from the type I to the type II mode of the telomerase maintenance process (Cohen and Sinclair 2001; Huang, Pryde et al. 2001; Johnson, Marciniak et al. 2001). Interestingly, it has been shown that Toposiomerase (Top3), a Sgs1 interaction partner, is also involved in type II telomere lengthening (Tsai, Huang et al. 2006). Recently, genetic data show that sumoylation of Sgs1 promotes telomere-telomere recombination (Lu, Tsai et al.).

sgs1 mutants are not dramatically sensitive to any DNA-damaging agents (Watt, Hickson et al. 1996; Frei and Gasser 2000), but show some increase in sensitivity to MMS (Miyajima, Seki et al. 2000; Mullen, Kaliraman et al. 2000), UV light (Gangloff, Soustelle et al. 2000; Saffi, Pereira et al. 2000) and HU (Miyajima, Seki et al. 2000). *sgs1* mutants display elevated rates of several different types of mitotic recombination events, including marker loss (Mullen, Kaliraman et al. 2000; Onoda, Seki et al. 2001), unequal sister chromatid exchange (SCE) (Onoda, Seki et al. 2000), gross chromosomal rearrangements (Myung, Datta et al. 2001), and all types of loss-of-heterozygosity events (Ajima, Umezu et al. 2002). They also show an increased rate of illegitimate recombination (Yamagata, Kato et al. 1998). Interestingly, the frequency of UV-induced heteroallelic recombination has been shown to be reduced in diploid *sgs1* cells compared with wild-type cells (Gangloff, Soustelle et al. 2000). Similarly, MMS-induced interchromosomal recombination was found to be significantly reduced in *sgs1* compared with wild-type cells, and little induction is observed in response to UV (Onoda, Seki et al. 2001). In yeast cells, a major pathway for the repair of DSBs is Rad52-dependent HR. A second pathway is NHEJ, which is dependent upon DNA ligase IV. An epistatic relationship has been demonstrated between mutations in *SGS1* and *RAD51*. This,

coupled with the demonstration of a direct physical interaction between C-terminal Sgs1 and Rad51 (Wu, Davies et al. 2001) and Rad51 DNA strand exchange activity stimulated by Blm (Bugreev, Mazina et al. 2009)implies that Sgs1 plays a role in HR.

Sgs1 shows physical and genetic interactions with all three topoisomerases expressed in *S. cerevisiae. sgs1 top1* double mutants grow very poorly, but the reason for this synthetic defect is not known. Sgs1 and Top2 have been shown to interact physically (Watt, Louis et al. 1995; Duno, Thomsen et al. 2000). Moreover, genetic analyses indicate that mutations in *SGS1* and *TOP2* are epistatic with regard to reducing chromosome non-disjunction, suggesting that Sgs1 and Top2 act on the same chromosome segregation pathway (Watt, Louis et al. 1995). Mutations in the *SGS1* gene suppress most of the phenotypic abnormalities displayed by *top3* mutants, including G_2 delay and elevated frequency (Gangloff, McDonald et al. 1994; Onodera, Seki et al. 2002)Sgs1 and Top3 also interact physically. The region of Sgs1 that interacts with Top3 has been mapped using different biochemical techniques to the extreme N-terminal region of the protein (Fig. 3). Studies with Sgs1–Top3 fusion proteins that lack the Top3 interaction segment on Sgs1 indicate that the N-terminal Top3 interaction domain probably has no function other than to recruit Top3 to sites of action (Bennett and Wang 2001). The molecular and genetic studies outlined above suggest that Top3 and Sgs1 function mainly as a complex. It seems likely that Sgs1 helicase creates a DNA structure that is resolved by the ssDNA strand passing activity of Top3. Top3 is highly specific for ssDNA, but probably lacks additional substrate specificity.

Mullen et al. have identified genes in a screen for mutations that show synthetic lethality in an *sgs1* background (Kaliraman, Mullen et al. 2001; Mullen, Kaliraman et al. 2001). These genes were designated *SLX*. The six *SLX* gene products form three distinct heterodimeric complexes, and all three have catalytic activity. Slx3-Slx2 (Mus81-Mms4) and Slx1-Slx4 are both heterodimeric endonucleases with a marked specificity for branched replication fork DNA, whereas Slx5-Slx8 is a SUMO (small ubiqutin-related modifier)-targeted E3 ubiquitin ligase (Ii, Fung et al. 2007; Ii, Mullen et al. 2007). All three complexes play important roles in different aspects of the cellular response to DNA damage and perturbed DNA replication.

sgs1 srs2 double mutants are synthetically lethal or very slow growing (Gangloff, Soustelle et al. 2000; McVey, Kaeberlein et al. 2001; Mullen, Kaliraman et al. 2001). Following sporulation of heterozygous diploids, approximate 40% of the *sgs1 srs2* double mutant spores form microcolonies of 2–100 cells. Lifespan analyses of cells from these colonies revealed that they survive on average for only three generations. The microcolonies contain a high percentage of large budded cells, which are probably arrested at the G_2/M checkpoint (McVey, Kaeberlein et al. 2001). Triple mutants having the combination of *sgs1 srs2* with *rad51*, *rad55* or *rad57* are viable, however, indicating that disabling HR rescues the *sgs1 srs2* inviability (Gangloff, Soustelle et al. 2000). The synthetic phenotype is likely to be a consequence of unconstrained recombination or the accumulation of recombination structures that cannot be resolved adequately in the absence of these helicases. There are apparently some overlapping functions of Sgs1 and Srs2. The *SGS1* gene has been identified as a multicopy suppressor of the sensitivity of *srs2* mutants to MMS and HU(Mankouri, Craig et al. 2002).

Mutation of *RAD51* or *RAD52* can also suppress the synthetic lethality of *mus81 sgs1* double mutants (Bastin-Shanower, Fricke et al. 2003; Ui, Seki et al. 2005). Similarly, *rad51* suppresses the synthetic lethality of *mms4 sgs1* double mutants. These data suggest that the Mus81–Mms4 complex acts in the HR pathway, but in a branch different from that in which Sgs1 is required. However, as *mus81 sgs1 rad51* triple mutants still grow more slowly than the corresponding single *rad* mutants, the effect of *mus81 sgs1* is unlikely to be restricted to HR (Fabre, Chan et al. 2002; Ii and Brill 2005).

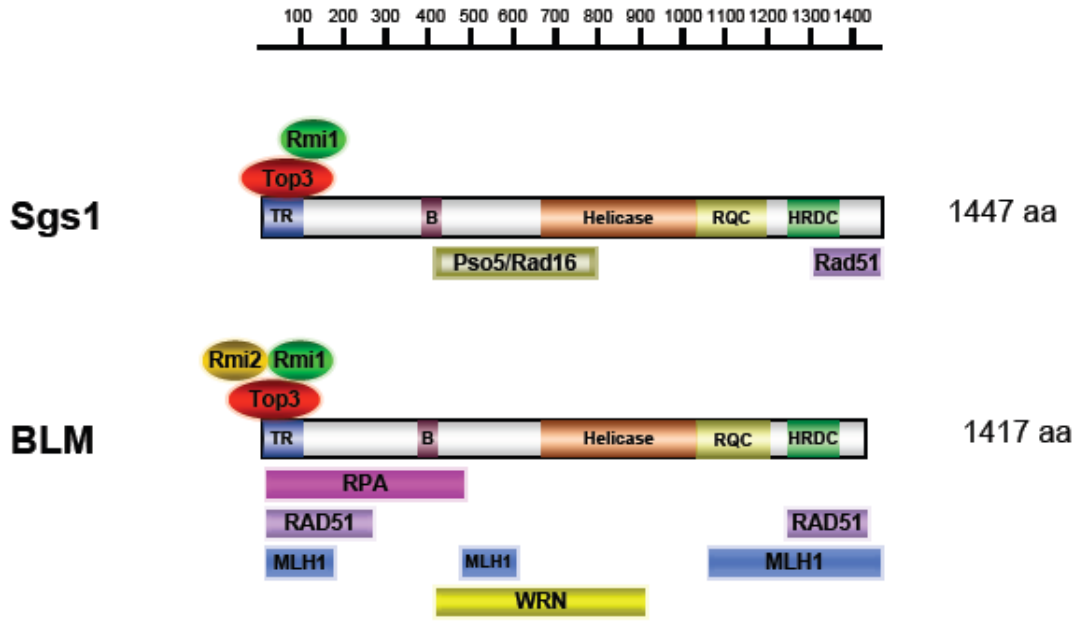

Figure 3. Selected Sgs1- and Blm-interaction proteins

The conserved regions in Sgs1 or Blm are shown in schematic diagram. Interacting proteins with Sgs1 (Blm) are identified by genetic or biochemical way.

Conserved complex Sgs1-Top3-Rmi1

Sgs1 interacts genetically and physically with its cognate DNA topoisomerase III (Top3) (Gangloff, McDonald et al. 1994; Fricke, Kaliraman et al. 2001; Wu, Davies et al. 2001). Eukaryotic Top3 is a type I enzyme that it is most active in unlinking single-strand catenanes (Kim and Wang 1992). Mutation of *TOP3* results in slow-growth phenotype, high levels of recombination and chromosome loss (Myung, Datta et al. 2001; Ui, Seki et al. 2005). Slow-growth of *top3* was suppressed by *sgs1*, and yeast two-hybrid data indicated that the Sgs1 N-terminus and Top3 interacted *in vivo* (Gangloff, McDonald et al. 1994). Physically interaction studies confirmed that Top3 interacts with the N-terminal 100 aa of Sgs1 (Bennett and Wang 2001; Fricke, Kaliraman et al. 2001). This interaction is conserved in the BLM-TOP3α and Rqh1-Top3 complexes (Wu, Davies et al. 2001; Laursen, Ampatzidou et al. 2003) and is essential for complementation of *sgs1* mutant phenotype (Duno, Thomsen et al. 2000; Mullen, Kaliraman et al. 2000; Ui, Satoh et al. 2001). Taken together, these results indicate that Sgs1-Top3 functions as a complex and confirm the idea that the *top3* slow-growth phenotype is primarily due to unrestrained Sgs1 DNA helicase activity in the absence of Top3 activity (Gangloff, McDonald et al. 1994).

The RecQ-Top3 complex is needed to complete a late step in homologous recombination (HR), and it may play a specific role in HR events that occur in response to DNA replication damage (Chu and Hickson 2009). Consistent with the DNA damage sensitivity of *sgs1 top3* mutants, yeast strains lacking *TOP3* either arrest or delay in G2, suggesting a role in repairing spontaneous S-phase damage (Gangloff, de Massy et al. 1999; Maftahi, Han et al. 1999). *SGS1* is required for UV- and MMS-induced

heteroalleleic recombination and, like *rqh1*$^{+}$, *SGS1* has been shown to act in an *RAD52*-dependent pathway (Murray, Lindsay et al. 1997; Gangloff, Soustelle et al. 2000; Ui, Seki et al. 2005). Additional support for a role of Sgs1-Top3 in recombination is provided by genetic suppression studies. Several *sgs1-top3* mutant phenotypes appear to result from toxic recombination intermediates, since they are suppressed in strains that are unable to initiate meitotic or mitotic recombination. Of particular relevance is the finding that *top3* homozygous diploids are capable of undergoing meiosis as long as recombination is not initiated (Gangloff, de Massy et al. 1999). Similarly, the *top3* slow-growth cells or the synthetic sickness of *sgs1 srs2* cells is relieved in cells lacking any of the *RAD52* epistasis genes that are required for HR (Gangloff, Soustelle et al. 2000; Maftahi, Hope et al. 2002; Oakley and Hickson 2002; Shor, Gangloff et al. 2002). Recent progress in explaining the molecular mechanism of RecQ-Top3 complexes has come from both genetic and biochemical studies (Chu and Hickson 2009). Similar to the increase in sister chromatid exchanges seen in Bloom syndrome cells, *sgs1* mutants display an increase in crossover frequency compared to wild-type (wt) cells (Ira, Malkova et al. 2003). This result suggests that the normal function of Sgs1-Top3 is to resolve recombination intermediates in a pathway leading to noncrossover products (Fig. 4). Furthermore*, in vitro* studies with BLM-TOP3α provide a mechanistic explanation for such a pathway. Consistent with BLM's role in HR, BLM is able to dissociate various DNA substrates that resemble HR intermediates such as the D-loop and HJ (Karow, Constantinou et al. 2000; Wu, Bachrati et al. 2006). In 2003, Wu et al show that BLM cooperates with TOP3α to catalyze the resolution of the dHJ intermediate to produce exclusively non-crossover recombinants, this process termed "dHJ dissolution" (Fig5)

(Wu and Hickson 2003). BLM appears to branch migrate double HJs until they collapse into a hemicatenane, which is then a substrate for strand passage by TOP3α (Fig. 5). Interestingly, BLM also disrupt the Rad51 presynaptic filament and stimulates DNA repair synthesis by DNA polδ (Bugreev, Yu et al. 2007). Taken together, the ability of BLM in HR is likely important for the regulation of HR to limit the formation of crossovers and prevent genome rearrangements (Fig. 4) (Wu and Hickson 2003; Bussen, Raynard et al. 2007).

Genes that are redundant with *SGS1-TOP3* have been identified by synthetic lethal screens. Newer methodologies such as as synthetic genetic arrays (SGA) (Tong and Evangelista, 2001; Thomas and Rothstein 1989) and synthetic lethal analysis by microarray (Ooi, Shoemaker et al. 2003) have been combined with a standard genetic screen (Mullen, Kaliraman et al. 2001) to identify over 30 mutations that result in a slow-growth or lethal phenotype in the absence of *SGS1*. This large number of interactors suggests that *SGS1* is a "hub" gene that overlaps multiple pathways (Tong, Evangelista et al. 2001). As an approach to identify genes in the Sgs1-Top3 pathway, Mullen et al. employed a synthetic lethal screen with the synthetic interactor *MUS81* (Mullen, Nallaseth et al. 2005). Analysis of synthetic-lethal screen candidate genes revealed that one of them, *RMI1*, encoded a component of the Sgs1-Top3 complex. RMI1, originally called BLAP75 in human, was also identified as a component of the BLM complex purified from human cells by immunopurified by BLM (Yin, Sobeck et al. 2005). Interestingly, RMI1's association with BLM appears to be accomplished by independent direct physical interactions with both BLM and Top3α (Raynard, Bussen et al. 2006), although it is not clear whether the interactions are mutually exclusive as the BLM and

Top3α interaction domains on RMI1 map to the same N-terminal region (Fig. 6) (Raynard, Zhao et al. 2008). Nevertheless, it has been shown that BLM-Top3α mediated HJ unwinding or dHJ dissolution reaction was enhanced by RMI1 (Wu, Bachrati et al. 2006; Raynard, Zhao et al. 2008). Human RMI1 (625 aa) contains two oligonucleotide-binding (OB)-fold domains and is capable of binding to ssDNA, dsDNA, or more complex DNA structures such as dHJs (Wu, Bachrati et al. 2006; Raynard, Zhao et al. 2008). Unlike human RMI1, yeast RMI1 (241 aa) contains one OB-fold and prefers to bind HJ structure (Fig 6) (Mullen, Nallaseth et al. 2005). Intriguingly, unlike RPA, the DNA-binding activity of RMI1 is dispensable for the stimulation of BLM dependent helicase activity (Raynard, Zhao et al. 2008). Thus, in contrast to the RPA-dependent stimulation that occurs through both DNA-protein and protein-protein interactions, RMI1 affects BLM function only through specific protein-protein contacts. The different function between OB-fold domain of proteins RPA and RMI1 exhibits functionally distinct mechanisms of stimulation of BLM-Top3α.

A novel BLM complex associated protein was identified and called RMI2 (Singh, Ali et al. 2008; Xu, Guo et al. 2008). This protein was found to be present in BLM or RMI1 immunoprecipitates and was subsequently identified as a 15.8 kDa polypeptide by mass spectrometry (Singh, Ali et al. 2008; Xu, Guo et al. 2008). RMI1 was found to interact with RMI2 via the C-terminal OB-fold domain of RMI1 and the OB-fold domain of RMI2. Purified recombinant RMI1 and RMI2 stably associate to form a heterodimeric complex that has greatly improved solubility compared with either of the two individual subunits (Fig. 6). Indeed, it is possible that the RMI1/RMI2 heterodimer is a functional protein, reminiscent of the RPA heterotrimer. Furthermore, mutation of RMI2 results in

an increased level of SCE in cells and RMI (RMI1-RMI2 complex) stimulates BLM-Top3α dependent dissolution of dHJ (Xu, Guo et al. 2008). Taken together, multi-OB-fold complexes are involved in BLM action via RPA-mediated protein-DNA interaction or RMI-mediated protein-protein interactions.

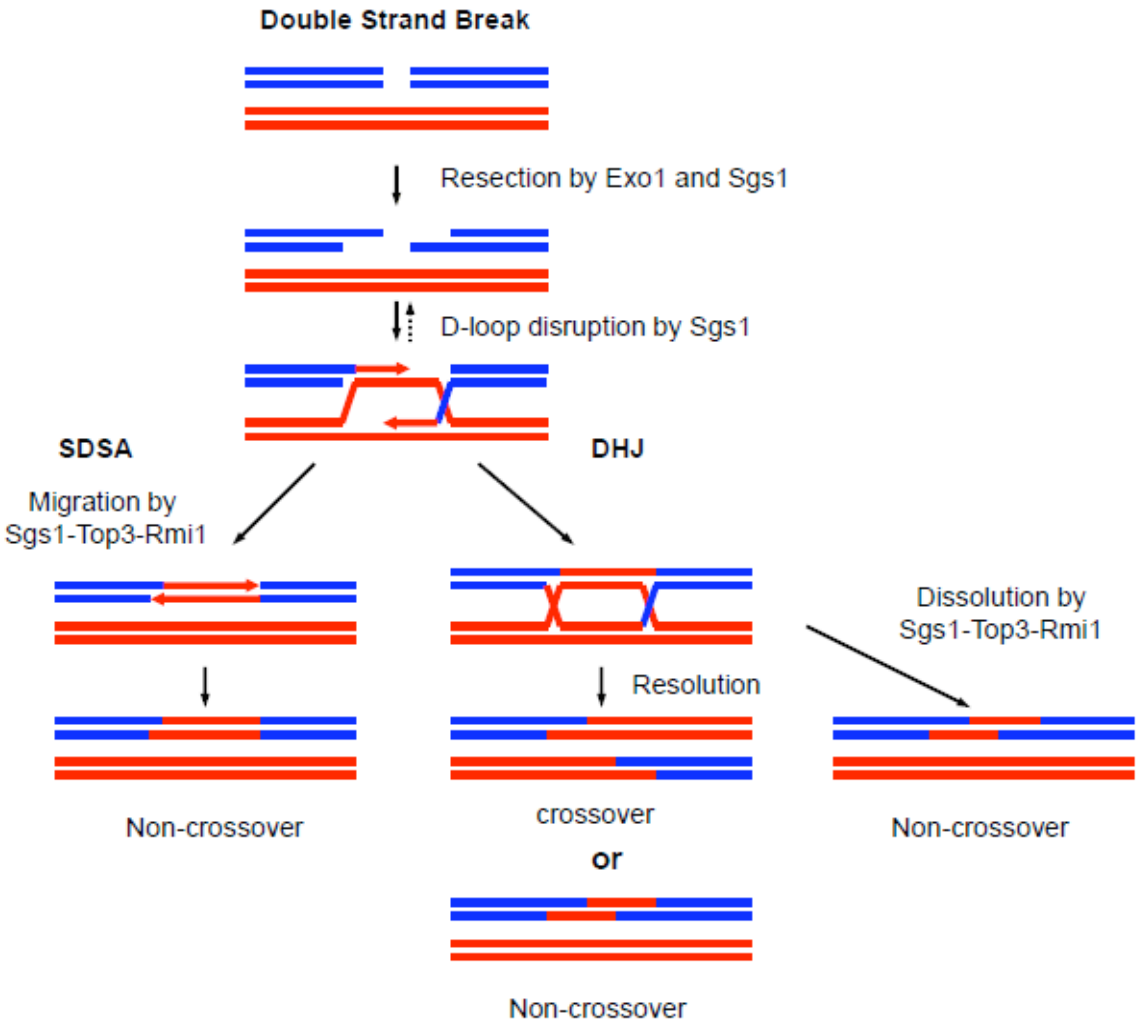

Figure 4. The role of Sgs1 to prevent crossover product in HR

In the early steps of DNA HR repair, Sgs1 promotes Exo1-dependent DNA resection (on left) to creat 3′ ssDNA tail required for Rad51 to facilitate DNA strand invasion. However, formation of D-loop can also be disrupted by Sgs1. In the latter steps of Synthesis-Dependent Strand Annealing (SDSA) or HR pathway, the Sgs1 complex (Sgs1-Top3-Rmi1) or other proteins can complete the reaction by dissolution or resolution.

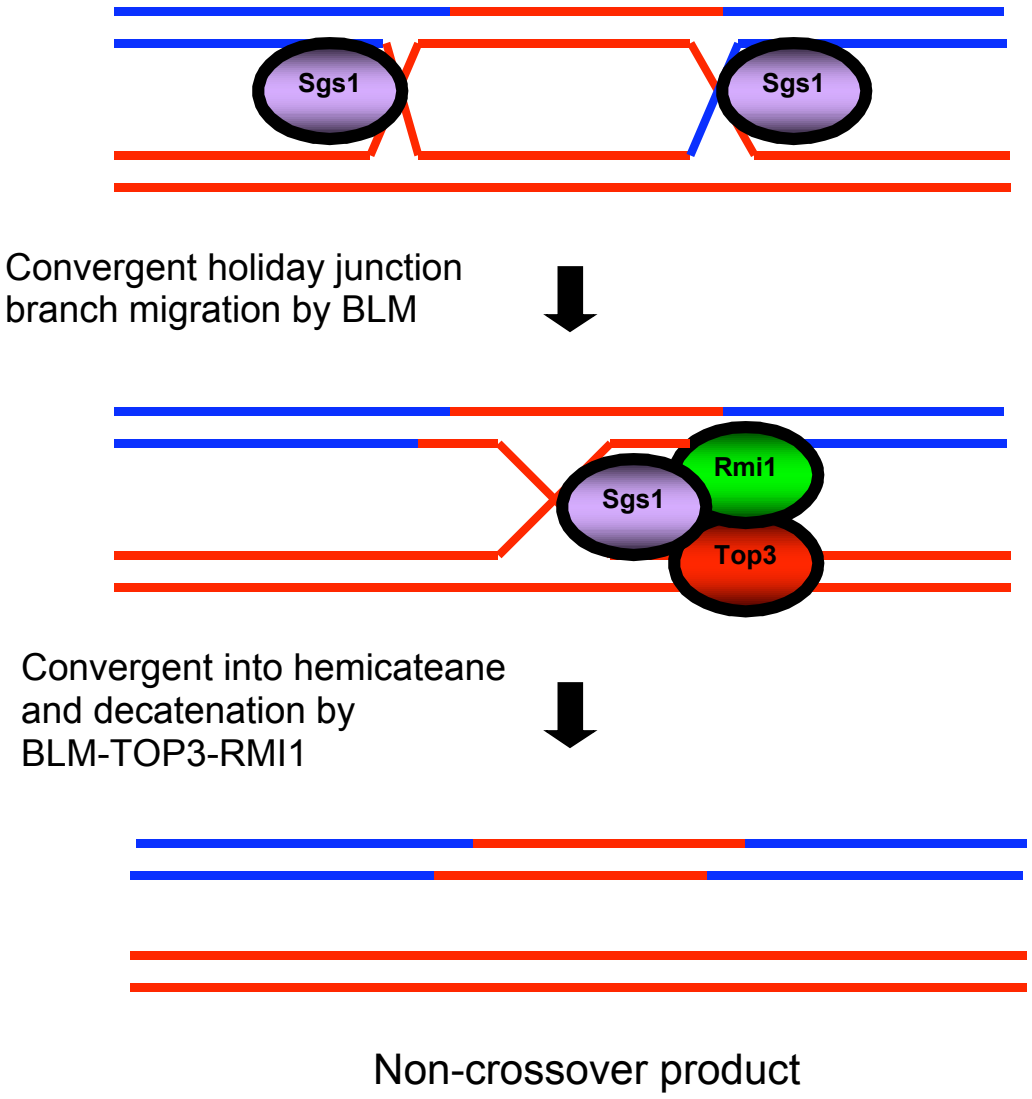

Figure 5. Proposed model for double holliday junction dissolution catalyzed by BLM-TOP3-RMI1

BLM promotes double holliday junction migration and creates hemicateane structure. Hemicateane is decatenated by single-strand passing acticity of TOP3α and this reaction is enhanced by RMI1. The non-crossover product is formed exclusively by dissolution of double holliday junction reaction.

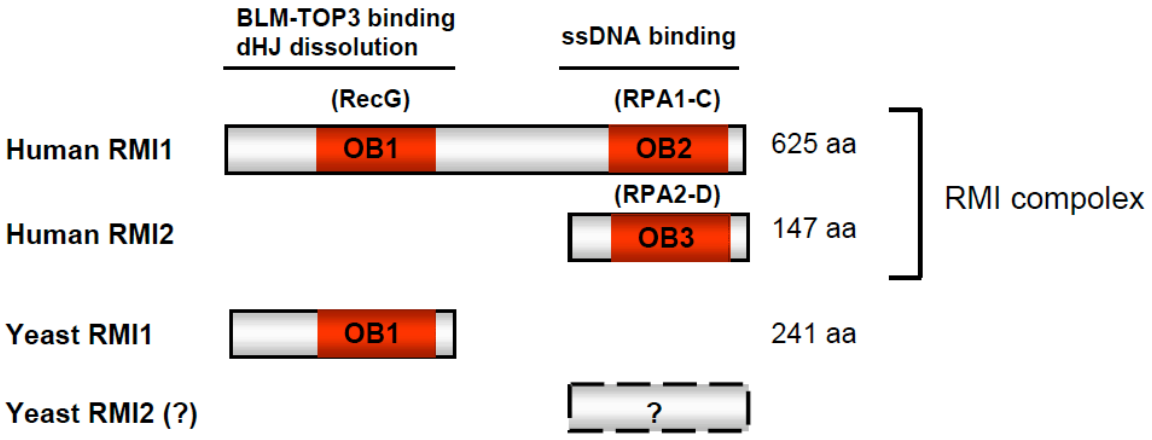

Figure 6. Schematic representation of human RMI1, RMI2 and yeast RMI1

hRMI1 contains two OB-fold domains: OB1 is most similar to the Wedge domain in bacterial RecG, whereas OB2 resembles RPA1-C. Biochemical studies demonstrate that N-terminal hRMI1 including OB1 binds BLM and TOP3 and is required for dHJ dissolution. Furthermore, C-terminal hRMI1 including OB2 contains ssDNA binding function. RMI2 has one OB-fold domain called OB3, which resembles RPA2-D. hRMI1 and hRMI2 form a complex and this complex promote dHJ dissolution. In yeast, only RMI1 was discovered and is similar to OB1 in hRMI1.

Chapter II

Binding and activation of DNA topoisomerase III by the Rmi1 subunit

Summary

Rmi1 is a conserved OB-fold protein that is associated with RecQ DNA helicase complexes from humans (BLM-TOP3α) and yeast (Sgs1-Top3). Although human Rmi1 stimulates the dissolution activity of BLM-TOP3α, its biochemical function is unknown. Here we examined the role of Rmi1 in the yeast complex. Consistent with the similarity of *top3Δ* and *rmi1Δ* phenotypes, we find that a stable Top3-Rmi1 complex can be isolated from yeast cells overexpressing these two subunits. Compared to Top3 alone, this complex displays increased superhelical relaxation activity. The isolated Rmi1 subunit also stimulates Top3 activity in reconstitution experiments. In both cases, elevated temperatures are required for optimal relaxation unless the substrate contains a ssDNA bubble. Interestingly, Rmi1 binds only weakly to ssDNA on its own, but it stimulates the ssDNA binding activity of Top3 five-fold. Top3 and Rmi1 also cooperate to bind the Sgs1 N-terminus and promote its interaction with ssDNA. These results demonstrate that Top3-Rmi1 functions as a complex and suggest that Rmi1 stimulates Top3 by promoting its interaction with ssDNA.

Introduction

Mutations in *BLM* result in Bloom Syndrome (BS), a rare autosomal disease characterized by a variety of symptoms including a predisposition to cancer (Ellis, Groden et al. 1995). Cells from BS patients display genomic instability characterized by elevated rates of sister chromatid exchange (SCE)(German, Archibald et al. 1965). BLM is a RecQ-family DNA helicase that forms a complex with DNA topoisomerase IIIa (Top3α)(Ellis, Groden et al. 1995; Karow, Chakraverty et al. 1997; Wu, Davies et al. 2000). This complex is conserved throughout eukaryotes where it acts to suppress recombination - especially in response to DNA damaging agents such as inter-strand crosslinkers (e.g., mitomycin C) or the alkylating agent methylmethanesulfonate (Krepinsky, Heddle et al. 1979; Hook, Kwok et al. 1984; Shiraishi, Yosida et al. 1985; Bachrati and Hickson 2003; Cheok, Bachrati et al. 2005; Sung and Klein 2006). The fact that the lesions created by these agents are known to impede replication forks has led to the notion that the hyper-SCE phenotype of BS cells is a consequence of an alternative repair pathway for replication-induced DNA damage.

Although the molecular function of BLM-TOP3α is not completely understood, the ability of the helicase-topoisomerase complex to "dissolve" double Holliday junction (HJ) substrates in vitro has suggested a compelling mechanism by which it could suppress crossing over during recombinational repair (Wu and Hickson 2003; Plank, Wu et al. 2006). Studies of orthologous RecQ complexes from model systems such as budding yeast (Sgs1-Top3), fission yeast (Rqh1-Top3) and *Drosophila* have provided genetic insight into the function of these proteins as well as support for the HJ dissolution model (Gangloff, McDonald et al. 1994; Watt, Louis et al. 1995; Bennett, Sharp et al.

1998; Maftahi, Han et al. 1999; Bennett, Noirot-Gros et al. 2000; Ira, Malkova et al. 2003; Plank, Wu et al. 2006).

Rmi1/BLAP75 is a conserved protein that was recently identified based on its association with BLM, Sgs1, and Rqh1. In human cells, Rmi1 co-purifies with a complex of proteins including BLM and Top3α (Yin, Sobeck et al. 2005). This complex has not been purified to homogeneity from yeast, but Rmi1 co-fractionates with a complex containing Sgs1 and Top3 (Chang, Bellaoui et al. 2005; Mullen, Nallaseth et al. 2005). Human Rmi1 is a 625 aa protein that contains a predicted oligonucleotide and oligosaccharide binding fold (OB-Fold) between residues 115 and 192 (Fig. 7A) (Yin, Sobeck et al. 2005). OB-folds are found in a large number of proteins that interact with single stranded DNA (ssDNA) and RNA (Murzin 1993; Theobald, Mitton-Fry et al. 2003). Although yeast Rmi1 is smaller than its human homolog and contains no obvious OB-fold motif, amino acid sequence similarity between these proteins is greatest in the region predicted to contain the OB-fold (Mullen, Nallaseth et al. 2005). This similarity suggests that Rmi1 should interact with ssDNA. Although some support for this idea was previously reported, UV-crosslinking was required to detect a specific interaction between Rmi1 and ssDNA (Mullen, Nallaseth et al. 2005). Moreover, the interaction between Rmi1 and several branched DNA stubstrates using an Electrophoretic Mobility Shift Assay (EMSA) (Mullen, Nallaseth et al. 2005) suggests that structure-specific DNA binding could be influenced by additional proteins in the complex.

In-vitro studies have shown that human Rmi1 can stimulate the BLM-Top3α-dependent HJ dissolution assay and that it interacts with human Top3α (Cheok, Bachrati et al. 2005; Raynard, Bussen et al. 2006; Sung and Klein 2006; Wu, Bachrati et al. 2006).

Consistent with these results, co-immunoprecipitation studies have shown that Rmi1 and Top3 can interact in yeast extracts even in the absence of the Sgs1 DNA helicase (Chang, Bellaoui et al. 2005; Mullen, Nallaseth et al. 2005). While these biochemical assays reveal a functional role for Rmi1 in stimulating BLM-Top3 activity, the mechanism by which it stimulates dissolution and the nature of the interaction between Top3 and Rmi1 has not been investigated.

To determine whether Top3 and Rmi1 formed a stable sub-complex with unique activities, we expressed and purified them from yeast. We found that the two proteins formed a stable complex and that the superhelical relaxation activity of Top3 was stimulated by the Rmi1 subunit. Interestingly, Rmi1 did not show appreciable ssDNA binding activity on its own, but it did stimulate the ssDNA binding activity of Top3. The two subunits also displayed cooperative binding to the Sgs1 N-terminal domain. These data demonstrate that Rmi1 and Top3 form a functional sub-complex and suggest a mechanism by which Rmi1 can regulate Top3 activity.

Results

Isolation of the Top3-Rmi1 complex

In order to test whether Top3 and Rmi1 formed a stable complex we simultaneously overexpressed both proteins in yeast. Top3 complexes were then affinity purified via a C-terminal hexahistidine tag. This Top3-V5His6-tagged protein was expected to be functional in-vitro because it had previously been shown to complement a variety of *top3Δ* phenotypes in yeast (Fricke, Kaliraman et al. 2001; Mullen, Nallaseth et al. 2005). Rmi1 was found to co-purify with Top3 following Ni-affinity and Mono-S chromatography. The resulting complex of 68- and 33-kD proteins was purified to apparent homogeneity based on Coomassie blue staining (Fig. 7B). A similar approach was used to purify Top3, which was overexpressed alone in yeast, while recombinant Rmi1 was purified from *E. coli* as previously described (Mullen, Nallaseth et al. 2005). The Top3-Rmi1 complex was stable to gel filtration chromatography (Fig. 7C) and glycerol gradient sedimentation (Fig. 7D).

Rmi1 stimulates Top3 superhelical relaxing activity

These proteins were tested for the ability to relax negatively supercoiled plasmid DNA. Top3 is most active when provided with ssDNA substates or incubated at elevated temperature (Kim and Wang 1992; Wilson, Chen et al. 2000) so we assayed at several temperatures. As shown in Fig. 8A, Top3-Rmi1 displayed a peak of relaxation activity at 58°C. Under the conditions used in this experiment, similar concentrations of Top3 or Rmi1 displayed no relaxation activity at any temperature. As shown below, the Top3 preparation used in this assay was active but required Rmi1 and a more sensitive assay to

detect relaxation. This suggests that the activity of Top3 in the complex was stimulated by Rmi1.

Figure 7. Purification and characterization of recombinant Top3-Rmi1 complex

(A) Comparison of full-length amino acid sequences of human Rmi1 and budding yeast Rmi1. Gray shading represents the predicted OB-fold domain while crosshatch represents the region of greatest amino acid sequence similarity. (B) Approximately 1.5 μg Top3-Rmi1, 1μg Top3, and 1μg Rmi1 were resolved by 17% SDS-PAGE and subjected to Coomassie blue staining. (C) Forty μg of purified Top3-Rmi1 complex was subjected to Superose 6 size exclusion chromatography and analyzed as in above. (D) Thirty μg of Top3-Rmi1 complex was subjected to 15-35% glycerol gradient sedimentation and analyzed as above.

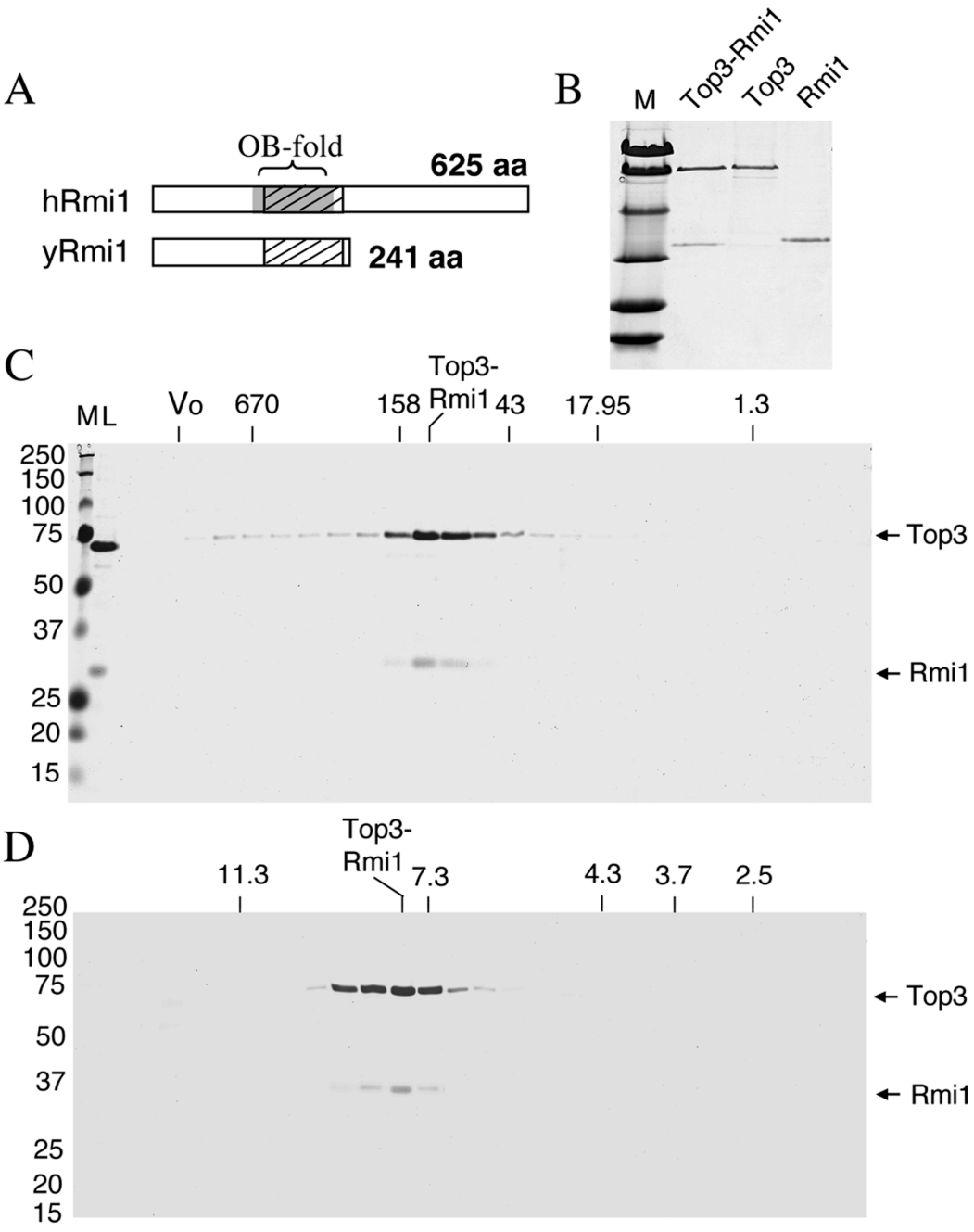
A
OB-fold
625 aa
hRmi1
yRmi1
241 aa
B
M
Top3-Rmi1
Top3
Rmi1
C
ML
Vo
670
158
Top3-Rmi1
43
17.95
1.3
250
150
100
75
50
37
25
20
15
Top3
Rmi1
D
11.3
Top3-Rmi1
7.3
4.3
3.7
2.5
250
150
100
75
50
37
25
20
15
Top3
Rmi1

To confirm this idea, we assayed Top3 in the presence of increasing amounts of Rmi1 and used chloroquine gel electrophoresis to detect any partial relaxation activity. Under these conditions negatively supercoiled DNA is resolved into a ladder of bands (I_n) (Fig. 8B, lane 2) while fully relaxed DNA migrates as a faster-moving species (I_o) that accumulates due to the intercalation of chloroquine (Fig. 8B, lane 20). Partial relaxation of negatively supercoiled DNA could be detected when Top3 was assayed on its own at 45°C or 55°C (Fig. 8B, lanes 9 and 15), but not at 40°C. Increasing levels of Rmi1 stimulated Top3 relaxation of negatively supercoiled DNA at 40°C as revealed by the accumulation of Form I products (Fig. 8B lanes 4 – 6). At 45°C and 55°C Rmi1 had a small effect of accelerating the migration of the Form I product (e.g., Fig. 8B, lanes 10-12). This result confirms that 100 to 200 nM Rmi1 can stimulate 5 nM Top3 in the relaxation of negatively supercoiled plasmid DNA. However, at 40°C this activity was far less than that obtained with 5 nM Top3-Rmi1 complex. This suggests that in vitro reconstitution of the Top3-Rmi1 complex from the individual subunits is inefficient.

The inability of Top3 to completely relax supercoiled DNA is likely due to its inability to gain access to ssDNA like its bacterial counterpart DNA topoisomerase III (Srivenugopal, Lockshon et al. 1984; DiGate and Marians 1988). The stimulation of Top3 by high temperature or its ability to relax hyper-negatively supercoiled DNA is consistent with this idea (Kim and Wang 1992; Wilson, Chen et al. 2000). Further, it has been shown that Top3 is capable of relaxing positively supercoiled DNA if the enzyme is provided acess to ssDNA strands via ssDNA extrusions or bubble DNA (Plank, Chu et al. 2005). We tested the abilility of Rmi1 to stimulate Top3 using a negatively supercoiled duplex DNA containing a 500 bp bubble (Plank, Chu et al. 2005). As previously

demonstrated (Plank, Chu et al. 2005), Top3 was able to partially relax this bubble substrate when assayed at low temperature (30°C) (Fig. 9A, lanes 2, 6, 10, and 14). Increasing concentrations of Rmi1 stimulated this activity especially when assayed in the presence of 100 – 400 nM Top3. The ability of Rmi1 to stimulate relaxation was confirmed by quantifying the level of unreacted negatively supercoiled bubble DNA (NSB) in the titrations. As shown in Fig. 9B, Rmi1 stimulated relaxation at all concentrations of Top3 that were used. Complete relaxation was obtained with 400 nM Top3 and 500 nM Rmi1 (Fig. 9A, lane 16). As before, Top3-Rmi1 complex (125 nM) was more active than Top3 alone (400 nM).

We used the bubble substrate to test whether Rmi1 could stimulate Top3 to relax positively supercoiled DNA. Bubble DNA was first incubated with 1.5 µg/ml EtBr to positively supercoil the DNA, and then incubated with either Top3 alone, or Top3 plus Rmi1. Following incubation the reaction was extracted and the product was analyzed by agarose gel electrophoresis. Under these conditions, the substrate DNA migrates as a ladder of bands between NSB and OCB, while Top1 treatment, which is known to relax positively supercoiled DNA, produces Form I DNA (Fig 9C, lane 2). Although Top3 or Rmi1 alone had little or no effect on the substrate, Rmi1 stimulated Top3 to relax the positively supercoiled substrate as indicated by the appearance of NSB (Fig. 9C, lanes 5 & 6, and 8 & 9). Quantifying the NSB confirmed this interpretation (Fig. 9D). Finally, the specificity of the Top3-Rmi1 interaction was determined by showing that Rmi1 failed to stimulate the relaxation activity of DNA topoisomerase I (Fig. 10).

Figure 8. Relaxation of negatively supercoiled DNA by Top3, Rmi1, and Top3-Rmi1

(A) Relaxation reactions containing 200 ng pKS+ supercoiled plasmid DNA were incubated at indicated temperature for 20 min. Following resolution on a native agarose gel the products were stained with ethidium bromide and photographed. Presented is the negative image. Top3 concentrations were 75 nM or 150 nM; Rmi1 concentrations were 75 nM or 150 nM; and the concentrations of Top3-Rmi1 complex were 45 nM or 90 nM. (B) Relaxation reactions containing 200 ng negatively supercoiled pKS+ plasmid DNA were incubated at the indicated temperature with 5 nM Top3-Rmi1, or 5 nM Top3 together with increasing concentrations of Rmi1. Following the reactions, the products were resolved by 0.8% agarose gel electrophoresis in presence of 5 μg/ml chloroquine and the gel was processed as above. The concentrations of Rmi1 were 25 (lanes 4, 9, 15), 100 (lanes 5, 10, 16), or 200 nM (lanes 7, 13, 19). The various topological states of the plasmid are indicated to the right of the gel as follows: I, negatively supercoiled DNA; I_n, topoisomers of negatively supercoiled DNA; II, open circle and nicked circle forms; III, linear DNA. B, pKS+ plasmid digested with *Bam*HI (lane 1); M, mock incubation; S, substrate relaxed with DNA topoisomerase I.

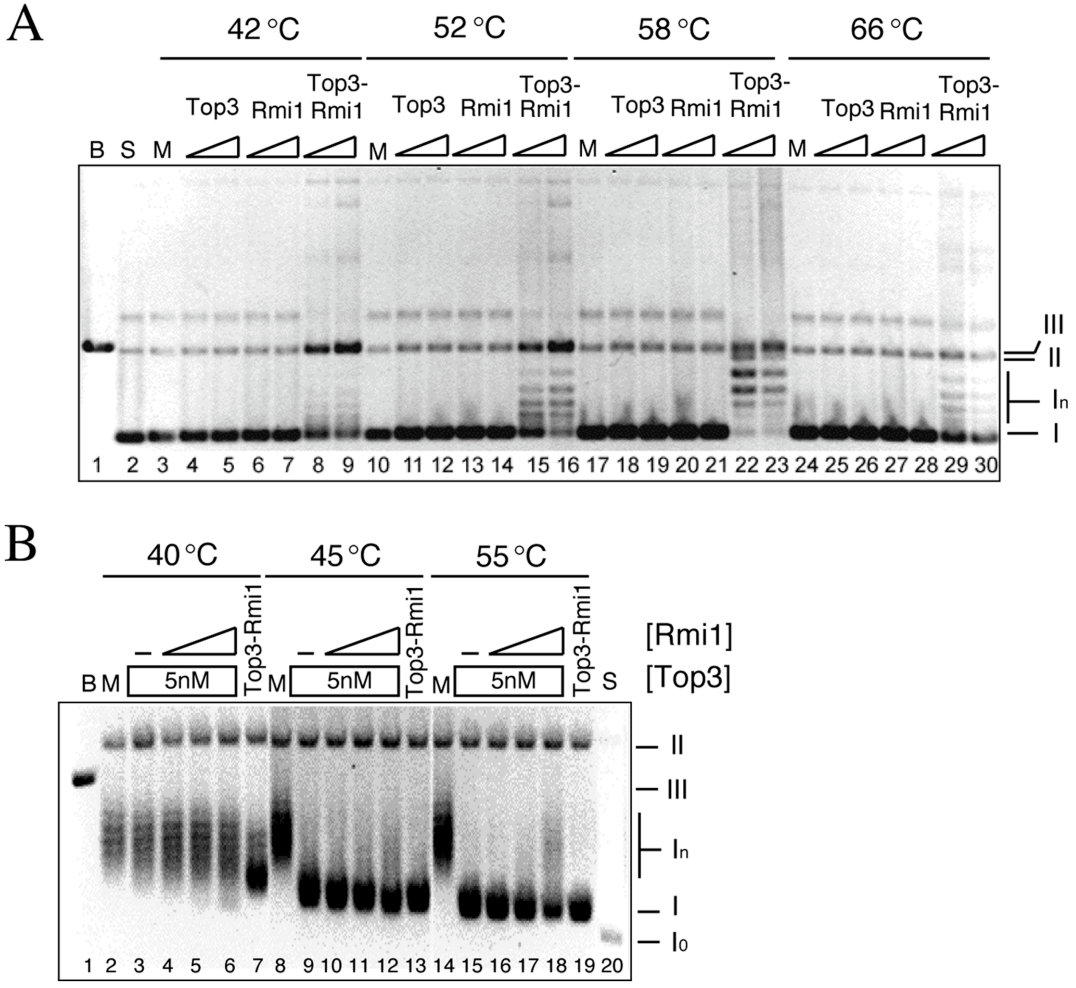
A
42 °C
52 °C
58 °C
66 °C
Top3
Rmi1
Top3-Rmi1
B S M
M
III
II
In
I
1 2 3 4 5 6 7 8 9 10 11 12 13 14 15 16 17 18 19 20 21 22 23 24 25 26 27 28 29 30
B
40 °C
45 °C
55 °C
–
Top3-Rmi1
[Rmi1]
[Top3]
B M
5nM
M
S
II
III
In
I
I0
1 2 3 4 5 6 7 8 9 10 11 12 13 14 15 16 17 18 19 20

Figure 9. Rmi1 stimulates Top3-dependent relaxation of supercoiled bubble DNA at 30°C

(A) Negatively supercoiled DNA containing a 500 bp bubble (NSB) was prepared as described in the Materials and Methods and incubated with the indicated concentrations of Top3 together with increasing concentrations of Rmi1 (0, 250, 500, or 1000 nM) for 20 min at 30°C. Alternatively, NSB was mock treated (lane 1), or treated with 125 nM Top3-Rmi1 (lane 18) or 1000 nM Rmi1 (lane 19). OCB, Open circular bubble DNA. The products were analyzed by native gel electrophoresis as in Fig 2A. (B) The percent of initial substrate DNA (NSB; mock = 100%) remaining in each reaction was quantified and is presented as a function of Top3 concentration. (C) Positively supercoiled DNA containing a 500 bp bubble (PSB) was prepared by pre-incubating OCB with EtBr. This substrate was then incubated with the indicated concentration of Top3 together with increasing amounts of Rmi1 (0, 100, 500 nM) for 20 min at 30°C. Alternatively, PSB substrate (S, lane 1) was treated with DNA topoisomerase I (Top1, lane 2), mock treated (M, lane 3), or treated with 100 nM (lane 12) or 1000 nM (lane 13) Top3-Rmi1. Following incubation, the DNA was purified away from protein and EtBr by phenol/chloroform extraction and analyzed by native agarose gel electrophoresis. Note that the relaxation of PSB DNA produces NSB DNA. (D) The NSB product DNA was quantified for each reaction and is presented as percent maximal relaxation (where M = 0% and Top1 = 100%).

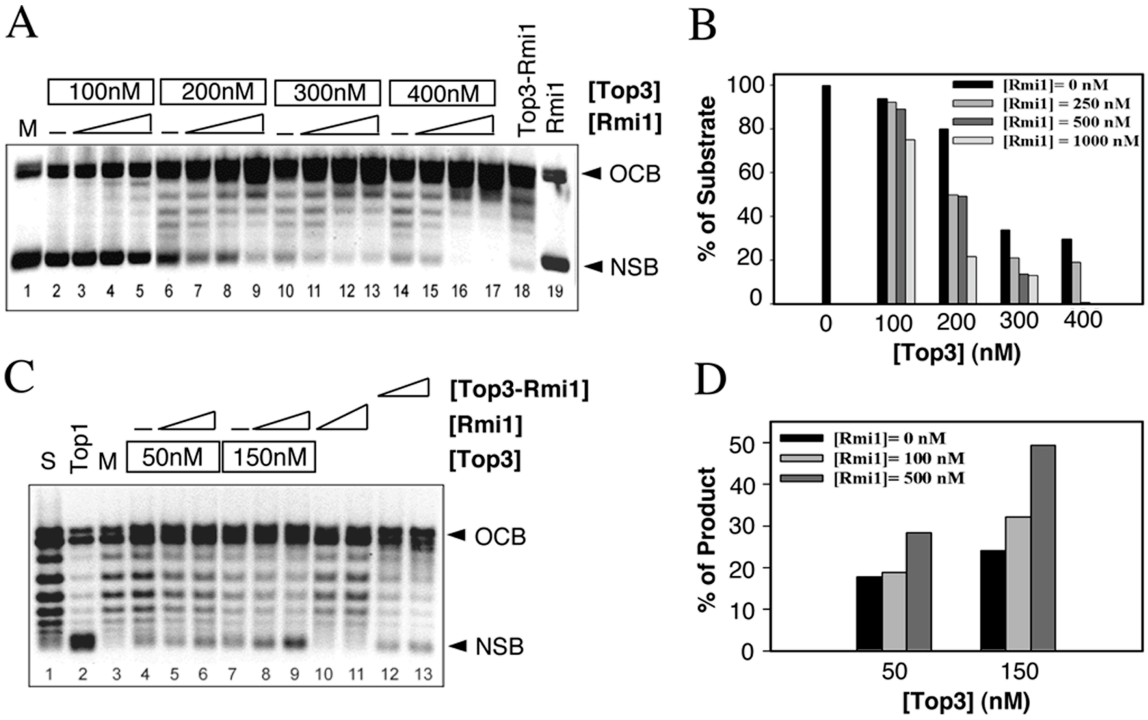
A
100nM
200nM
300nM
400nM
M
Top3-Rmi1
Rmi1
[Top3]
[Rmi1]
OCB
NSB
1 2 3 4 5 6 7 8 9 10 11 12 13 14 15 16 17 18 19
B
[Rmi1]= 0 nM
[Rmi1] = 250 nM
[Rmi1] = 500 nM
[Rmi1] = 1000 nM
% of Substrate
100
80
60
40
20
0
0 100 200 300 400
[Top3] (nM)
C
[Top3-Rmi1]
[Rmi1]
[Top3]
S Top1 M
50nM
150nM
OCB
NSB
1 2 3 4 5 6 7 8 9 10 11 12 13
D
[Rmi1]= 0 nM
[Rmi1]= 100 nM
[Rmi1]= 500 nM
% of Product
50
40
30
20
10
0
50 150
[Top3] (nM)

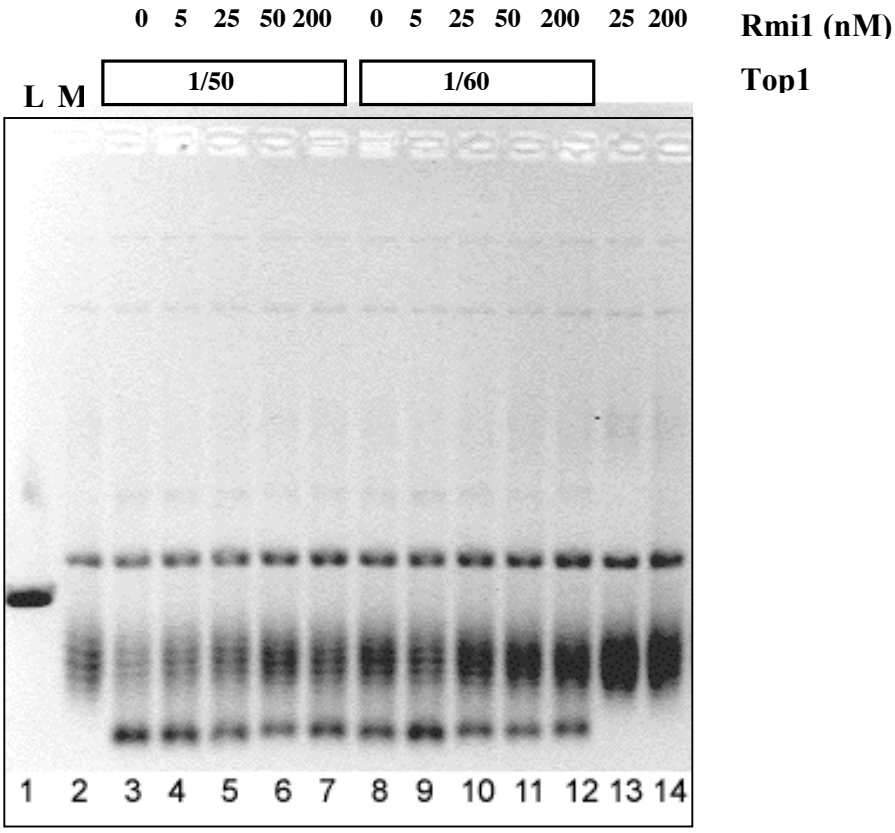

Figure 10. Rmi1 fails to stimulate the relaxation activity of DNA topoisomerase I

Eukaryotic Top1 (GE Healthcare) was diluted 50-fold or 60-fold and incubated with negatively supercoiled pKS+ plasmid DNA at 37°C for 20 min using the manufacturer's buffer conditions. Following the reaction, the products were resolved using 0.8% agarose gel electrophoresis in the prescence of 5 µg/ml chloroquine. The gel was then stained with EtBr.

Rmi1 stimulates the ssDNA binding activity of Top3

Given the possibility of an OB-fold within the yeast Rmi1 subunit, we investigated whether the Rmi1-Top3 complex displayed specific DNA binding activity. Using an EMSA assay we first tested the ability of the Rmi1 or Top3 subunits to bind ^{32}P-labeled ssDNA, dsDNA, or HJ probes that were 50 nt in length. Consistent with previous data (Mullen, Nallaseth et al. 2005), high concentrations of Rmi1 interacted weakly with ssDNA, producing a diffuse smear following gel electrophoresis (Fig. 11A, lanes 2-6). Also, some signal was observed in the well at maximal Rmi1 concentrations. Small amounts of Rmi1 bound the dsDNA and HJ probes, although a majority of these complexes could not enter the gel, suggesting that it was aggregated (Fig. 11A, lanes 7 - 17). As previously reported (Bennett, Noirot-Gros et al. 2000), low concentrations of Top3 bound the ssDNA probe and formed a discrete band in the gel (Fig. 11B, lane 2). At higher concentrations, Top3 bound the dsDNA and HJDNA probes (Fig. 11B) with evidence of aggregation at the highest concentrations. Like Top3, the Top3-Rmi1 complex bound the ssDNA probe at low concentrations and produced a single band within the gel (Fig. 11C, lanes 1 - 11). Higher concentrations of Top3-Rmi1 complex were required for dsDNA and HJ binding and a specific band was obtained (Fig. 11C, right panels). Under these conditions little or no signal was observed in the well suggesting that Top3-Rmi1 is resistant to aggregation.

To measure substrate preference, we quantified the amount of each substrate that was bound by Top3, Rmi1, or Top3-Rmi1 as a function of protein concentration (Figures 11D-F). These results indicated that Top3 and Top3-Rmi1 complex bound preferentially to the ssDNA probe. In the case of the Top3-Rmi1 complex, this preference is reflected

by a Kd (0.18 nM) that was four to ten-fold lower than those obtained for HJDNA or dsDNA (Table 2). Consistent with this result, unlabelled ssDNA was a better competitor than dsDNA (Fig. 11G). Using this assay, 50% of the ssDNA binding was completed by 0.12 nM ssDNA or 6.5 nM dsDNA, which is a 50-fold difference.

Using a 50 nt substrate there was little if any difference in ssDNA binding affinity between Top3 and the Top3-Rmi1 complex (Fig. 11D). Because Top3 was previously shown to bind a 41 nt substrate (Bennett, Noirot-Gros et al. 2000), we tested whether shorter ssDNA substrates could distinguish these proteins. A difference between Top3 and the Top3-Rmi1 complex was observed using a low concentration of a 30 nt substrate (Fig. 12A). To compare binding affinities we performed titration experiments using a higher concentration of the 30 nt ssDNA probe as this resulted in detectable Top3 band-shifts by EMSA (Fig. 12B). Under these conditions ssDNA binding required significantly less Top3-Rmi1 complex than Top3 alone (Fig. 12C). This difference was reflected in a dissociation constant for Top3-Rmi1 (2.25 nM) that was five-fold lower than that of Top3 (Table 3). Taken together, these results indicate that the Top3-Rmi1 complex has a reduced tendency to aggregate on DNA and that it has a higher affinity for ssDNA than Top3 alone.

To confirm this result, we tested whether exogenous Rmi1 could directly stimulate ssDNA binding by Top3. For this analysis increasing amounts of Rmi1 were incubated together with a fixed concentration of Top3 and the 30 nt probe. As shown in Fig. 12D (lanes 3-7), increasing levels of Rmi1 resulted in increased probe being retarded in the gel. The migration of this band was retarded relative to that of Top3 alone and its position approximated that of the purified Top3-Rmi1 complex (Fig. 12D, lane 2). This is

consistent with the idea that Top3-Rmi1 binds the probe as a complex. This experiment was repeated with increasing Top3 concentrations and the results were quantified. As shown in Figure 12E, Rmi1 stimulated Top3-dependent ssDNA binding with maximal stimulation occurring at lower concentrations of Top3.

Figure 11. DNA binding specificity of Rmi1, Top3, and the Top3-Rmi1 complex

EMSA probes were made by gel-purifying ^{32}P-labeled DNA substrates that were assembled from 50-mer oligonucleotides. Standard binding reactions (Materials and Methods) were carried out at a final DNA concentration of 0.25 nM. Following incubation, the reactions were subjected to 5% PAGE after which the gel was dried and analyzed on a phosphorimager. (A) The indicated substrates were incubated with Rmi1 at the following concentrations: 0 (*lanes 1, 7, 13*), 162 (*lanes 2, 8, 14*), 325 (*lanes 3, 9, 15*), 650 (*lanes 4, 10, 16*), 1300 (*lanes 5, 11, 17*), or 2600 nM (*lanes 6, 12*). (B) Top3 was incubated with the indicated substrates exactly as in (A). (C) Top3-Rmi1 complex was incubated with either the ssDNA substrate (0, 0.037, 0.075, 0.15, 0.3, 0.75, 1.5, 2.25, 3, 4.5, or 9 nM protein; lanes 1 - 11), the HJ substrate (0, 1.5, 3, 6, 15, 23, 30, 45, or 90 nM protein; lanes 12 - 20), or the dsDNA substrate (0, 6, 15, 23, 30, 45, 60, 90, or 150 nM protein; lanes 21 – 29). The fraction of free and bound probe was then determined using IP LabGel software. (D) Quantification of ssDNA binding. (E) Quantification of dsDNA binding. (F) Quantification of HJDNA binding. Each data point represents the mean of three independent experiments presented along with the standard deviation as error. (G) The specificity of ssDNA binding by Top3-Rmi1 was confirmed by competition assay. Six nM Top3-Rmi1 was incubated together with 0.25 nM ^{32}P-labeled $(dT)_{60}$ ssDNA in a 20 µl reaction volume. Where indicated, reactions included unlabeled competitor DNA consisting of either boiled pKS+ plasmid (ssDNA) at 0.00064, 0.0032, 0.0016, 0.08, 0.4, 2, 10 nM or untreated pKS+ plasmid (dsDNA) at 0.0032, 0.0016, 0.08, 0.04, 0.2, 1, 5, 25

nM. The products were analyzed as above. For each reaction, the percentage of initial ssDNA binding (obtained in the absence of unlabeled DNA) was determined.

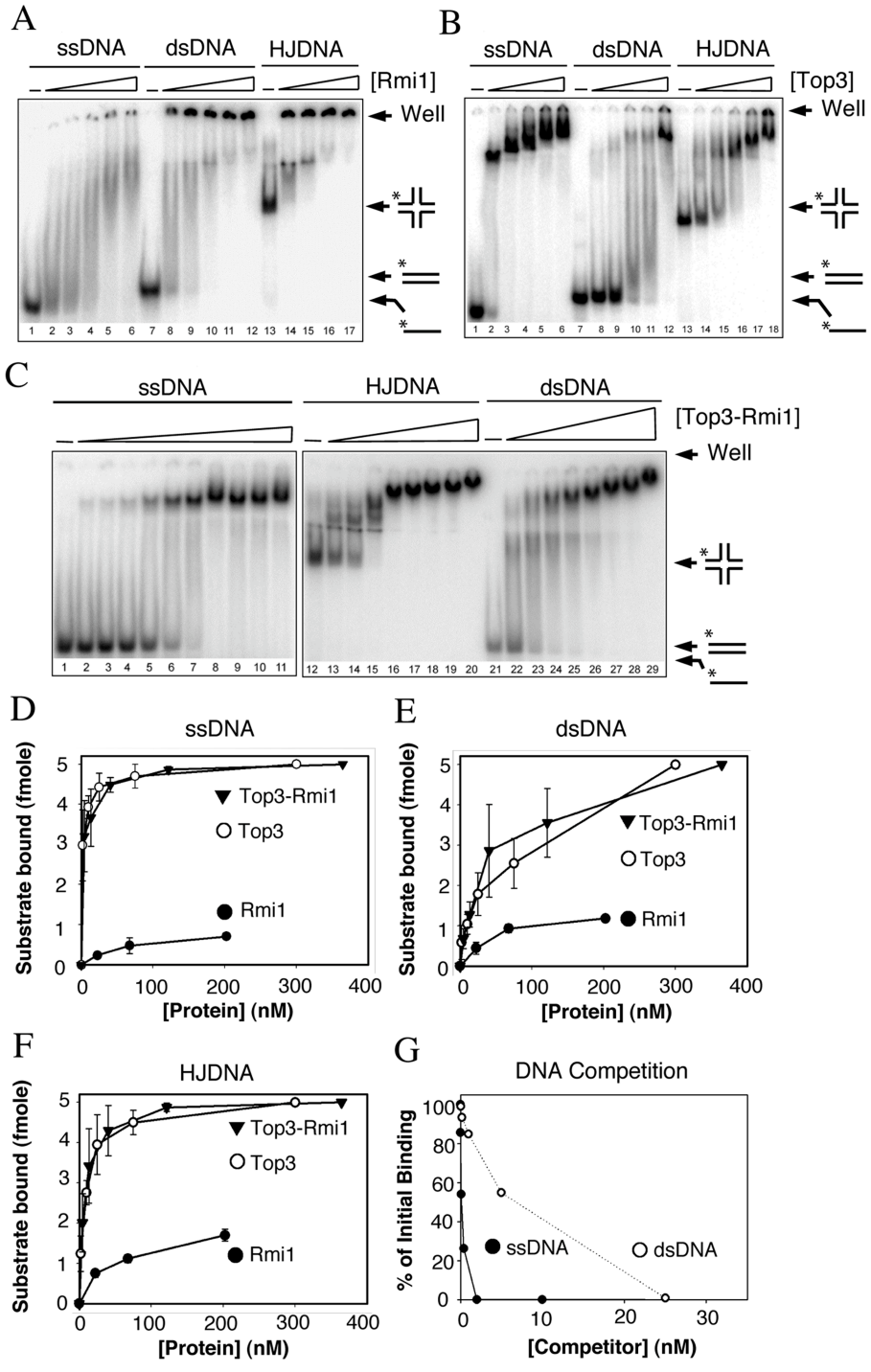

Figure 12. Top3-Rmi1 displays enhanced ssDNA binding activity

(A) A ^{32}P-labeled 30-mer oligonucleotide (0.25 nM) was incubated under standard conditions with either no protein (lane 1), Top3 protein (7.5, 30, or 60 nM; lanes 2-4) or Top3-Rmi1 complex (7.5, 30, or 60 nM; lanes 5-7). Products were then analyzed by EMSA as in Fig. 4, except for use of a 4% polyacrylamide gel. (B) The ^{32}P-labeled 30-mer oligonucleotide (100 nM) was incubated with either no protein (ssDNA; lane 1), Top3 (28, 56, 112, 225, 450, 670 nM; lanes 2 – 7), Top3-Rmi1 (4.5, 9, 18, 38, 75, 150 nM; lanes 8 - 13), or Rmi1 (32, 64, 125, 250, 500, 1000 nM; lanes 14 - 19). (C) The experiment shown in panel (B) was repeated and the signal corresponding to bound DNA was quantified for each protein. Presented is the mean value obtained from three experiments together with its standard deviation. (D) The ^{32}P-labeled 30-mer oligonucleotide (30 nt) was incubated with either no protein (ssDNA; lane 1), Top3-Rmi1 (112 nM; lane 2), or the indicated concentrations of Top3 together with increasing concentrations of Rmi1 (0, 250, 500, 750, or 1000 nM). As control, the probe was incubated with Rmi1 alone (500, 750, or 1000 nM; lanes 13 - 15). (E) The signal corresponding to bound ssDNA in panel (D) was quantified and is presented graphically.

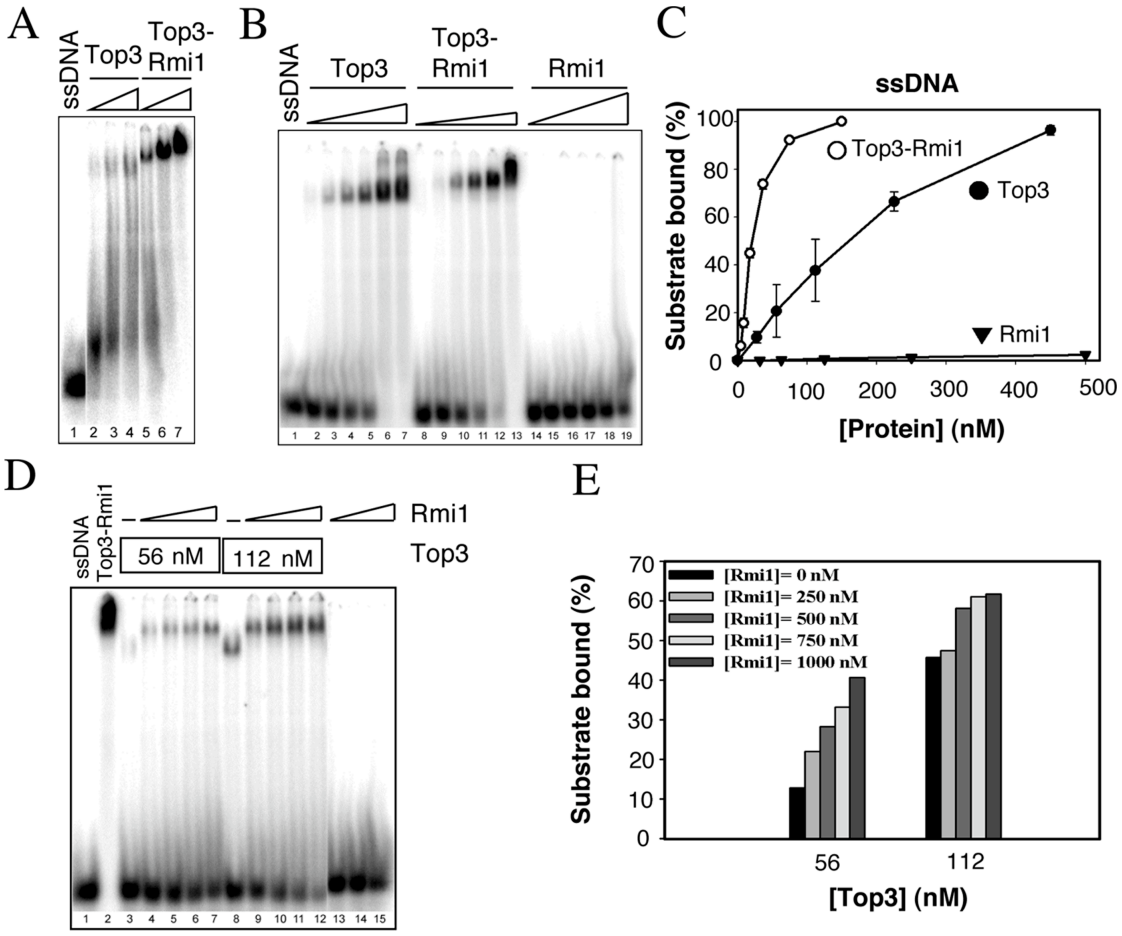
A
ssDNA
Top3
Top3-Rmi1
1 2 3 4 5 6 7
B
ssDNA
Top3
Top3-Rmi1
Rmi1
1 2 3 4 5 6 7 8 9 10 11 12 13 14 15 16 17 18 19
C
ssDNA
Substrate bound (%)
Top3-Rmi1
Top3
Rmi1
[Protein] (nM)
D
ssDNA
Top3-Rmi1
56 nM
112 nM
Rmi1
Top3
1 2 3 4 5 6 7 8 9 10 11 12 13 14 15
E
Substrate bound (%)
[Rmi1]= 0 nM
[Rmi1]= 250 nM
[Rmi1]= 500 nM
[Rmi1]= 750 nM
[Rmi1]= 1000 nM
[Top3] (nM)

Table 2

DNA binding affinity of Top3·Rmi1

Substrate	K_d
	nM
$ssDNA_{50}$	0.18 ± 0.038
$HJ\text{-}DNA_{50}$	0.72 ± 0.11
$dsDNA_{50}$	1.5 ± 0.14

Table 3

ssDNA (30 nt) binding affinity of Top3·Rmi1 and its subunits

Protein	K_d
	M
Top3·Rmi1	2.25 ± 0.05
Top3	11.7 ± 1.5
Rmi1	227 ± 19

Top3 and Rmi1 cooperate to bind Sgs1

Top3 has been shown to interact directly with N-terminal domain of Sgs1 (Bennett, Noirot-Gros et al. 2000; Fricke, Kaliraman et al. 2001) and fractionation of yeast extracts indicates that these proteins exist in a complex with Rmi1 (Chang, Bellaoui et al. 2005; Mullen, Nallaseth et al. 2005). To examine these subunit interactions more completely, we tested whether Rmi1 modulated the interaction between Top3 and the Sgs1 N-terminus. To do this, we exploited a GST-fusion protein consisting of GST plus residues 1 – 158 of Sgs1 (Fricke, Kaliraman et al. 2001). Constant amounts of Top3 and GST-$Sgs1_{1\text{-}158}$ were first incubated together with increasing levels of Rmi1, and the amount of Top3 or Rmi1 that bound to GST-$Sgs1_{1\text{-}158}$ was then measured by glutathione-bead pull down and immunoblotting. Under the conditions used here, Top3 failed to interact with Sgs1 alone (Fig. 13A, lane 3). However increasing levels of Rmi1 stimulated the binding of Top3 to Sgs1 (lanes 4-9). As expected, Rmi1 precipitated along with GST- $Sgs1_{1\text{-}158}$ and Top3 consistent with the formation of a tertiary complex. Control reactions showed that neither Rmi1 nor Top3 bound to GST alone (Fig. 13A, lanes 17 – 19). In the reciprocal experiment, increasing levels of Top3 were found to stimulate the binding of Rmi1 to GST-$Sgs1_{1\text{-}158}$ (Fig. 13A, lanes 10-16). We conclude that Rmi1 and Top3 act together as a complex to bind Sgs1.

Given the ability of Top3-Rmi1 to bind ssDNA and Sgs1, we asked whether the Top3-Rmi1 complex could mediate the binding of Sgs1 to ssDNA. It has previously been shown that the N-terminal 640 amino acids of BLM are dispensible for ssDNA binding by BLM (Cheok, Wu et al. 2005). Consistent with this result, the Sgs1 N-terminal domain ($Sgs1_{1\text{-}652}$) did not bind ssDNA on its own (Fig. 13B, lanes 18-19) and

increasing concentrations of this domain had no effect on the binding of a 50 nt ssDNA probe by Top3 (Fig. 13B, lanes 2 - 5). However, when incubated in the presence of Top3-Rmi1 and the probe, $Sgs1_{1-652}$ promoted the formation of a slower-migrating band (Fig. 13B, lane 10 – 13). The migration of this band is consistent with a quaternary complex of Top3-Rmi1-$Sgs1_{1-652}$-ssDNA. To confirm that the $Sgs1_{1-652}$ protein was present in the complex we incubated the mixture with antibodies against the Sgs1 N-terminal 18 amino acids. As shown in Fig. 13B (lanes 14 – 17), this antibody supershifted the complex into the wells. Taken together, we conclude that Top3-Rmi1 functions as a complex to bind ssDNA and Sgs1.

Figure 13. Top3 and Rmi1 cooperate to bind the N-terminus of Sgs1 and promote its interaction with ssDNA

(A) Constant amounts of Top3 (220 ng) and GST-$Sgs1_{1-158}$ (300 ng) were incubated on ice together with increasing amounts of Rmi1 (0, 3.1, 6.3, 12.5, 25, 50, or 100 ng; lanes 3 - 9). Alternatively, constant amounts of Rmi1 (125 ng) and GST-$Sgs1_{1-158}$ (300 ng) were incubated with increasing amounts of Top3 (0, 6.8, 13.8, 27.5, 55, 110, or 220 ng; lanes 10 - 16). Glutathione beads were added to the mixture and bound proteins were detected by immunoblot. Top3 and Rmi1 markers are shown in lanes 1 and 2. Control reactions (lanes 17 – 19) were performed as above by incubating GST together with the indicated proteins in ng. (B) Constant amounts of Top3 (lanes 2 – 9) or Top3-Rmi1 (lanes 10 – 17) were incubated with increasing concentrations of $Sgs1_{1-652}$ (10, 40, or 160 nM) on ice. After 15 min, a ^{32}P-labeled oligonucleotide (50 nt) was added to a final concentration of 0.25 nM and the incubation was continued at room temperature for 15 min. Where indicated, an antibody to the Sgs1 N-terminus was added and the incubation continued for 30 min. The probe was also left untreated (ssDNA; lane 1) or incubated with $Sgs1_{1-652}$ (lane 18) or $Sgs1_{1-652}$ followed by anti-Sgs1 antibody (lane 19). Following the incubation the samples were subjected to standard EMSA analysis.

A

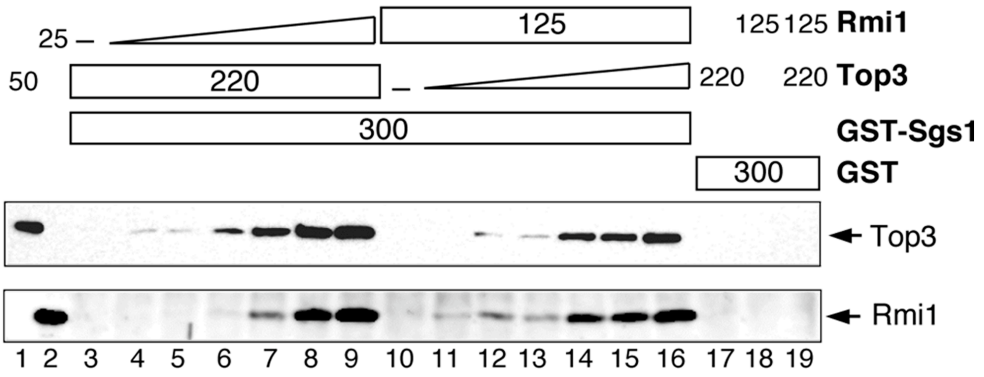
25
125
125 125 Rmi1
50
220
220 220 Top3
300
GST-Sgs1
300
GST
Top3
Rmi1
1 2 3 4 5 6 7 8 9 10 11 12 13 14 15 16 17 18 19

B

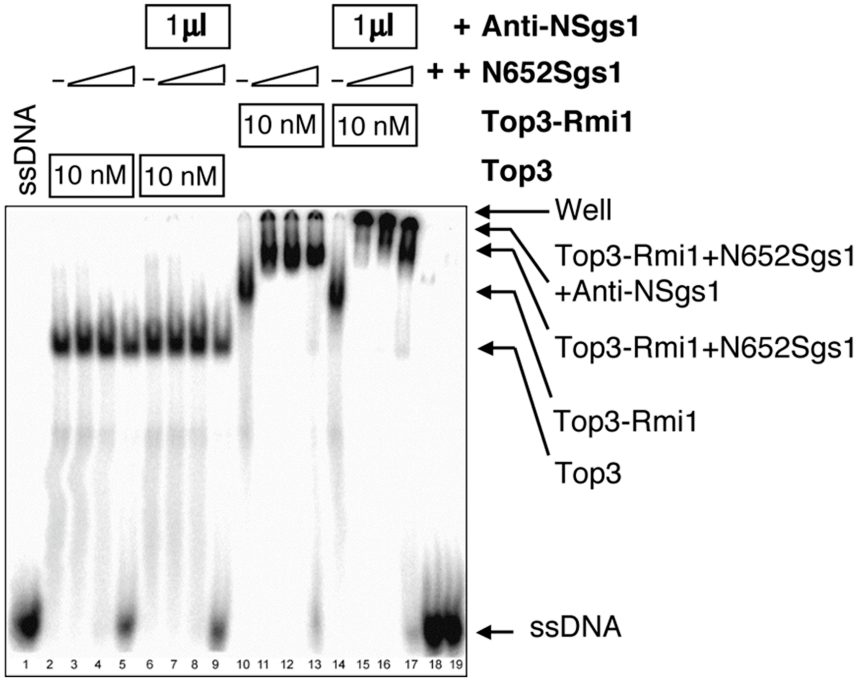
1µl
1µl
+ Anti-NSgs1
+ + N652Sgs1
10 nM
10 nM
Top3-Rmi1
ssDNA
10 nM
10 nM
Top3
Well
Top3-Rmi1+N652Sgs1
+Anti-NSgs1
Top3-Rmi1+N652Sgs1
Top3-Rmi1
Top3
ssDNA
1 2 3 4 5 6 7 8 9 10 11 12 13 14 15 16 17 18 19

Discussion

In this study we report that Rmi1 interacts stably with DNA topoisomerase III and that the Top3-Rmi1 complex displays enhanced superhelical relaxation activity compared to Top3 alone. The Top3-Rmi1 complex is stable to low concentrations of SDS (Mullen, Nallaseth et al. 2005) and displays improved solubility compared to its individual subunits (CFC and SJB, unpublished results). In addition to its enhanced relaxation activity, the complex binds a variety of DNA structures without aggregation and displays unique functional interactions with the Sgs1 N-terminus. Previously, it has been difficult to interpret EMSA results obtained with the individual subunits since much of the signal is retained in the well of the gel (Fig. 12) (Mullen, Nallaseth et al. 2005). Thus, it appears that the Top3-Rmi1 complex is an improved reagent to identify biologically relevant substrates for Top3 activity.

So, which of these substrates is bound preferentially? Our data on Top3-Rmi1 do not support preferential binding to either dsDNA or a single HJ. First, although Top3-Rmi1 binds HJDNA with twice the affinity of dsDNA, this can be explained by the fact that our HJ probe contains twice the amount of DNA as the dsDNA probe (i.e., approximately two 50-mer duplexes). Second, competition experiments confirmed that Top3-Rmi1 preferred ssDNA over dsDNA. Third, the preference for ssDNA is apparent from its 10-fold lower K_d. It will be interesting to test whether the Sgs1-Top3-Rmi1 complex retains this specificity given that its DNA helicase domain has been shown to bind a variety of branched DNAs including HJs (Bennett, Keck et al. 1999). Since there are multiple enzymatic activities in the Sgs1-Top3-Rmi1 complex, we would not be surprised to find that the full complex recognizes a variety of DNA structures. Future

studies should be able to address this question by measuring the interaction of Top3-Rmi1 or Sgs1-Top3-Rmi1 with more complex substrates including those with multiple HJs (Wu and Hickson 2003; Plank and Hsieh 2006).

Amino acid sequence analysis predicts that human Rmi1 contains a single OB-fold (Yin, Sobeck et al. 2005). OB-folds are found in numerous proteins that interact with ssDNA or RNA (Theobald, Mitton-Fry et al. 2003). This includes a number of well-characterized DNA replication proteins such as the ssDNA binding protein Replication Protein A (RPA), BRCA2 and POT1 (Yang, Jeffrey et al. 2002; Lei, Podell et al. 2003; Bochkarev and Bochkareva 2004). Although little evidence for an OB-fold can be extracted from yeast Rmi1 sequences, OB-folds are known to tolerate considerable sequence variation (Agrawal and Kishan 2003). In addition, we think it is revealing that the region of human Rmi1 with greatest amino acid sequence similarity to its homologs overlaps significantly with the predicted OB-fold (Chang, Bellaoui et al. 2005; Mullen, Nallaseth et al. 2005; Yin, Sobeck et al. 2005). Thus, the ability of Rmi1 to stimulate ssDNA binding by Top3 may be due to the presence of an OB-fold. Structural studies of Rmi1 will be necessary to make this conclusion definitively, but other results are consistent with this idea. In the case of RPA, a pair of OB-folds (the A-B dimer) bound stably to 8 nt of ssDNA (Bochkarev, Pfuetzner et al. 1997). In contrast, the interaction between a solitary OB-fold and ssDNA (A or B) was not stable to EMSA analysis and required UV crosslinking to fix the interaction (Philipova, Mullen et al. 1996). Interestingly, we observed weak ssDNA binding by the isolated Rmi1 subunit that could be stabilized by UV crosslinking (Mullen, Nallaseth et al. 2005). Taking RPA as a

model, we suggest that Rmi1's ssDNA binding activity is enhanced in the Top3-Rmi1 complex where it synergizes with that of Top3.

Like DNA topoisomerase III from *E. coli*, the eukaryotic enzyme is limited in its ability to relax superhelical stress at low temperature (Srivenugopal, Lockshon et al. 1984; DiGate and Marians 1988; Kim and Wang 1992). The requirement for elevated temperatures has been taken as evidence of a requirement for ssDNA access by Top3, and a number of elegant studies have proved this idea by demonstrating that DNA topoisomerase III is capable of decatenating circular DNA and relaxing negative or positive supercoils if the protein is given access to ssDNA (DiGate and Marians 1988; Kim and Wang 1992; Wilson, Chen et al. 2000; Plank, Chu et al. 2005). In vitro, this access can be provided by altering the secondary structure of the substrate using hyper-negative supercoiling or by engineering non-homologous bubbles or hairpins into the DNA. In the case of decatenation, which does not require elevated temperatures, Top3 can be stimulated by RecQ DNA helicases (Harmon, DiGate et al. 1999; Wu and Hickson 2003; Plank, Wu et al. 2006). In turn, RPA has been shown to stimulate this reaction (Plank, Wu et al. 2006). Taken together, these findings suggest that Rmi1 may have evolved to assist eukaryotic Top3 in binding ssDNA present in its substrates. Future experiments might address this idea by identifying mutants of Rmi1 that lack ssDNA binding activity. Interestingly, Rmi1 stimulated Top3's relaxation activity but only slightly reduced the temperature needed for this reaction. Indeed, we were surprised to find that a ssDNA bubble was necessary for relaxation at 30°C. This may reflect the fact that relaxation of superhelical stress is not a biological activity of Top3. In decatenation

reactions, such as the dissolution assay, Rmi1 has been shown to stimulate at 37°C (Raynard, Bussen et al. 2006; Wu, Bachrati et al. 2006).

An alternative model for Rmi1 function is that regulates Top3's access to ssDNA. It has previously been shown that the N-terminal domain of Sgs1 inhibits the ssDNA binding activity of Top3 (Bennett, Noirot-Gros et al. 2000). In contrast to this result, we have shown that the Top3-Rmi1 complex binds ssDNA stably in the presence of the Sgs1 N-terminus. In fact, the N-terminal domain of Sgs1 forms a quaternary complex with the Top3-Rmi1-ssDNA assembly. The ability of Rmi1 to simultaneously stimulate binding to ssDNA and Sgs1 places it in a position to regulate Top3's interaction with the helicase or the DNA substrate. At present it is unclear how Rmi1 mediates these two interactions. It will be interesting to identify the domains of Rmi1 required for these interactions and test whether they are regulated by proteins involved in homologous recombination or if they are modified in response to DNA damage.

Experimental Methods

Yeast strains, plasmids, and antibodies

Yeast strains were constructed and maintained following standard procedures (Rose, Winston et al. 1990). Strain JEL1 (*MAT***a** *leu2 trp1 ura3-52 prb1-1122 pep4-3 Δhis::PGAL10-GAL4::ura3*) (Lindsley 1999) was used as the host for expressing galactose-induced proteins. Derivative NJY2063 expresses a previously-described C-terminal V5-His6-tagged Top3 (Top3-V5) (Fricke, Kaliraman et al. 2001) under the control of the *GAL1-10* promoter on each of two plasmids, pNJ2585 and pNJ2588. Derivative NJY2062 contains plasmids pNJ2585 and pNJ2586, and was used for the purification of Top3-Rmi1 complex. Plasmid pNJ2586 expresses Top3-V5 and wild type Rmi1 under the control of the *GAL1-10* promoter. A rabbit anti-serum was raised against recombinant yeast His6-Rmi1 (Covance). Antibodies against the following epitopes were obtained commercially: V5 (Invitrogen), Sgs1 N-terminus (Santa Cruz Biotechnology), and HA (Roche).

Expression and purification of recombinant proteins

Top3-Rmi1 was expressed in yeast strain NJY2062 by growing it at 30°C in 100 ml of synthetic complete medium lacking leucine and uracil and supplemented with 2% (w/v) glucose. After reaching saturation, the culture was diluted 20-fold into the same medium and grown until OD_{600}= 1.25. Cells from 2 L of culture were collected by centrifugation, washed with sterile distilled water, and resuspended in 4 L synthetic complete medium lacking leucine and uracil and containing 2% galactose and 2% sucrose. At OD_{600} = 1.5 the cells were harvested by centrifugation, washed as above, and

resuspended in an equal volume of 2X buffer N (1X = 25 mM Tris·HCl, pH 7.5, 0.1 mM phenylmethylsulfonyl fluoride [PMSF], 0.01% NP-40, 1 mM dithiothreitol [DTT], 10% glycerol, and 500 mM NaCl) and the following protease inhibitors: pepstatin, 10 μg/ml; leupeptin, 5 μg/ml; benzamidine, 10 mM; and bacitracin, 100 μg/ml. Cells were packed into a syringe and extruded through an 18-gauge needle into liquid nitrogen. The frozen material was then ground in a coffee grinder with dry ice for 3 min. This mixture was placed on ice, allowed to sublime, and diluted with 1 volume of cold 2X buffer N plus protease inhibitors. The insoluble material was pelleted by centrifugation at 13,000 RPM in an SS34 rotor for 20 min at 4°C, and the soluble portion was taken as extract. The extract was filtered through a 0.45 μm syringe filter (Nalgene) and made 10 mM in imidazole before loading onto a 5 ml Ni His-Trap column attached to an AKTA FPLC (GE Healthcare). The column was washed with 10 column-volumes (CVs) of Buffer N plus 10 mM imidazole and eluted with a six CV gradient from 10 to 500 mM imidazole in Buffer N. The Top3-Rmi1 complex eluted at 170 mM imidazole based on SDS-PAGE and Coomassie blue staining. The peak fractions were pooled and dialyzed against buffer B (25 mM HEPES [pH 6.9], 1 mM EDTA, 0.01% NP-40, 10% glycerol, 0.1 mM PMSF, 1 mM DTT) containing 50 mM NaCl. The dialyzed pool was loaded onto a 1 ml MonoS column, washed with Buffer B plus 50 mM NaCl and resolved into 0.3 ml fractions across a 6 CV gradient from 50 to 1000 mM NaCl. Peak fractions eluted at 375 mM NaCl.

Top3 was expressed in yeast strain NJY2063 and purified by Ni-column chromatography as described above, except that Top3 eluted from the Ni-column at 200 mM imidazole. Following dialysis, the sample was fractionated by Mono S column

chromatography as described above. Peak fractions (425 mM NaCl) were identified by SDS-PAGE and Coomassie blue staining. Recombinant His6-Rmi1-HA protein was expressed in *E. coli* BL21(DE3)-RIL cells (Stratagene) and purified as described (Mullen, Nallaseth et al. 2005).

The N-terminal 652 amino acids of Sgs1 was expressed as a $(His)_6$-$Sgs1_{1-652}$-V5 fusion protein from plasmid pKR6318 , which was transformed into *E. coli* BL21(DE3)-RIL cells. Freshly transformed colonies were pooled and grown in 1L LB media containing 0.1 mg/ml ampicillin at 37°C until OD_{600} = 0.4. The recombinant protein was induced by addition of 0.4 mM isopropyl-1-thio-D-galactopyranoside and the cells were grown at 16°C for 16 hours. Induced cells were pelleted and resuspended in 40 ml Buffer N containing 10 mM imidazole and protease inhibitors as above. The cells were sonicated for 2 min with a Branson sonifer 450 microtip at setting 2 and 25% duty cycle. The lysate was centrifuged at 13,500 rpm in an SS34 rotor at 4°C for 15 min and the supernatant was filtered before loading onto a 5 ml Ni column. The column was washed with 10 CVs of Buffer N plus 10 mM imidazole and eluted with a 6 CV gradient from 10 to 500 mM imidazole in Buffer N. Peak fractions were pooled and dialyzed against buffer B plus 50 mM NaCl. The dialyzed pool was loaded onto a 1 ml HiTrap SP column (Amersham Bioscience) and washed with 10 CVs Buffer B plus 50 mM NaCl and then eluted into 0.3 CV fractions across an 8 CV gradient from 50 to 1000 mM NaCl and 2 additional CVs of 1000 mM NaCl in Buffer B. Peak fractions were pooled and dialyzed against Buffer A (25 mM Tris-HCl [pH 7.5], 1 mM EDTA, 0.01% NP-40, 10% glycerol, 0.1 mM PMSF, and 1 mM DTT) containing 50 mM NaCl. The dialyzed pool was loaded onto a HiTrap Q HP 1 ml column (GE Healthcare), washed with 10 CVs Buffer A plus

50 mM NaCl and eluted with an 8 CV gradient from 50 to 1000 mM NaCl in Buffer A. Peak fractions were pooled based on SDS-PAGE and Coomassie blue staining.

Superose 6 HR10/30 chromatography was performed on an AKTA FPLC system in the presence of Buffer A containing 150 mM NaCl but lacking glycerol. Approximately 40 µg protein was fractionated at a flow rate of 0.4 ml/min. Thirty µg of Top3-Rmi1 complex was subjected to 15–35% glycerol gradient sedimentation by centrifugation for 24 h at 45,000 RPM in a Beckman SW55 Ti rotor. 0.2 ml fractions were collected from the top. Fractions from both treatments were analyzed by SDS-PAGE and Coomassie blue staining.

GST pulldown assay

For GST-pulldown experiments, a GST-fusion to the N-terminal 158 amino acids of Sgs1 (Fricke, Kaliraman et al. 2001) was incubated with various amounts of Rmi1-HA and Top3-V5 in 30 µl of Buffer A containing 150 mM NaCl at 4°C for 30 min. Protein solutions were mixed by rotation with 10 µl glutathione-Sepharose beads (GE Healthcare) for 30 min at 4°C. Beads were washed twice with 150 µl of Buffer A containing 150 mM NaCl. Bound proteins were eluted by SDS-PAGE loading buffer, resolved by 17% SDS-PAGE, and visualized via western blotting as described (Mullen, Nallaseth et al. 2005).

Preparation of DNA substrates - The pKS bubble substrate was prepared by annealing and linking the plus- and minus-strands of pBlueScript KS using ADP and *Archaeoglobus fulgidus* reverse gyrase (Plank, Wu et al. 2006), a kind gift of Dr. Tao Hsieh. Negatively supercoiled bubble DNA was prepared by incubating circular bubble

DNA (50 ng/µl) with yeast DNA topoisomerase I (5 ng/µl) and ethidium bromide (EtBr; 1.5 µg/ml) in DNA topoisomerase I relaxation assay buffer : 35 mM Tris-HCl [pH 8.0], 72 mM KCl, 5 mM $MgCl_2$, 5 mM DTT, 5 mM spermidine, and 0.01% bovine serum albumin. The reaction was incubated at 37°C for 1 hr and stopped by treatment with 0.5% SDS and 0.05 mg/ml proteinase K at 37°C for 20 min. DNA was extracted by phenol/chloroform, precipitated, and redissolved in TE buffer.

Relaxation of negatively supercoiled DNA

The standard DNA topoisomerase III reaction contained 40 mM HEPES (pH 7.0), 40% glycerol, 5 mM sodium acetate, and 10 µg/ml bovine serum albumin in a final volume of 20 µl. The reactions were assembled on ice, initiated by shifting to 30°C for 20 min, and stopped by treatment with SDS and proteinase K as above. Loading dye was added and the samples were resolved on a 0.8% agarose gel by overnight electrophoresis at 1.5 V/cm in 1X TBE buffer at room temperature. The gel was stained with 0.5 µg/ml EtBr and visualized with UV light.

Relaxation of supercoiled bubble DNA – Standard assays were performed as above, stopped by the addition of EDTA to 25 mM and incubation at room temperature for 2 min. SDS was then added to 0.5% for a 2 min incubation, followed by the addition of proteinase K to 0.05 mg/ml and incubation at 37°C for 15 min. The samples were analyzed by electrophoresis through 0.8% agarose containing _ X TBE buffer. For positively supercoiled bubble DNA, EtBr was first added to 1.5 µg/ml.

Electrophoretic mobility shift assay (EMSA)

^{32}P-labeled DNA substrates were prepared and assayed in a 20 µl reaction volume as previously described (Mullen, Nallaseth et al. 2005). The sequences of the oligonucleotide substrates were taken from (Whitby and Dixon 1998) as follows: ssDNA, oligo 1253 (5'-TGGGTCAACGTGGGCAAAGATGTCCTA GCAATGTAATCGTCTATGACGTT-3'); linear dsDNA, oligos 1253 and 2148 (5'-AACGTCATAGACGATTACATTGCTAGG ACATCTTTGCCCACGTTGACCCA-3'); or branch-migratable Holliday junction, oligos 1253, 1254 (5'-TGCCGAATTCTACCA GTGCCAGTGATGGACATCTTTGCCCACGTTGACCC-3'), 1255 (5'-GTCGGATCCTCTAGACAGCTCCATGATCACTGGCACTGGTAGAATTCGGC-3'), and 1256 (5'-CAACGTCATAGACGATTACATTGCTACATGGAGCTGTCTAGAGGATCCGA-3'). Also used was oligo 1313 (5'-TGGCGTTAGGAGATACCGATAAGCTTCGGC-3').

Chapter III

An Essential DNA strand exchange activity is conserved in the divergent N-termini of BLM orthologs

Summary

The gene mutated in Bloom's syndrome, *BLM*, encodes a member of the RecQ family of DNA helicases that is needed to suppress genome instability and cancer predisposition. BLM is highly conserved and all BLM orthologs, including budding yeast Sgs1, have a large N-terminus that binds Top3-Rmi1 but has no known catalytic activity. Here we describe a sub-domain of the Sgs1 N-terminus that displays *in vitro* single-strand DNA (ssDNA) binding, ssDNA annealing and strand exchange (SE) activities. These activities are conserved in the human and *Drosophila* orthologs. Strand exchange between duplex DNA and homologous ssDNA requires no cofactors and is inhibited by a single mismatched base-pair. The SE domain of Sgs1 is required *in vivo* for the suppression of hyper-recombination, suppression of synthetic-lethality and heteroduplex rejection. The *top3*Δ slow-growth phenotype is also SE-dependent. Surprisingly, the highly divergent human SE domain functions in yeast. This work identifies SE as a new molecular function of BLM/Sgs1, and we propose that at least one role of SE is to mediate the strand-passage events catalyzed by Top3-Rmi1.

Introduction

The RecQ family of DNA helicases comprises five eukaryotic members that participate in homologous recombination (HR) to repair double-stranded DNA breaks (DSBs) and stalled replication forks. Defects in all five helicases are associated with genome instability, and defects in three (BLM, WRN, and RecQ4) are known to cause cancer predisposition syndromes in humans (Wang, Seki et al. 2003; Hu, Lu et al. 2005; Chu and Hickson 2009). Structurally, these enzmes are well characterized. All members contain a highly-conserved DNA helicase domain (Fig. 14a), and most contain an RQC domain that participates in DNA binding and protein-protein interactions (Bernstein, Zittel et al. 2003; Bennett and Keck 2004) (Fig. 14a). Some RecQ members also contain a C-terminal HRDC domain that assists in DNA binding (Bernstein and Keck 2005) and is required for *in vitro* activity (Wu, Chan et al. 2005). These helicases efficiently unwind a variety of model recombination intermediates such as Holliday Junctions (HJs), D-loops, replication forks, and G-quadruplex DNA (Sun, Karow et al. 1998; LeRoy, Carroll et al. 2005; Bachrati, Borts et al. 2006; Ralf, Hickson et al. 2006; Capp, Wu et al. 2009). However, a clear understanding of how these enzymes suppress inappropriate recombination *in vivo* is lacking.

The only RecQ DNA helicase conserved in lower eukaryotes is the ortholog of the gene defective in Bloom's Syndrome (BS) *BLM*. BS is a rare autosomal disease associated with elevated levels of sister chromatid exchange (SCE) and susceptibility to a wide variety of cancers (Chaganti, Schonberg et al. 1974; German, Sanz et al. 2007). Like human BLM, budding yeast Sgs1 forms a tight complex with two other subunits, Top3 and Rmi1 (Chaganti, Schonberg et al. 1974; Gangloff, McDonald et al. 1994;

Bennett, Noirot-Gros et al. 2000; Wu, Davies et al. 2000; Fricke, Kaliraman et al. 2001; Ui, Satoh et al. 2001; Mullen, Nallaseth et al. 2005; German, Sanz et al. 2007). The hyper-recombinational phenotypes of BS cells and yeast *sgs1*Δ mutants (Gangloff, McDonald et al. 1994) indicates that the BLM-TOP3-RMI1 complex functions as an anti-recombinase that may be related to its ability to dissolve double HJs and/or unwind D-loops *in vitro* (Wu and Hickson 2003; Bachrati, Borts et al. 2006). However, the complex is known to be multi-functional. It interacts with the Rad51 strand-exchange protein (Wu, Davies et al. 2001; Bugreev, Mazina et al. 2009), it is required for recombination in model systems such as *S. pombe* and *Drosophila* (Adams, McVey et al. 2003; Cromie, Hyppa et al. 2008), and it promotes 5'-end resection (Mimitou and Symington 2008; Nimonkar, Ozsoy et al. 2008; Zhu, Chung et al. 2008). Further, BLM promotes ssDNA annealing (SA) *in vitro*. Considerable evidence indicates that this SA activity is intrinsic to the RecQ helicase domain: annealase activity has been identified in all five RecQ members, including the two smallest (RecQ1 and RecQ5), and although it is ATP-independent, it is typically inhibited by non-hydrolyzable ATP analogs (Garcia, Liu et al. 2004; Cheok, Bachrati et al. 2005; Machwe, Xiao et al. 2005; Mullen, Nallaseth et al. 2005; Macris, Krejci et al. 2006; Muftuoglu, Kulikowicz et al. 2008; Xu and Liu 2009). For RecQ5 and WRN, SA activity has been localized to RecQ C-terminal domains (Garcia, Liu et al. 2004; Muftuoglu, Kulikowicz et al. 2008). Similarly, the N-terminal extension of BLM is dispensible for a SA activity that maps to residues 642-1350 (Cheok, Wu et al. 2005). Lastly, BLM displays DNA strand-exchange (SE) activities that are both ATP-dependent (Machwe, Xiao et al. 2005; Weinert and Rio 2007) and ATP-independent (Machwe, Xiao et al. 2005; Bugreev, Mazina et al. 2009). For reasons

that are unclear, the ATP-independent SE activities are sensitive to non-hydrolyzable ATP analogs and certain DNA helicase mutations (Machwe, Xiao et al. 2005; Bugreev, Mazina et al. 2009).

Apart from the DNA helicase domain, BLM/Sgs1orthologs contain a poorly characterized N-terminal domain of about 650 amino acids (aa) (Fig. 15a). Functional analysis of the N-terminus has been hindered in part by the lack of sequence conservation between orthologs (Fig. 14b). In yeast, this domain ($Sgs1_{1\text{-}652}$) is known to be physiologically important (Mullen, Kaliraman et al. 2000; Rockmill, Fung et al. 2003; Bernstein, Shor et al. 2009) although it's only known role is to bind Top3 and Rmi1 through its N-terminal 100 aa. In searching for a biochemical function of $Sgs1_{1\text{-}652}$ we identified a sub-domain that displays ssDNA binding and SA activity. Despite the lack of sequence conservation, this domain is functionally conserved in multiple BLM orthologs and it displays a SE activity that is inactive on homologous templates containing a single mismatch. To determine the physiological role of this activity we characterized an *SGS1* allele lacking the SE domain. This *sgs1-*Δ*SE* allele displayed a null phenotype in most *in vivo* assays including suppression of hyper-recombination. These data indicate that DNA strand exchange is an essential conserved function of BLM/Sgs1 orthologs, and we speculate that its *in vivo* role is to promote DNA strand exchange in conjunction with Top3-Rmi1 at double HJs and D-loops.

FIGURE 14.

Clustal W alignment of BLM orthologs was performed using default parameters (http://www.ebi.ac.uk/Tools/clustalw2/index.html). Note that highlighting identifies similar residues. Sequence names include the aa residues used in the alignment: *Hs, human; Dr, Danio rerio; Ol, Oryzias latipes; Xl, Xenopus laevis, Gg, Gallus gallus; Dm, Drosophila melanogaster; Kl, Kluvermyces lactis; Sc, Saccharomyces cerevisiae.* (**a**)RecQ domains. (**b**) N-terminal domains. The BDHCT region is underlined.

A

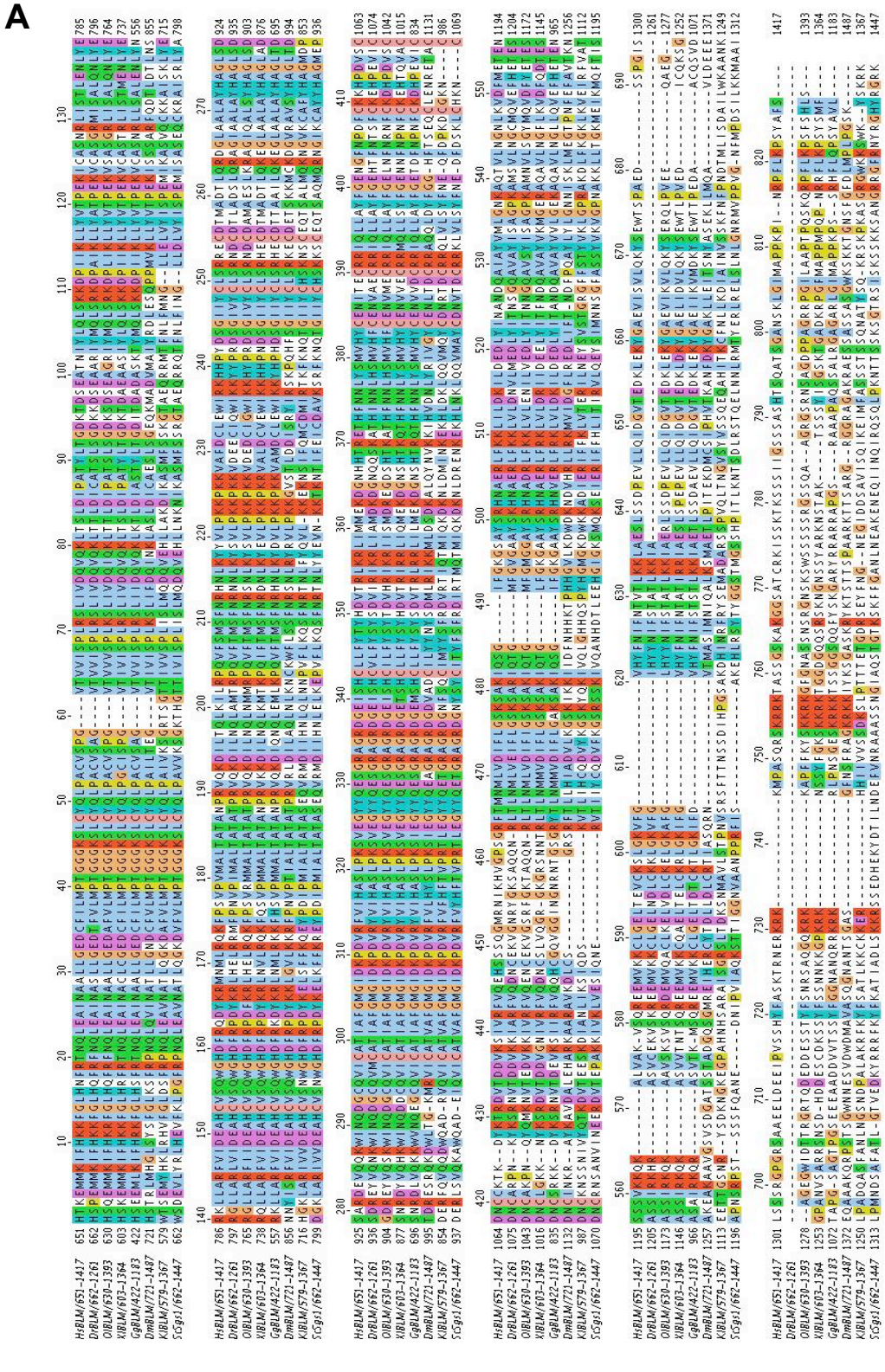

B

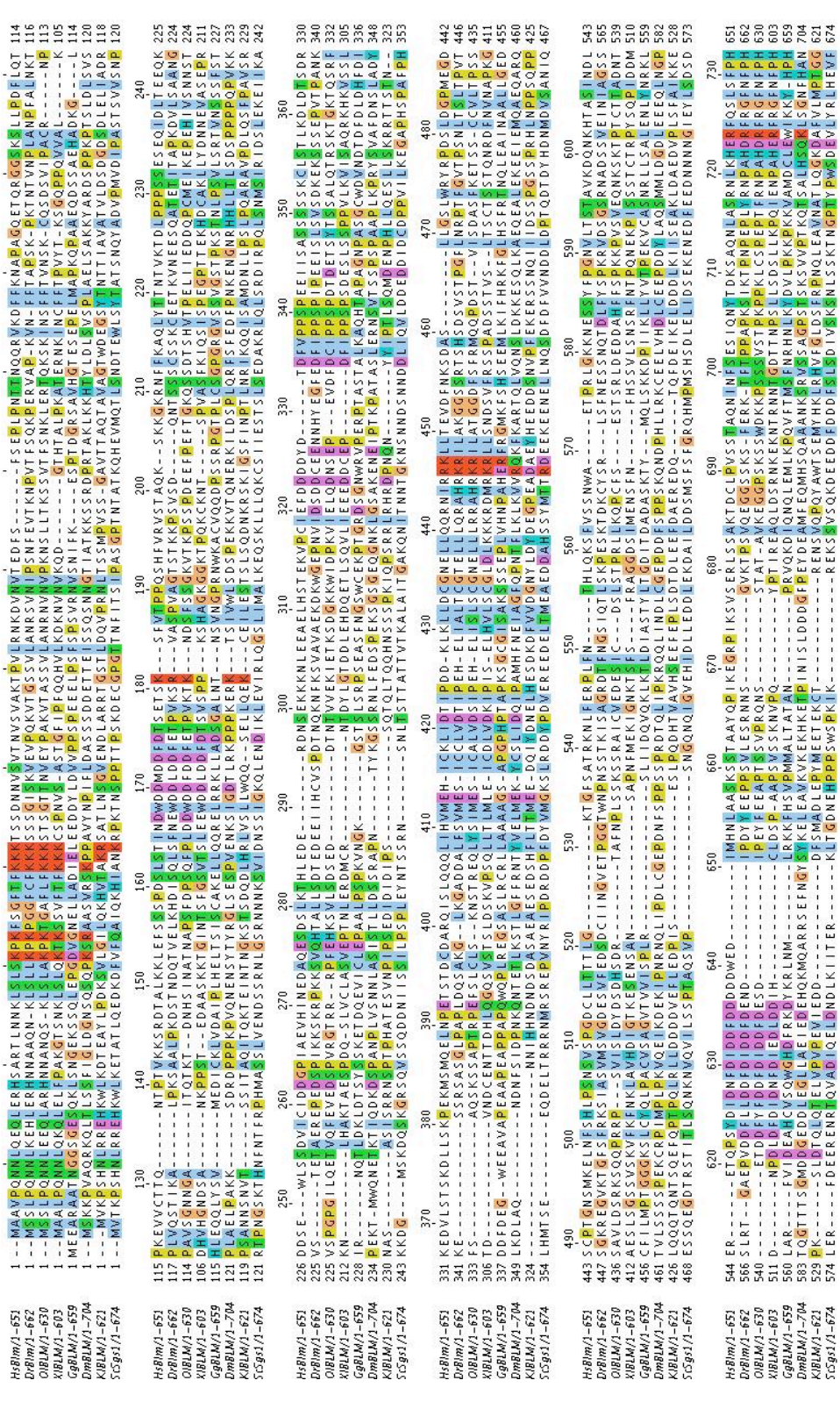

Results

Identification of a novel ssDNA binding activity in BLM orthologs

Structure-function analysis of Sgs1 previously showed that deletion of the Top3-Rmi1 binding domain (TR; Fig. 15a) creates a hypermorphic phenotype in yeast (Mullen, Kaliraman et al. 2000; Bennett and Wang 2001; Weinstein and Rothstein 2008). That is, removal of the first 80-150 aa results in slow-growth and hyper-recombinational phenotypes that are more extreme than the *sgs1*Δ null. These hypermorphic phenotypes are suppressed by either a point mutation that eliminates Sgs1 DNA helicase activity, or by deleting more of the N-terminus to aa 323 (Mullen, Kaliraman et al. 2000; Weinstein and Rothstein 2008). The simplest interpretation of this result is that the first 323 aa of Sgs1 contain a helicase-dependent activity that is toxic when untethered to Top3-Rmi1. Because prior studies had failed to identify deoxyoligonucleotide (oligo) binding activity in the N-terminus of Sgs1 or BLM (Cheok, Bachrati et al. 2005; Chen and Brill 2007), we assayed it for structure-specific DNA binding activity. To this end, we incubated $Sgs1_{1\text{-}652}$ protein with two large radiolabled probes consisting of either primed øX174 ssDNA or a plasmid-based D-loop. Analysis by electrophoretic mobility shift assay (EMSA) indicated that the migration of both probes was retarded by $Sgs1_{1\text{-}652}$ (Fig. 15b). Surprisingly, further characterization showed that the binding of $Sgs1_{1\text{-}652}$ to primed øX174 ssDNA was sensitive to unprimed plasmid-length ssDNA competitor (Fig. 15c). This suggested that $Sgs1_{1\text{-}652}$ does bind ssDNA and that it might bind oligonucleotide substrates if they were unusually long. To test this idea, we incubated $Sgs1_{1\text{-}652}$ with oligonucleotides of 60, 90, or 174 nt. As predicted, Sgs1 efficiently bound d(T)174, but bound the 90- and 60-mer oligos progressively less well (Fig. 15d). We note that $Sgs1_{1\text{-}}$

$_{652}$ binds d(T)174 with high affinity because it could be detected at nM concentrations of both protein and substrate. Because the D-loop is unlikely to contain significant ssDNA character, its binding by Sgs1$_{1\text{-}652}$ may involve different structural determinants.

To further localize this activity, we expressed and purified sub-domains of Sgs1$_{1\text{-}652}$ as GST-fusion proteins and assayed them for ssDNA binding (Fig. 16a). Based on these assays we determined that the C-terminal half of Sgs1$_{1\text{-}652}$ was dispensible for binding, and that Sgs1$_{103\text{-}322}$ was the minimal region required for activity (Fig. 16b). To confirm this result, and show that ssDNA binding could be detected by methods other than EMSA, we performed nitrocellulose filter-binding assays with His6-tagged proteins. These assays confirmed that ssDNA binding activity could be detected in both Sgs1$_{1\text{-}322}$ and Sgs1$_{103\text{-}322}$ (Fig. 16c).

To determine whether these results generalized to other BLM orthologs, we assayed comparable regions of human and *Drosophila* BLM for ssDNA binding. Pairwise amino acid sequence alignments were of limited usefulness in identifying homologous regions in these orthologs. However, vertebrate BLM orthologs contain a conserved 40 aa region of unknown function, BDHCT, (InterPro: IPR012532; hsBLM$_{372\text{-}411}$) that showed weak similarity to the fly and yeast orthologs in multiple sequence alignments (Fig. 14b). Using this alignment we chose to express hsBLM$_{1\text{-}294}$ and dmBLM$_{1\text{-}380}$ as approximations of Sgs1$_{1\text{-}322}$ and Sgs1$_{1\text{-}386}$, respectively (Fig. 16d). These domains were then purified as GST-fusion proteins for use in an EMSA assay. As shown in Figure 17e, titrations of both metazoan proteins resulted in a mobility shift of the d(T)174 probe. When the reaction products were incubated with an antibody to GST prior to electrophoresis, the resulting signals were further retarded indicating that the

GST-Sgs1 and GST-hsBLM fusion proteins are responsible for this activity (Fig. 16f). The GST portions of the proteins did not contribute to this activity as hexahistidine-tagged versions of all three proteins (Figure 17a) bound ssDNA (Fig. 17b).

FIGURE 15. Identification of a ssDNA binding activity in Sgs1$_{1-652}$

(**a**) Schematic representations of the full length 1447 aa Sgs1 protein and Sgs1$_{1-652}$. Domains: TR, Top3-Rmi1 binding; B, C-terminal domain in Bloom's Syndrome DEAD helicases (BDHCT) homology; RQC, RecQ C-terminal homology; HRDC, Human RecQ and RnaseD C-terminal homology. (**b**) EMSA assays contained the indicated concentrations of His6-tagged Sgs1$_{1-652}$ and 1 nM of either primed ssDNA (oligo #16 annealed to øX174 ssDNA) or a plasmid-based D-loop (oligo #17 transferred into pSK+ DNA). Asterisks represent positions of ^{32}P-labelling. The reaction mixtures were incubated for 20 min at room temperature under standard conditions as described in the Methods. After incubation, the products were subjected to electrophoresis in composite 2.5% polyacrylamide/0.8% agarose gels followed by phosphorimager analysis. (**c**) Sgs1$_{1-652}$ (300 nM) was incubated together with 1 nM primed ssDNA and various concentrations of the four unlabeled versions of pSK+ DNA as indicated. Incubation and analysis was performed as in **b**. M is a mock incubation in the absence of Sgs1 protein. (**d**) The indicated concentrations of Sgs1$_{1-652}$ were incubated with one of three ^{32}P-labeled ssDNAs at a concentration of 1 nM: poly(dT)174, a 90 nt oligo of random sequence (oligo #18), or oligo(dT)60. Incubation and analysis was performed as in **b** except for the use of 10% PAGE.

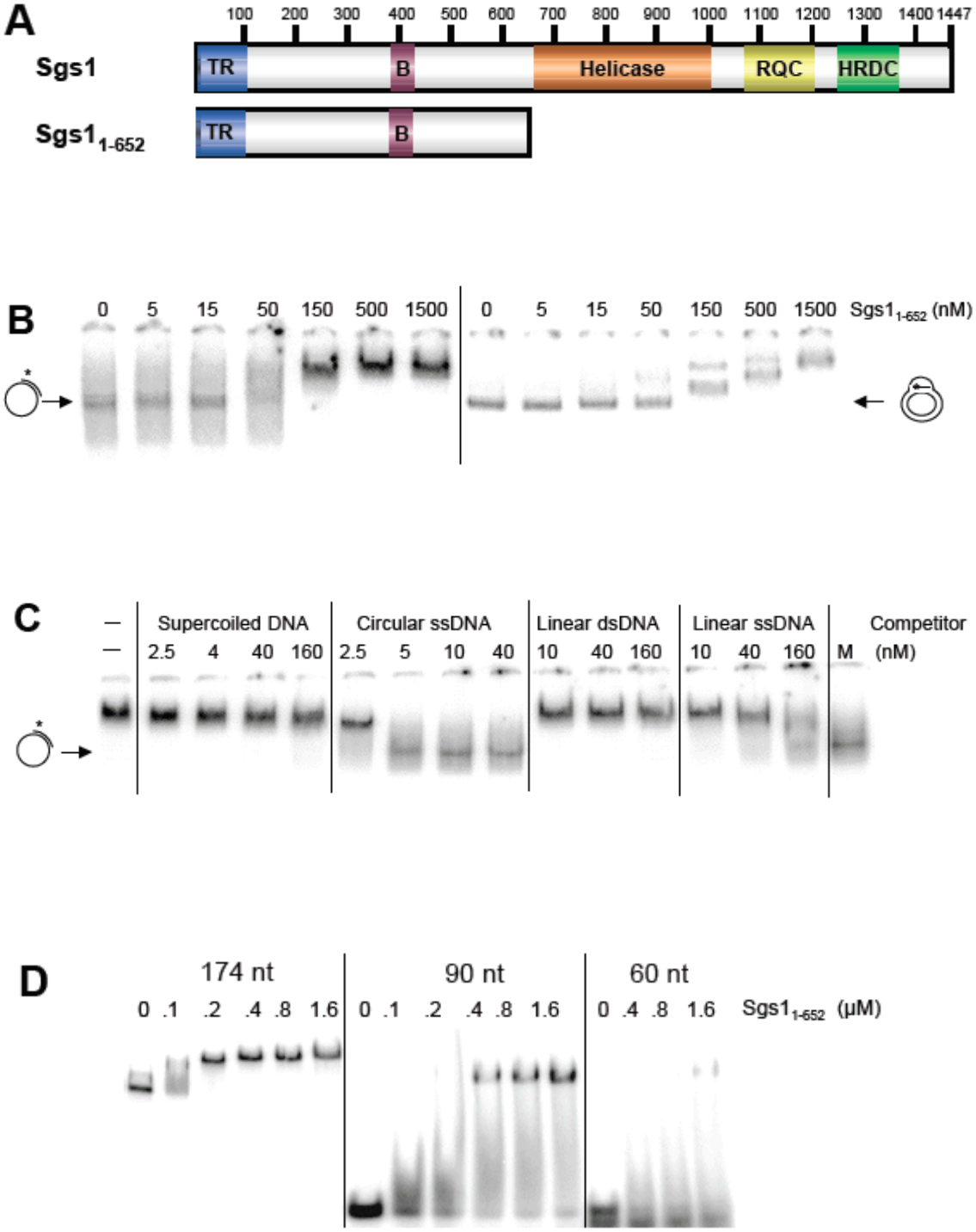
A
100 200 300 400 500 600 700 800 900 1000 1100 1200 1300 1400 1447
Sgs1
TR
B
Helicase
RQC
HRDC
Sgs1 1-652
TR
B
B
0 5 15 50 150 500 1500 0 5 15 50 150 500 1500 Sgs1 1-652 (nM)
C
– Supercoiled DNA Circular ssDNA Linear dsDNA Linear ssDNA Competitor
– 2.5 4 40 160 2.5 5 10 40 10 40 160 10 40 160 M (nM)
D
174 nt
90 nt
60 nt
0 .1 .2 .4 .8 1.6 0 .1 .2 .4 .8 1.6 0 .4 .8 1.6 Sgs1 1-652 (μM)

FIGURE 16. The ssDNA binding activity of Sgs1$_{1-652}$ maps to a sub-domain and is conserved in human and *Drosophila* BLM orthologs

(**a**) The following GST-Sgs1 fusion proteins were subjected to EMSA assay as in Fig. 1d using ^{32}P-labeled poly(dT)174 as probe: Sgs1$_{1-158}$, Sgs1$_{1-322}$, Sgs1$_{1-652}$, and Sgs1$_{322-652}$ at 18, 37, 75, 150 and 300 nM; Sgs1$_{50-322}$, Sgs1$_{103-322}$, and Sgs1$_{158-484}$ at 100, 200, 400 and 800 nM; and Sgs1$_{103-250}$ at 150, 300, 600 and 1200 nM. Dashes (-) indicate no-protein control lanes. (**b**) Summary of ssDNA binding and SA results. Symbols in the ssDNA-binding column represent the following results: +, strong; +/-, weak; and -, no ssDNA-binding activity. Symbols in the SA column represent the following results: +, strong; +/-, weak; and -, no SA activity. (**c**) The indicated His6-tagged proteins were assayed for ssDNA-binding using a nitrocellulose filter binding assay. Reactions were performed as in Fig. 1d, but were analyzed by filtering through alkalai-treated nitrocellulose and quantifying the bound products by scintillation counting. The data are presented as a percentage of input CPM. (**d**) The N-termini of Sgs1, hsBLM and dmBlm are presented schematically with putative domain boundaries indicated by dotted lines. ST, strand transfer domain. (**e**) EMSA assays were performed as above using GST-hsBLM$_{1-294}$ at 0, 100, 200, 400 and 800 nM, and dmBlm$_{1-380}$ at 0, 140, 280, 560 and 840 nM. (**f**) The indicated GST fusion proteins were subjected to EMSA as above, but the reaction products were incubated for 30 min on ice with or without α-GST prior to gel electrophoresis.

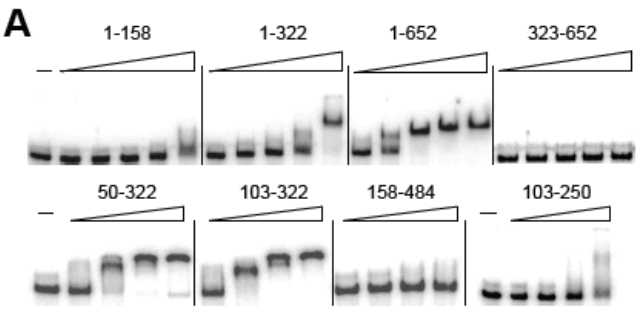
A
1-158
1-322
1-652
323-652
50-322
103-322
158-484
103-250

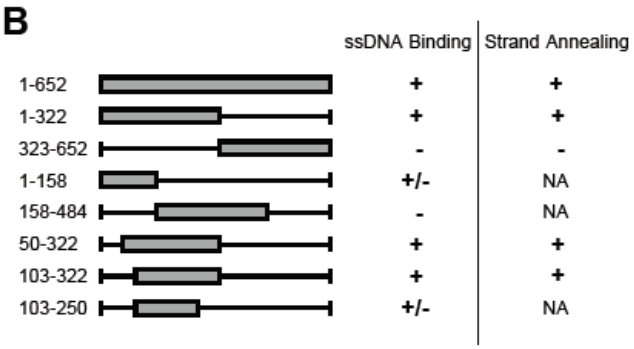
B
ssDNA Binding
Strand Annealing
1-652 + +
1-322 + +
323-652 - -
1-158 +/- NA
158-484 - NA
50-322 + +
103-322 + +
103-250 +/- NA

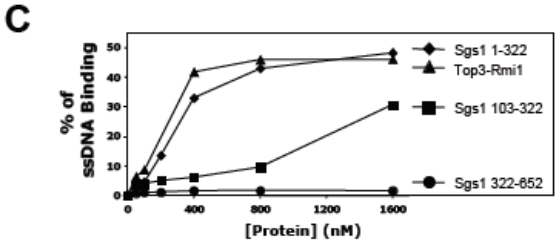
C
% of ssDNA Binding
[Protein] (nM)
Sgs1 1-322
Top3-Rmi1
Sgs1 103-322
Sgs1 322-652

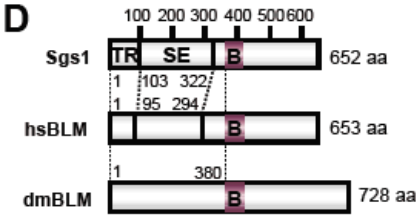
D
100 200 300 400 500 600
Sgs1
TR
SE
B
652 aa
hsBLM
653 aa
dmBLM
728 aa

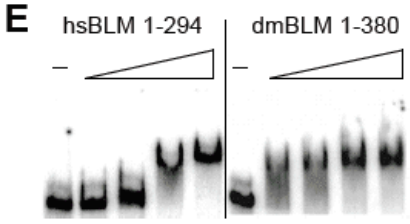
E
hsBLM 1-294
dmBLM 1-380

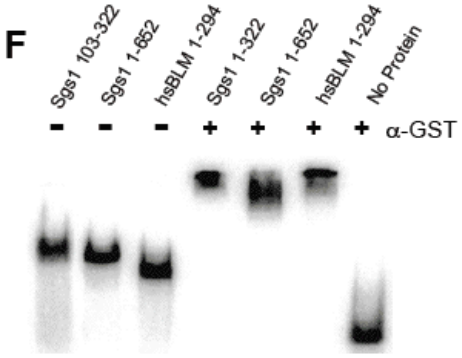
F
Sgs1 103-322
Sgs1 1-652
hsBLM 1-294
Sgs1 1-322
Sgs1 1-652
hsBLM 1-294
No Protein
α-GST

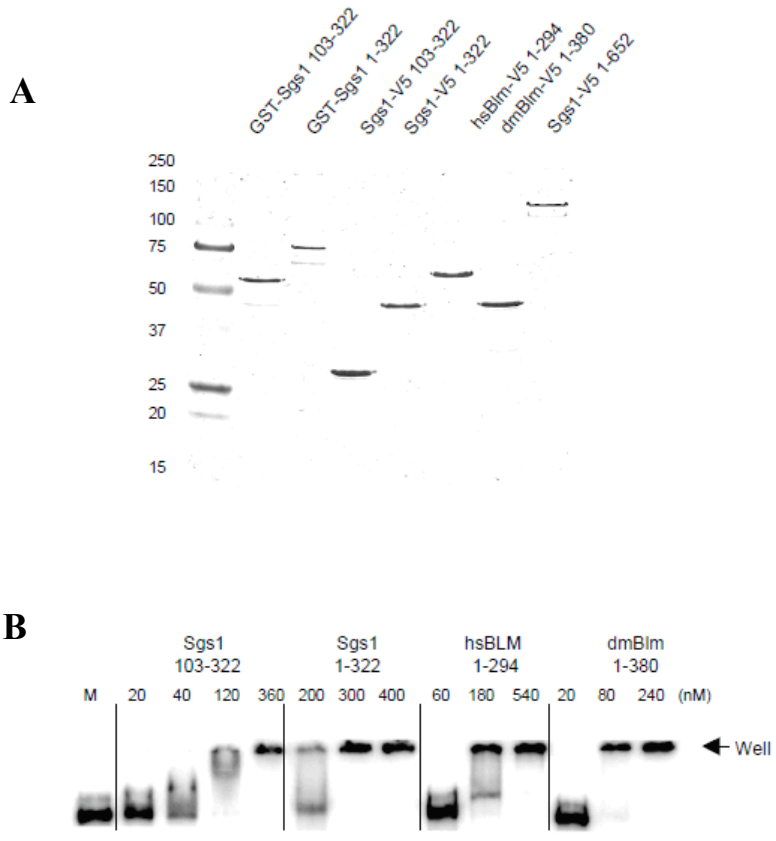

FIGURE 17. Proteins used for this study and ssDNA binding of His-tag recombinant proteins

(a) Proteins were expressed and purified from bacteria with either an N-terminal GST-tag (GST) or a C-terminal V5-His6 tag (V5). Approximately 1.5 µg of each recombinant protein was resolved by 15% SDS-PAGE and the gel was stained with Coomassie blue. Molecular weight standards are shown in kDa. (**b**) His6-tagged N-terminal domains of BLM orthologs bind d(T)174. The indicated His6-tagged proteins were assayed by EMSA as described in Figure 3d.

Characterization of a strand annealing activity

We assayed GST-tagged Sgs1 proteins for SA activity by incubating them with two partially homologous oligos one of which was ^{32}P-labeled. Compared to mock treatment, Sgs1 proteins that included residues 103-322 accelerated the rate of strand pairing (Fig. 18a, upper). By assaying a variety of subdomains we observed a correlation between ssDNA binding and SA activity (Fig. 18b). Sgs1$_{103\text{-}322}$ is the minimal domain required for this activity and, for reasons described below, we hereafter refer to it as the SE. SA activity was conserved in the human and fly domains as His6-tagged versions of all three proteins accelerated strand pairing (Fig. 18a, lower). The His6-tagged proteins, which displayed SA activity at concentrations as low as 5 nM, were judged to be superior to the GST-tagged versions presumably due to the smaller size of the epitope tag.

Further characterization of the SA activity indicated that it is rapid. In contrast to spontaneous annealing which was just detectable at 20 min, the enzyme-catalyzed reaction was complete within 1 min (Fig. 18b). The effect of non-homologous competitor ssDNA was tested by including high concentrations of an unrelated oligo in the reaction. As shown in Figure 18c, SA was resistant to a 100-fold excess of competitor, while a 1000-fold excess resulted in inhibition. Thus, high levels of non-homologous ssDNA are required to inhibit SA activity. We next examined the role that cofactors may play in SA. As shown in Figure 18d, the SA activities of all three orthologous SE domains were unaffected by ATP, ADP, or the non-hydrolyzable analog AMPPNP. Thus, the BLM/Sgs1 SA activity identified here behaves differently than activities identified in the full-length protein which are presumably dependent on the RecQ helicase domain.

FIGURE 18. The ST domains from BLM/Sgs1 orthologs display strand annealing activity

(**a**) SA assays contained the indicated concentrations of GST- (upper) or His6-tagged (lower) proteins plus 1 nM each of a ^{32}P-labeled 50 nt oligo (#1) and an unlabeled 50 nt oligo (#2) that share 25 nt of perfect complementarity. The reactions were incubated at 37°C for 5 min under standard conditions as described in the Methods. Reactions were stopped and the products were resolved by 10 % PAGE followed by phosphorimager analysis. M is a mock reaction lacking protein. (**b**) GST-Sgs1$_{1\text{-}322}$ (50 nM) or Sgs1$_{103\text{-}322}$ (20 nM) were assayed as in **a** except that the reactions were stopped at the indicated times prior to analysis. (**c**) The indicated ST domain proteins (50 nM) were were assayed as in **a** except that the reactions contained either no competitor (-) or a 10-, 100- or 1000-fold excess of oligo #16 prior to the addition of proteins. (**d**) The indicated ST domain proteins (50 nM) were assayed as in **a** except that the reaction contained either no additions (-) or 1 mM of the indicated cofactor. Throughout, all proteins are His6-tagged unless indicated as GST-tagged.

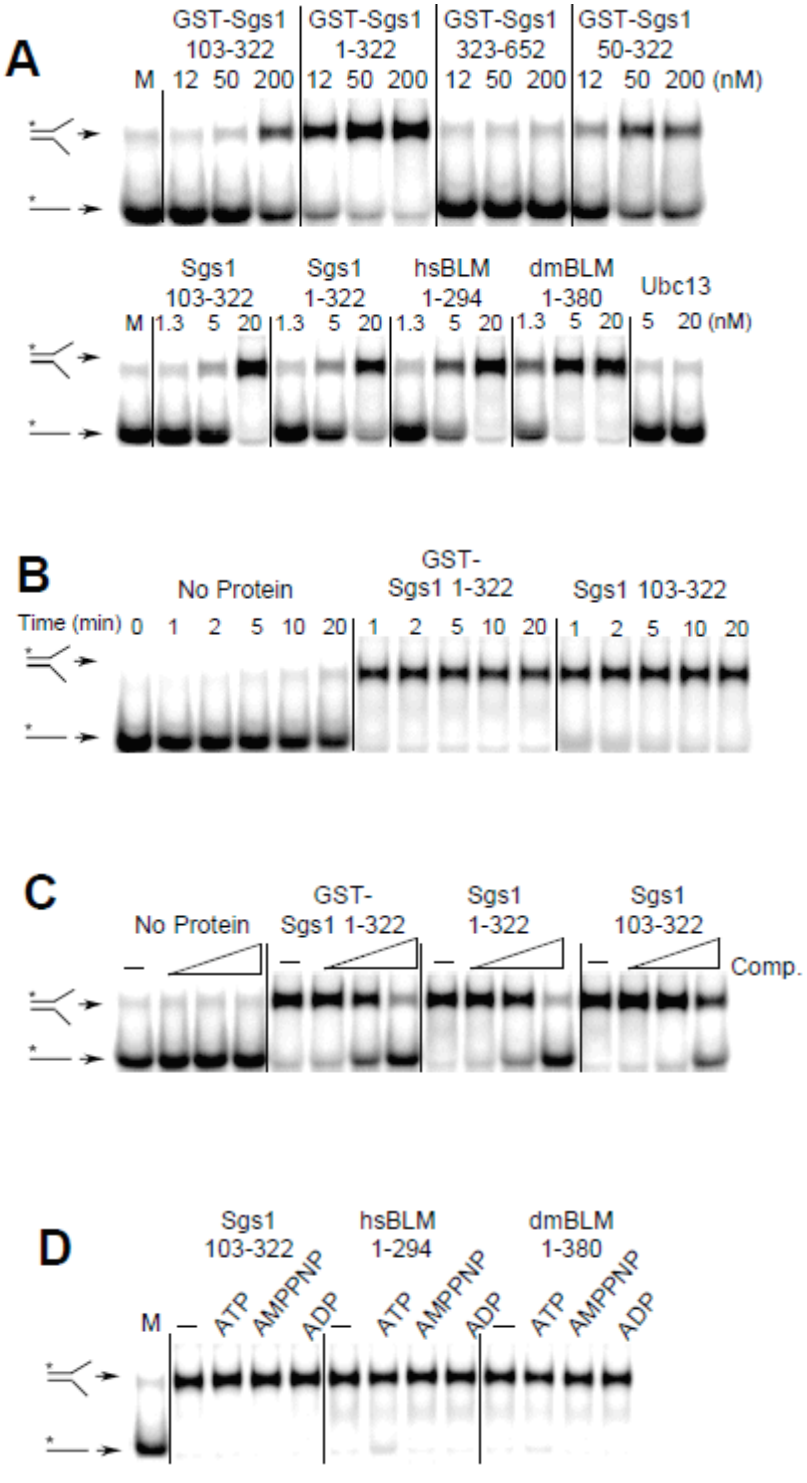
A
GST-Sgs1 103-322
GST-Sgs1 1-322
GST-Sgs1 323-652
GST-Sgs1 50-322
M 12 50 200 12 50 200 12 50 200 12 50 200 (nM)
Sgs1 103-322
Sgs1 1-322
hsBLM 1-294
dmBLM 1-380
Ubc13
M 1.3 5 20 1.3 5 20 1.3 5 20 1.3 5 20 5 20 (nM)
B
No Protein
GST-Sgs1 1-322
Sgs1 103-322
Time (min) 0 1 2 5 10 20 1 2 5 10 20 1 2 5 10 20
C
No Protein
GST-Sgs1 1-322
Sgs1 1-322
Sgs1 103-322
Comp.
D
Sgs1 103-322
hsBLM 1-294
dmBLM 1-380
M — ATP AMPPNP ADP — ATP AMPPNP ADP — ATP AMPPNP ADP

The SE domain displays DNA strand-exchange activity

The SE domain was tested for the ability to catalyze strand exchange between a duplex DNA substrate containing one labeled strand and a complementary ssDNA oligo. A similar ATP-dependent or ATP-stimulated reaction has been observed with multiple RecQ homologs (Machwe, Xiao et al. 2005; Weinert and Rio 2007; Xu and Liu 2009). One version of this reaction uses an excess of recipient ssDNA that has the same sense as the duplex's labeled strand. Denaturation of the fork is expected to result in annealing of the unlabeled complementary strands and release of the free ^{32}P-labeled ssDNA oligo. This reaction is essentially unidirectional as there is little chance of the duplex's unlabeled strand exchanging back to the less abundant labeled strand. Therefore, our substrates consisted of a synthetic forked donor DNA with a radiolabeled top strand plus a 5-fold molar excess of unlabeled top strand as recipient. As shown in Figure 19a, SE domains from all three species promoted the transfer reaction. Strand exchange was catalyzed by SE protein, and was not due to spontaneous denaturation of the duplex, because neither incubation with non-specific protein (GST), nor excess complementary DNA alone, resulted in strand exchange (Fig. 19a). To eliminate the possibility that the donor DNA was simply melted by SE after which it passively annealed to the recipient oligo during the protease step prior to electrophoresis, we included a high concentration of a second recipient oligo during the protease incubation. The failure to detect annealing to this larger 94 nt oligo during the protease reaction indicates that ssDNA was not present following the assay or during protease treatment (Fig. 20a). Moreover, the SE protein lacked detectable nuclease activity that might result in an artifactual DNA strand-exchange activity (Fig. 20b). Thus, the simplest explanation for strand transfer is that the

SE domain melts double-stranded DNA while it simultaneously anneals complementary DNA strands. Such a coordinated reaction might explain why higher protein concentrations were required for SE (200-400 nM) than for SA (5-20 nM).

The substrate requirements for SE were examined by preparing radiolabeled duplex substrates whose ends were either flush or contained a free 5'-tail or 3'-tail. $Sgs1_{103-322}$ was then titrated into the reactions which contained different concentrations of unlabeled recipient DNA. In all cases, SE required a 5-fold excess of recipient DNA (Fig. 19b-d). ST also took place using the blunt donor, however lower levels of protein were required when the donor duplex contained a 3'-tail (Fig. 19e). The stimulation by a 3'-tail suggests that unwinding and annealing has a specific polarity.

To further characterize the $Sgs1_{103-322}$ protein, we employed a SE reaction in which the recipient DNA was complementary to the labeled strand of the duplex but larger in size. Thus, the appearance of a retarded signal in native gel electrophoresis is diagnostic for SE. Using these substrates, the SE domains from three BLM orthologs efficiently converted the donor DNA signal into a slower-migrating form (Fig. 21a). Time course experiments confirmed that the three orthologs had similar kinetics and that the reactions were essentially complete within 5 min (Fig. 21b). The impact of ssDNA binding proteins on SA and SE activities was then assessed. The annealling of complementary 32- and 94-nt oligos (2 nM each) was inhibited by approximately 8 nM of both yeast RPA and *E. coli* SSB (Fig. 21c). Under these conditions we estimate that both ssDNA binding proteins occlude 30 nt of ssDNA, so that there are 8 nM of binding sites in the substrate. Thus, access of $Sgs1_{103-322}$ to ssDNA appears to be blocked by stoichiometric levels of RPA and SSB. The corresponding substrates were then assayed

in an analogous SE reaction: a 32 bp duplex (0.5 nM) and 94-nt recipient oligo (2.5 nM). *E. coli* SSB again inhibited the reaction at 8 nM, which is expected to saturate the 7.5 nM binding sites. Higher levels of RPA partially inhibited the SE reaction (Fig. 21d). Thus, although there are quantitative differences, $Sgs1_{103\text{-}322}$ -promoted SE is inhibited by high levels of both ssDNA binding proteins.

Two additional experiments were performed to characterize the SE reaction. First, because the above experiments were performed in the presence of EDTA, we tested whether it was influenced by divalent cations. The results (Fig. 22A and B) indicated that the SE reaction was unaltered by physiological levels of Mg^{2+}. Second, to examine its stoichiometry we titrated $Sgs1_{103\text{-}322}$ into a SE reaction and quantified the products. The results indicated that 40 – 54% of the flush-end DNA duplex was exchanged onto the recipient ssDNA over a range of 0.4 to 1.6 μM $Sgs1_{103\text{-}322}$ (Fig. 22C). Based on these values, strand exchange requires a minimum of one molecule of protein for each 7 nts of ssDNA.

FIGURE 19. The SE domains from BLM/Sgs1 orthologs display DNA strand transfer activity

(**a**) The SE assay is illustrated at the top of the panel. Reactions contained the indicated SE domain proteins at 0 (-), 50, 200, or 400 nM plus 2 nM forked DNA (where oligo #1 is ^{32}P-labeled) plus 10 nM oligo #1. Substrate DNAs were incubated with GST at 50, 200, or 800 nM as negative control. The reactions were incubated at 37°C for 30 min under standard conditions and the products were analyzed by 8% PAGE and phosphorimaging. The first lane (Δ) contains ^{32}P-labeled oligo #1 as marker. (**b**) $Sgs1_{103-322}$ (0, 100, 200, 400, 800 and 1600 nM) was used in a SE assay using blunt-ended substrate as indicated in the reaction at the top of the panel. Reactions contained 1 nM duplex DNA plus the indicated amounts of oligo 3. Assays were performed as in **a** except for use of 10% PAGE. (**c**) $Sgs1_{103-322}$ was assayed using 5'-tail duplex DNA as substrate as in **b**. (**d**) $Sgs1_{103-322}$ was assayed using 3'-tail duplex DNA as substrate as in **b**. (**e**) The strand transfer reactions shown in **b-d** (20 nM unlabled oligo) were quantified and are presented as a function of protein concentration. Sequences of the indicated oligos are presented in Table 4.

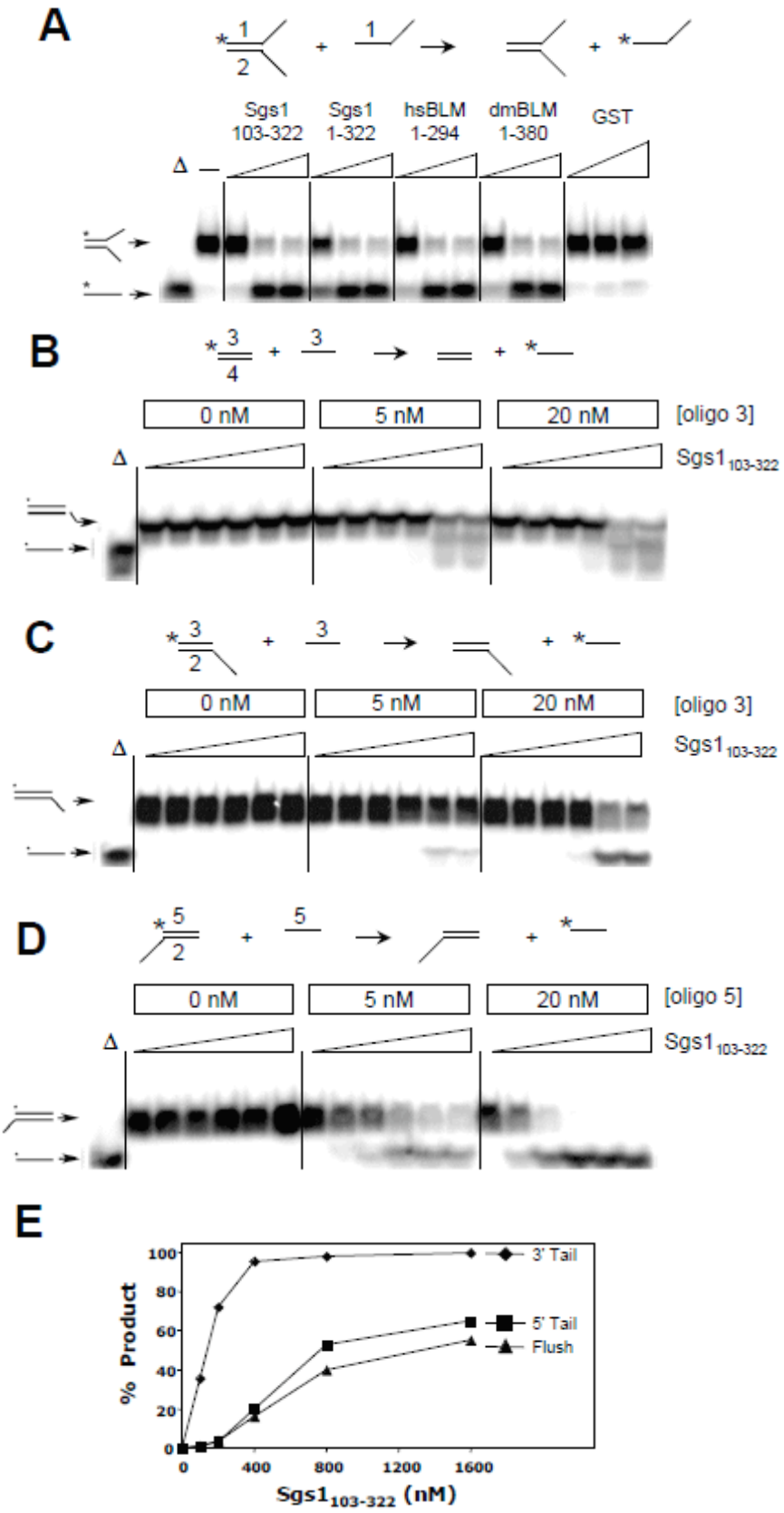
A
Sgs1 103-322
Sgs1 1-322
hsBLM 1-294
dmBLM 1-380
GST
Δ
B
0 nM
5 nM
20 nM
[oligo 3]
Sgs1103-322
C
0 nM
5 nM
20 nM
[oligo 3]
Sgs1103-322
D
0 nM
5 nM
20 nM
[oligo 5]
Sgs1103-322
E
% Product
3' Tail
5' Tail
Flush
Sgs1103-322 (nM)

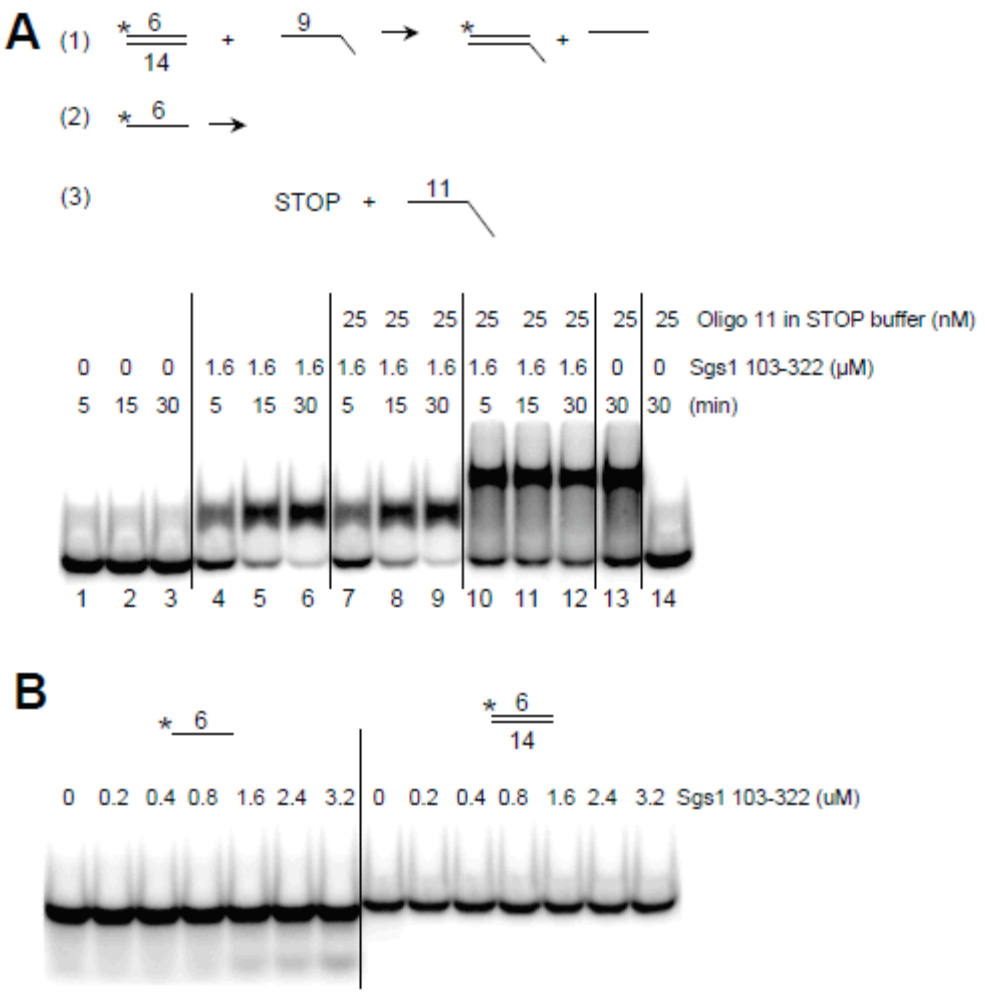

FIGURE 20. The SE domain lacks meltase and nuclease activity

(**a**) A SE reaction (1) was carried out using 1 nM of a ^{32}P-labeled donor DNA with flush ends plus 5 nM of recipient oligo (lanes 1-9, 14). In reaction (2) the substrate consisted of 1 nM ^{32}P-labeled oligo 6 alone (lanes 10-13). Both reactions were performed as described in the standard SE assay except that oligo 11 (25 nM final concentration) was added with the stop buffer in lanes 7-14 and incubated at 37ºC for 30 min (3). (**b**) One nM of ^{32}P-labeled oligo 6 or 1 nM of ^{32}P-labeled dsDNA (oligo 6 plus 14) was incubated with the indicated amount of protein at 37°C for 30 min and analyzed as described in SE reaction.

FIGURE 21. Characterization of SA and SE reactions

(**a**) The indicated SE reaction was performed by titrating $Sgs1_{103-322}$, $hsBLM_{1-294}$ or $dmBLM_{1-380}$ into the standard SE assay. Following incubation at 37°C for 30 min, the products were analyzed as in Figure 4. Δ, boiled substrate; M, mock reaction without protein. (**b**) Time courses of the SE reaction illustrated in (**a**) were carried out with $Sgs1_{103-322}$ (2.4 μM), $hsBLM_{1-294}$ (1.2 μM) or $dmBLM_{1-380}$ (1.2 μM). A, annealed oligos were obtained by slow cooling and used as marker. (**c**) The indicated SA reaction was performed by incubating 2 nM each of oligo #6 (32-nt) and oligo 11 (94-nt) together with various concentrations of either *E. coli* SSB or yeast RPA. Reactions were assembled on ice prior to incubation at 37°C for 5 min. (**d**) A SE reaction was performed using the indicated duplex DNA (0.5 nM) as donor and a 94-nt ssDNA (2.5 nM) as recipient. Reactions were assembled on ice prior to incubation at 37°C for 30 min.

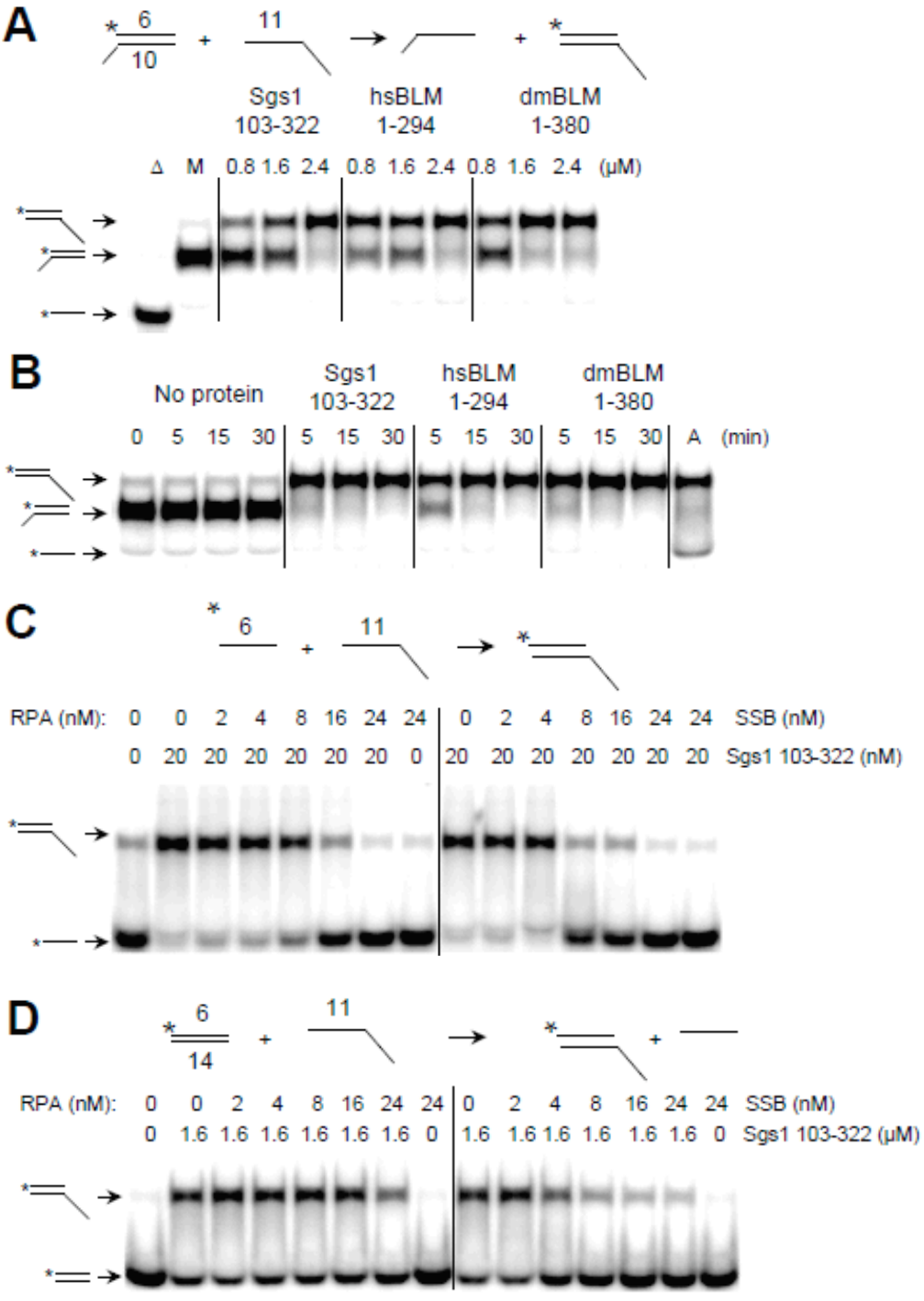
A
6
10
11
Sgs1
103-322
hsBLM
1-294
dmBLM
1-380
Δ M 0.8 1.6 2.4 0.8 1.6 2.4 0.8 1.6 2.4 (μM)
B
No protein
Sgs1
103-322
hsBLM
1-294
dmBLM
1-380
0 5 15 30 5 15 30 5 15 30 5 15 30 A (min)
C
6
11
RPA (nM): 0 0 2 4 8 16 24 24 0 2 4 8 16 24 24 SSB (nM)
0 20 20 20 20 20 20 0 20 20 20 20 20 20 20 Sgs1 103-322 (nM)
D
6
14
11
RPA (nM): 0 0 2 4 8 16 24 24 0 2 4 8 16 24 24 SSB (nM)
0 1.6 1.6 1.6 1.6 1.6 1.6 0 1.6 1.6 1.6 1.6 1.6 1.6 0 Sgs1 103-322 (μM)

FIGURE 22. SE reaction is Mg^{2+}-independent

(A) A SE reaction was carried out in the presence of $Sgs1_{103-322}$ and the indicated concentrations of Mg^{2+}. (**B**) A SE reaction containing two potential recipient ssDNAs was carried out in the presence or absence of Mg^{2+}. (**C**) $Sgs1_{103-322}$ was titrated into a SE reaction employing 10 nM flush-ended duplex as donor and 50 nM ssDNA as recipient. The products of the indicated reactions were quantified and its efficiency is presented as the percent of total signal present in the slower migrating band. Shown below these values is the ratio of molecules of ssDNA (in nucleotides) to molecules of protein used in the reaction.

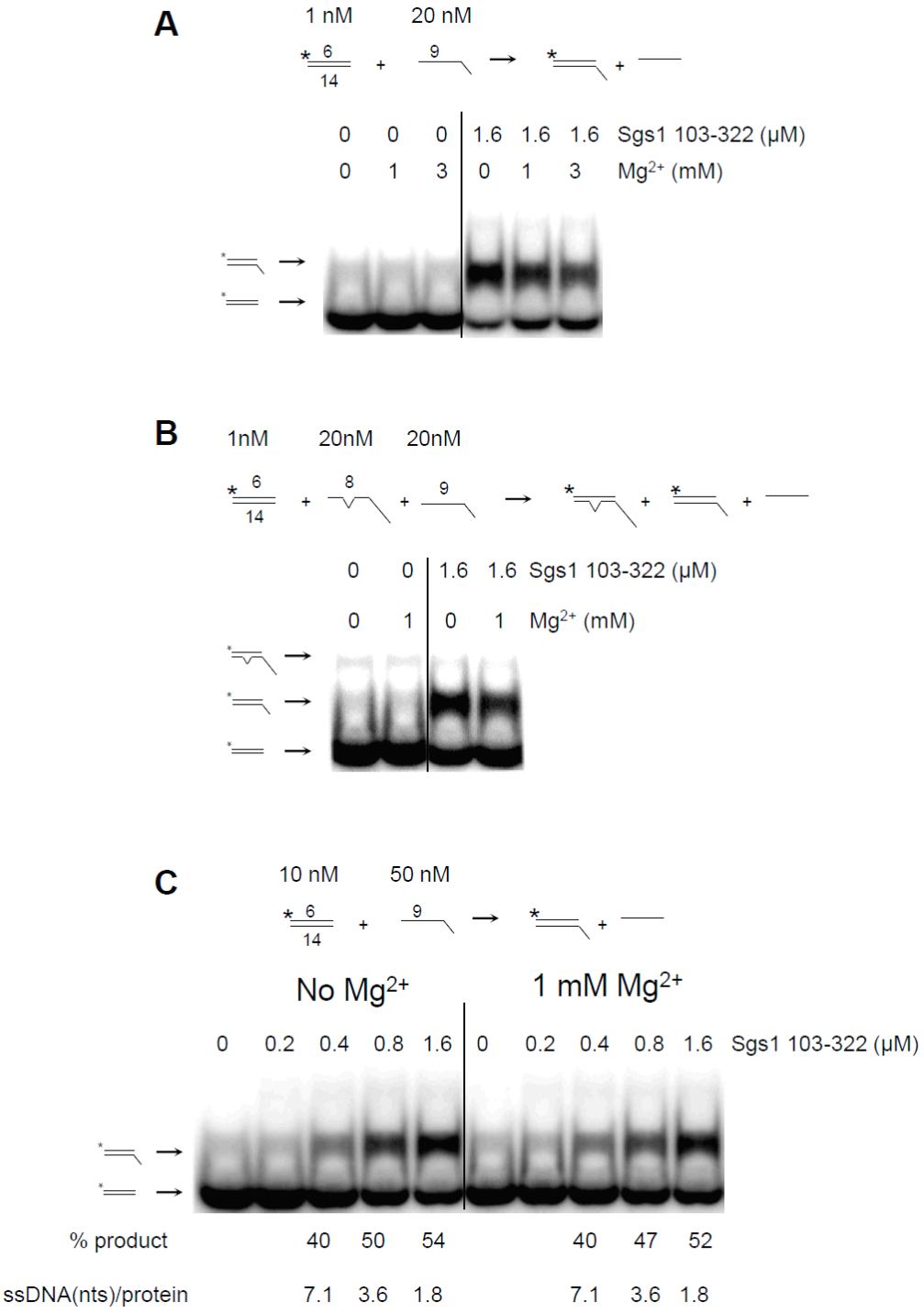
A
1 nM
20 nM
6
14
9
0 0 0 1.6 1.6 1.6 Sgs1 103-322 (μM)
0 1 3 0 1 3 Mg2+ (mM)
B
1nM
20nM
20nM
6
14
8
9
0 0 1.6 1.6 Sgs1 103-322 (μM)
0 1 0 1 Mg2+ (mM)
C
10 nM
50 nM
6
14
9
No Mg2+
1 mM Mg2+
0 0.2 0.4 0.8 1.6 0 0.2 0.4 0.8 1.6 Sgs1 103-322 (μM)
% product 40 50 54 40 47 52
ssDNA(nts)/protein 7.1 3.6 1.8 7.1 3.6 1.8

The SE domain is required for Sgs1 function *in vivo*

In order to determine the *in vivo* function of the SE domain, we constructed the *sgs1-ΔSE* allele that lacks the SE coding region. This allele, which expresses $Sgs1_{\Delta 103\text{-}322}$ from its own promoter, was tested for its ability to complement *sgs1Δ* phenotypes. To eliminate the possibility that *sgs1-ΔSE* phenotypes were due to a defect in Top3-Rmi1 binding, we first assayed the interaction by immunoprecipitating (IP'ing) $Sgs1_{\Delta 103\text{-}322}$ and immunoblotting for Top3 and Rmi1. As previously demonstrated for wt Sgs1 (Mullen, Nallaseth et al. 2005), epitope-tagged versions of Top3 and Rmi1 were present in precipitates of FLAG-tagged $Sgs1_{\Delta 103\text{-}322}$, and $Sgs1_{\Delta 103\text{-}322}$ was found in Rmi1 precipitates (Fig. 23 a). In a side-by-side comparison, approximately equal amounts of the Top3 and Rmi1subunits were co-IP'd with Sgs1-wt and $Sgs1_{\Delta 103\text{-}322}$, respectively (Fig. 23b). Based on these results and the data presented below, we conclude that $Sgs1_{\Delta 103\text{-}322}$ interacts properly with Top3 and Rmi1.

Different alleles of *SGS1* have been shown to confer distinct slow-growth phenotypes (Weinstein and Rothstein 2008). For example, the *sgs1Δ* null strain grows more slowly than wt, but a strain lacking the Top3-Rmi1 binding domain of Sgs1 (e.g., *sgs1-ΔN158* encoding $Sgs1_{159\text{-}1447}$) grows even more slowly than *sgs1Δ* (Fig. 23c). As previously observed (Mullen, Kaliraman et al. 2000), this hypermorphic phenotype was eliminated by a larger N-terminal truncation (e.g., *sgs1-ΔN322* encoding $Sgs1_{323\text{-}1447}$). In contrast to these mutants, the doubling time of the *sgs1-ΔSE* strain was identical to wt (Fig. 23c). Further, when we examined its ability to complement the MMS sensitivity of *sgs1Δ*, the *sgs1-ΔSE* allele conferred a wt-level of resistance (Fig. 23d). This result is

consistent with other internal deletions made within the Sgs1 N-terminus (Ui, Satoh et al. 2001) and indicates that the *sgs1-ΔSE* allele functions like wt in these assays.

The *sgs1-ΔSE* allele was then used to test whether it would complement the *sgs1Δ* hyper-recombination phenotype. Intrachromosomal recombination was measured using a marker-excision assay in which *CAN1* and *URA3* are inserted between direct-repeat sequences at *LYS2* and the rDNA, respectively (Mullen, Kaliraman et al. 2000). Compared to wt, the *sgs1Δ* null strain displayed a 2.9-fold increase in recombination frequency at *LYS2* and a 4.2-fold increase at the rDNA (Fig. 24a), and consistent with its hypermorphic phenotype, *sgs1-ΔN158* displayed 7- and 32-fold increases at these loci. The *sgs1-ΔSE* allele generated recombination rates that were elevated by 3.8 and 4.2-fold, respectively. These levels closely match those obtained with *sgs1Δ* and *sgs1-ΔN322*. Thus, the SE domain is required to suppress hyper-recombination.

The prototypical phenotype of *SGS1* loss-of-function alleles is the suppression of *top3Δ* slow growth (Gangloff, McDonald et al. 1994). However some separations of function alleles, such as sgs1-D664Δ, confer this phenotype as well (Bernstein, Shor et al. 2009). To test the effect of *sgs1-ΔSE* in the *top3Δ* background, we introduced a variety of plasmid-borne *SGS1* alleles into an *sgs1Δ top3Δ* double mutant that contained plasmid pJM555 (*TOP3*/*URA3*/*CEN*). These strains were then serially diluted and spotted onto medium containing 5-FOA which selects against pJM555. As expected, the *sgs1Δ* allele allowed good growth on this medium while *SGS1* promoted slow growth (Fig. 24b). The *sgs1-ΔSE* allele behaved like *sgs1Δ* (and *sgs1-ΔN322*) as indicated by the good growth of this strain on 5-FOA. Based on this data, *sgs1-ΔSE* resembles *sgs1-D664Δ* in that both alleles suppress *top3Δ* slow-growth but remain MMS resistant. To test whether this

phenotype was due to the loss of the SE activity, we replaced residues 103-322 of Sgs1 with residues 95-300 of hsBLM. Despite the fact that these domains are only 13% identical in aa sequence, this chimeric allele *SGS1-BLM*$_{95\text{-}300}$, displayed wt function by promoting the slow growth of *top3Δ* cells (Fig. 23b). This result supports the notion that SE activity is required for *SGS1* to promote *top3Δ* slow growth.

One of the most sensitive assays for *SGS1* function is its ability to complement *sgs1Δ slxΔ* synthetic lethality (Mullen, Kaliraman et al. 2001). This was tested in two strains, *sgs1Δ slx4Δ* and *sgs1Δ slx5Δ,* that are kept alive by plasmid pJM500 (*SGS1*/*URA3*/*CEN*). Both strains were transformed with plasmid-borne *SGS1* alleles, and the transformants were then streaked onto media that selects against pJM500. In contrast to wt *SGS1*, which promoted growth on 5-FOA, *sgs1-ΔSE* failed to complement either strain (Fig. 24c). In this regard *sgs1-ΔSE* resembled the null allele and *sgs1-ΔN322*. To test whether the loss of SE activity was responsible for this phenotype, we also transformed these tester strains with *SGS1-BLM*$_{95\text{-}300}$. Again the human SE domain restored activity to the chimeric yeast protein as revealed by the growth of yeast in the absence of *SLX4* or *SLX5*. As control, we showed that another domain from the N-terminus of BLM could not provide SE function as the chimeric allele *SGS1-BLM*$_{421\text{-}640}$ failed to complement synthetic lethality (Fig. 24c). It should be noted that the ability of *SGS1-BLM*$_{95\text{-}300}$ to function in this assay most likely depended on productive interactions between the Sgs1 TR domain and Top3-Rmi1 because *SGS1* alleles that replace Sgs1$_{1\text{-}322}$ with BLM$_{1\text{-}300}$ fail to complement *sgs1Δ slx4Δ* or *sgs1Δ slx5Δ* synthetic lethality (J.R. Mullen and S.J.B., unpublished data). We conclude that the SE domain is essential for *SGS1* function in these genetic backgrounds.

In *S. cerevisiae*, Rad52 is a central recombination protein, whereas its paralogue, Rad59, plays a more subtle role in homologous recombination. Rad59 protein is a 238-residue protein with high homology to the N-terminus of Rad52 (34-198 aa, Fig. 25a). Rad59 and N-terminal Rad52 (34-270 aa) encompass DNA binding and annealing activities (Mortensen, Bendixen et al. 1996; Wu, Siino et al. 2006; Wu, Sugiyama et al. 2006). It has been proven that human N-terminal Rad52, not Rad59, possesses ATP-independent SE activity (Bi, Rybalchenko et al. 2004; Garcia, Liu et al. 2004). Interestingly, in the study of Rad59-Rad52 chimeric proteins, Rad59-Rad52 chimeras complement the γ-ray sensitivity of *rad59Δ*, but not of *rad52Δ* strains. This showed that N-terminus Rad52 provides unique function to DSB repair that can not be replaced by Rad59 (Feng, During et al. 2007). To test whether Rad52 SE domain or full-length Rad59 can replace SE activity of Sgs1 *in vivo,* we perform *sgs1Δ slxΔ* synthetic lethality. As a result (Fig. 25b), Rad52 SE domain, not full-length Rad59, restored activity to the chimeric protein as revealed by the growth of yeast in the absence of *SLX4* or *SLX5*. Importantly, the N-terminal Rad52 and Sgs1 SE domain may possess the same function not supplied by Rad59, which may account for SE activity.

SGS1 has been shown to prevent recombination between homeologous DNA sequences in a single-strand annealing (SSA) assay (Sugawara, Goldfarb et al. 2004). SSA is a DSB repair pathway in which a DSB between two direct-repeat (DR) sequences can be repaired by the annealing of the homologous 3'-ssDNA sequences that arise following 5'-end resection. We used strains engineered to contain an HO endonuclease site between two 205 bp DRs that have either 100% sequence homology (A-A strains) or 97% homeology (F-A strains) (Sugawara, Goldfarb et al. 2004). Failure to repair the

HO-induced break results in the loss of cell viability, which is exacerbated in F-A strains because wt cells prevent homeologous repair. For example, the viability of A-A strains following HO induction is 5-fold better than that of F-A strains (Fig. 24d). As previously demonstrated, *sgs1Δ* cells display efficient repair using homeologous sequences such that the A-A/F-A ratio is 1.1 (Sugawara, Goldfarb et al. 2004; Goldfarb and Alani 2005). We found that *sgs1-ΔSE* strains display an A-A/F-A cell-viability ratio of 1.4 which is indicative of efficient homeologous repair. Thus, the SE domain is required for heteroduplex rejection. This result is consistent with the finding that $Sgs1_{1\text{-}652}$, as well as the Sgs1 DNA helicase domain, are required for heteroduplex rejection in this assay (Goldfarb and Alani 2005).

FIGURE 23. $Sgs1_{\Delta 103\text{-}322}$ physically interacts with Top3-Rmi1

(**A**) Yeast strains were constructed to express integrated versions of Top3-V5, Rmi1-HA, and either $Sgs1_{\Delta 103\text{-}322}$-FLAG (ΔSE) or no Sgs1 (-) as the sole copies of these subunits Cell extracts were prepared and either immunoblotted directly (Extract) or subjected to IP with α-FLAG beads (IP-FLAG) prior to immunoblotting with α-FLAG, α-V5, and α-HA antibodies. Like wt Sgs1-FLAG, $Sgs1_{\Delta 103\text{-}322}$-FLAG is insufficiently abundant to be detected in crude cell extracts (Mullen, Nallaseth et al. 2005). In the lower panel, extracts were IP'd with α-HA and immunoblotted with α-FLAG to detect $Sgs1_{\Delta 103\text{-}322}$-FLAG. (**B**) Cell extracts were prepared from strains expressing Top3-V5, Rmi1-HA, and either Sgs1-FLAG (WT) or $Sgs1_{\Delta 103\text{-}322}$-FLAG (ΔSE) as above. Extracts containing 2 mg of total protein were subjected to IP with α-FLAG beads (IP-FLAG) and immunoblotted with α-FLAG, α-V5, and α-HA antibodies. (**C**) Cells of the indicated genotype were grown in liquid YPD at 30°C and doubling times were determined. Shown are the average values ± SD. (**D**) Cells of the indicated genotype were resuspended at OD = 3, serially diluted in 3-fold increments, and approximately 5 µl were spotted onto YPD plates with or without 0.03% MMS. Plates were photographed following 2 (YPD) or 3 days (MMS) growth at 30°C.

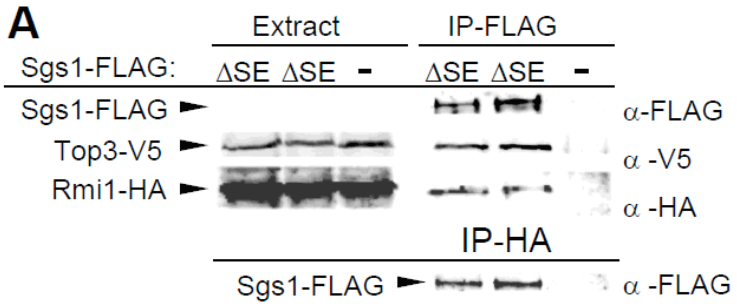
A
Extract
IP-FLAG
Sgs1-FLAG:
ΔSE ΔSE -
ΔSE ΔSE -
Sgs1-FLAG
Top3-V5
Rmi1-HA
α-FLAG
α -V5
α -HA
IP-HA
Sgs1-FLAG
α -FLAG

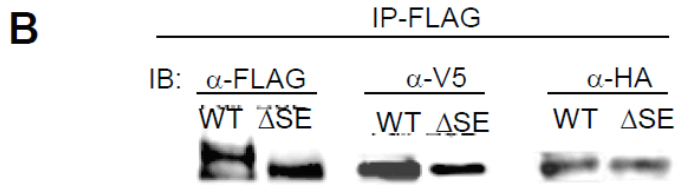
B
IP-FLAG
IB: α-FLAG
α-V5
α-HA
WT ΔSE
WT ΔSE
WT ΔSE

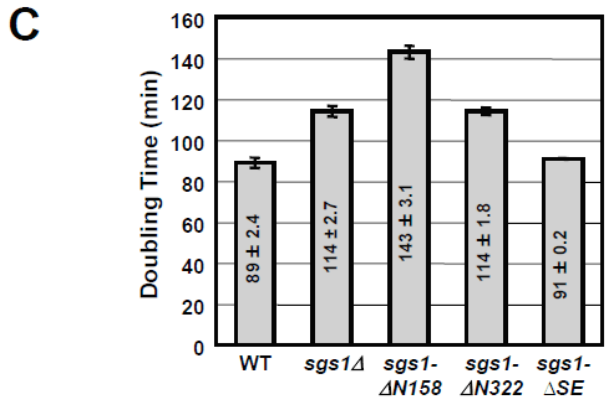
C
Doubling Time (min)
160
140
120
100
80
60
40
20
0
89 ± 2.4
114 ± 2.7
143 ± 3.1
114 ± 1.8
91 ± 0.2
WT
sgs1Δ
sgs1-ΔN158
sgs1-ΔN322
sgs1-ΔSE

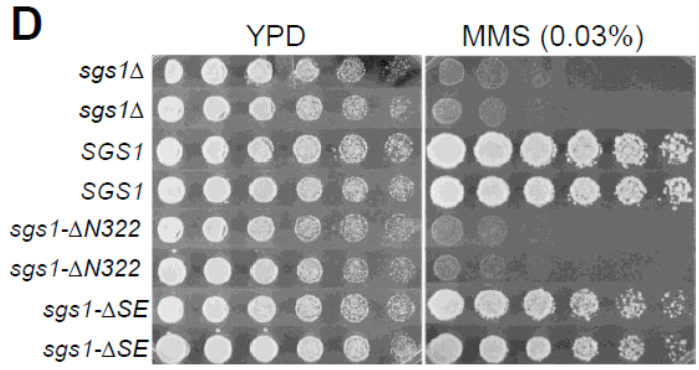
D
YPD
MMS (0.03%)
sgs1Δ
sgs1Δ
SGS1
SGS1
sgs1-ΔN322
sgs1-ΔN322
sgs1-ΔSE
sgs1-ΔSE

FIGURE 24. The SE domain is required for multiple *SGS1* functions

(**a**) Yeast strains of the indicated genotype were assayed for excision recombination at the *LYS2* and rDNA loci as previously described (Mullen, Kaliraman et al. 2000). Recombination frequencies were determined and are presented as fold increase over wt. (**b**) Strain NJY728 [*sgs1Δ top3Δ* plus pJM555 (*TOP3/URA3/ADE3/CEN*)] was transformed with the indicated *SGS1* alleles in pRS415 (*LEU2/CEN*). Transformants were streak purified on SD-leu plates, resuspended to OD600 = 3.0 and serially diluted in five-fold increments. Approximately 5 µl were spotted onto SD plates lacking leucine but with or without 5-FOA. Plates were photographed following 2 (-Leu) or 3 (5-FOA/-Leu) days growth at 30°C. (**c**) Strains NJY2083 [*sgs1-11::loxP slx4-11::loxP* plus pJM500 (*SGS1/URA3/ADE3/CEN*)] and NJY602 [*sgs1-11::KAN slx5-10::TRP1* plus pJM500] were transformed with various *SGS1* alleles in pRS415 as indicated in the key. Transformants were streaked onto YPD plates containing 5-FOA and the plates were photographed following 2 (*sgs1Δ slx4Δ*) or 3 (*sgs1Δ slx5Δ*) days growth at 30°C. (**d**) Cells of the indicated genotype were assayed for viability after inducing HO endonuclease in SSA reporter strains that contained either homologous (A-A) or homeologous (F-A) direct repeats flanking the HO cut site (Sugawara, Goldfarb et al. 2004). Results shown are the average viability ± SD.

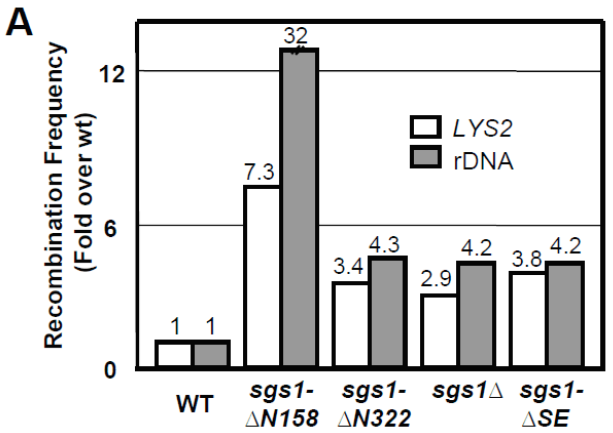

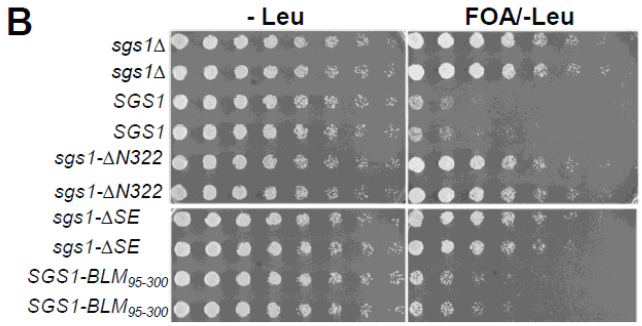

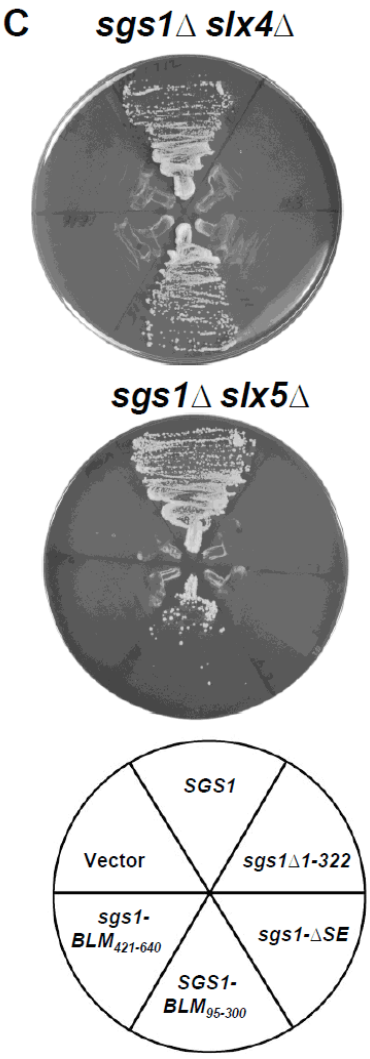

D

Genotype	A-A	F-A	A-A/F-A
WT	0.69 ± 0.07	0.13 ± 0.02	5.3
sgs1Δ	0.83 ± 0.07	0.75 ± 0.08	1.1
sgs1-ΔSE	0.64 ± 0.07	0.45 ± 0.04	1.4

FIGURE 25. Rad52 SE domain complements Sgs1 SE domain in *sgs1*Δ*slx*Δ synthetic lethality

(**a**) Schematic representations of the full length 504 aa Rad52 protein, 238 aa Rad59 and N-terminus $Sgs1_{1\text{-}652}$. Domains: TR, Top3-Rmi1 binding; SE, Strand-Exchange domain in Rad52 and Sgs1. (**b**) Strains NJY2083 [*sgs1-11::loxP slx4-11::loxP* plus pJM500 (*SGS1/URA3/ADE3/CEN*)] and NJY602 [*sgs1-11::KAN slx5-10::TRP1* plus pJM500] were transformed with various *SGS1* alleles in pRS415 as indicated in the key. Transformants were streaked onto YPD plates containing 5-FOA and the plates were photographed following 3 (*sgs1Δ slx4Δ*) or 5 (*sgs1Δ slx5Δ*) days growth at 30°C.

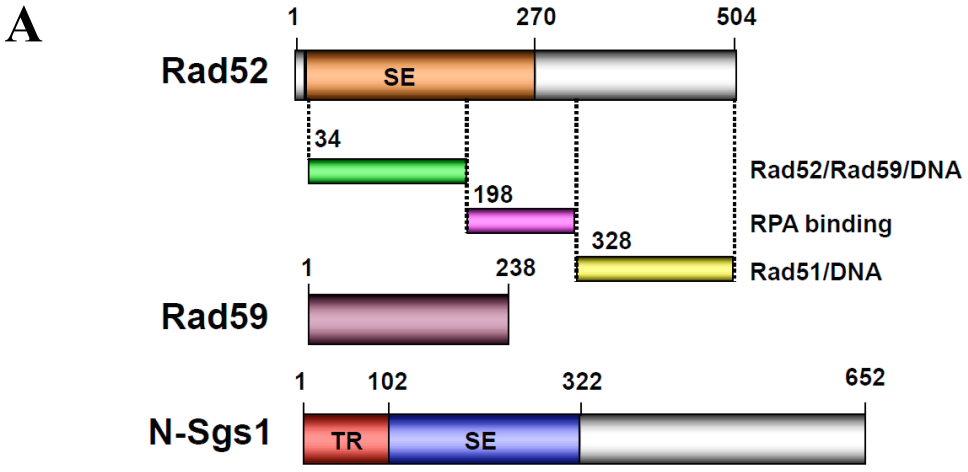

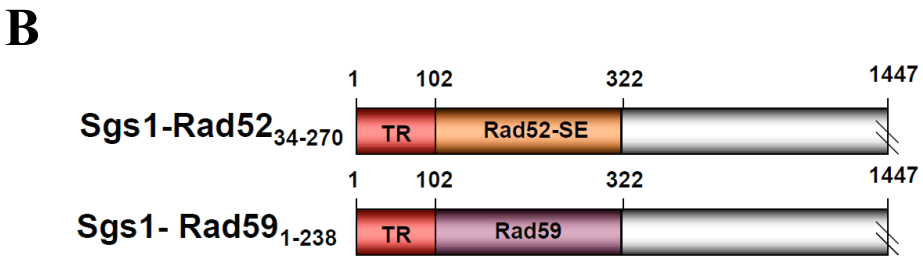

sgs1Δ slx4Δ

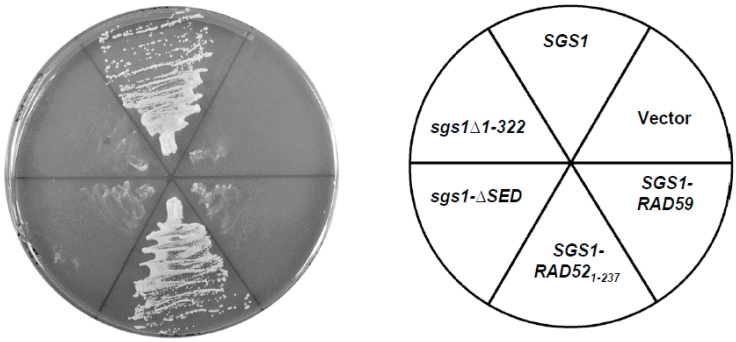

sgs1Δ slx5Δ

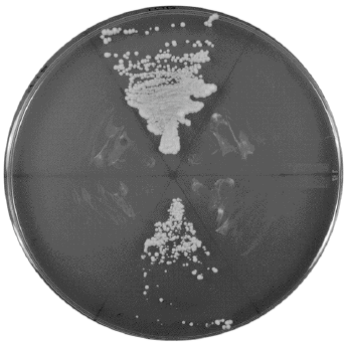

Role of DNA homology in DNA strand exchange *in vitro*

The results from the above experiment predicted that the SE domain might discriminate between homologous and homeologous DNA in *in vitro* assays. To test this idea, we designed SA and SE assays using synthetic substrates that contained a single mismatched base-pair within a 32 bp region of homology. The resulting 97% homeology would then approximate the *in vivo* conditions used in the experiment of Fig. 24d. For the SA assay we incubated a radiolabeled oligo (#6 in Fig. 26a) with two versions of its complement: a perfectly homologous oligo that contained a long tail (#8, 94 nt), and one with a shorter tail that contained a single mismatched base at the center of its 32 nt homologous region (#9; 57 nt). Following SA, homologous and homeologous products were distinguishable by their differential migration in gel electrophoresis. As shown in Fig. 26a, $Sgs1_{103\text{-}322}$ promoted strand annealing on both complementary oligos regardless of the mismatch. Note that the ratio of homologous to homeologous products was identical to mock incubation controls used to measure spontaneous annealing following 5 or 60 min incubations (Fig. 26a, left). This result was independent of whether the homologous strand or the homeologous strand contained the longer tail (Fig. 26a, right). Homeologous DNA was also annealled as efficiently as homologous DNA in standard two-oligo reactions (data not shown). Thus, SE-stimulated annealling does not distinguish between homologous and homeologous DNA, at least at this level of homeology. It should also be noted that the Tm's of the substrates used here must be sufficiently high that there is no impediment to the annealing of homeologous DNA in either spontaneous or SE-promoted reactions.

We next examined the effect of mismatches in SE reactions using standard methodology. Compared to substrates with perfect homology (Fig. 26b, upper), $Sgs1_{103-322}$ was unable to stimulate strand exchange using an oligo with a single mismatch in the center of the 32 nt region of homology (Fig.26b, middle). To compensate for the lower Tm of the mismatched products, substrates were designed such that the mismatched product would contain two additional bases of complementarity not found in the substrate (Fig. 26b, lower). However, strand transfer by $Sgs1_{103-322}$ remained negligible.

Because the above experiment compared individual reactions, we designed a competitive SE reaction in which the labeled strand of the duplex would be allowed to transfer onto either homologous or homeologous ssDNA analogous to the experiment in Fig. 26a. The diagram of Figure 27a illustrates the flush 32 bp duplex donor with a labeled top strand, and recipient DNAs consisting of either a 57 nt oligo with perfect homology or a 94 nt homeologous oligo containing a single mismatch. When incubated with the recipient DNAs individually, $Sgs1_{103-322}$ efficiently transferred the labeled donor strand onto the homologous substrate (#9) but not the homeologous substrate (#8). Note that the level of transfer onto oligo #8 (Fig. 27a, lanes 9-11) approximated that obtained in the absence of protein (Fig. 27a, lanes 1-4). Importantly, incubation of all three substrates together resulted in transfer exclusively onto the homologous substrate (Fig. 27a, lanes 5-8).

To test whether this result was biased by the fact that the homologous oligo contained a smaller non-homologous tail, we performed the control reaction in Figure 27b. Again transfer occurred exclusively onto the homologous oligo even when it contained the larger non-homologous tail. Thus, in contrast to strand annealing, strand

exchange catalyzed by the SE domain *in vitro* is inhibited by as little as 3% non-homology. The ability of the SE domain to discriminate between homologous and homeologous substrates may be related to *SGS1*'s role in heteroduplex rejection *in vivo*.

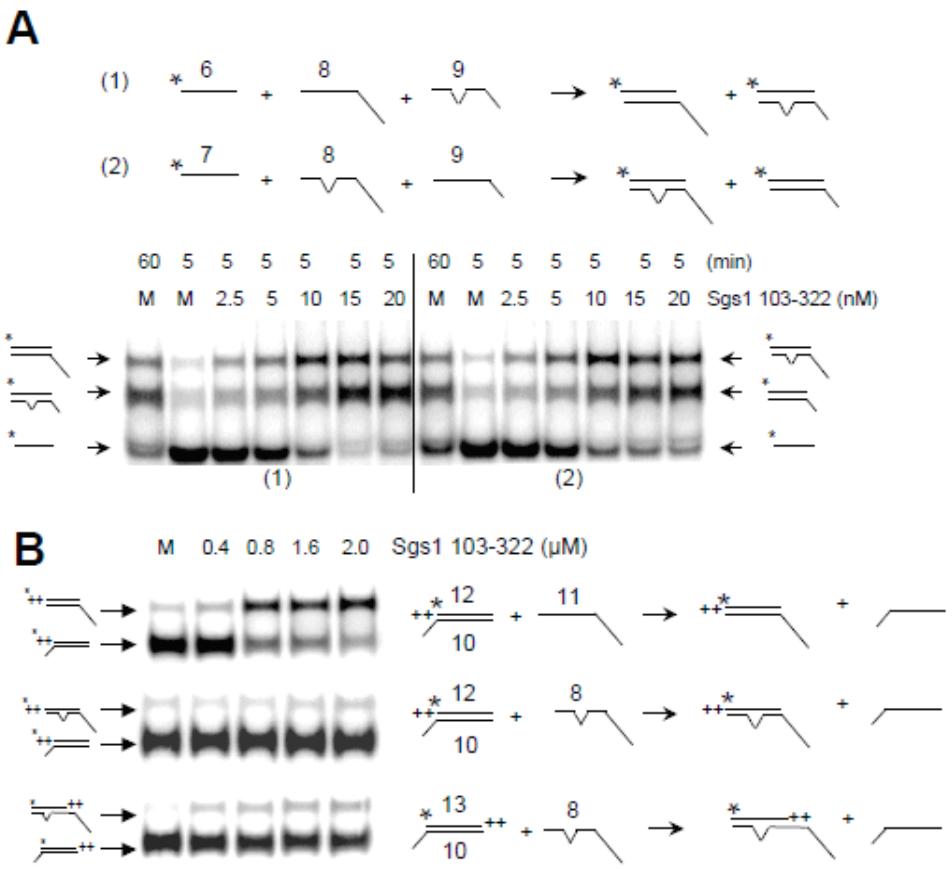

FIGURE 26. Differential response of SA and SE to non-homology

(**a**) Two SA reactions are illustrated schematically in which a single non-complementary nucleotide at the center of the 32 nt homologous region is indicated by a bulge. Reactions (1) and (2) differ by the lengths of the non-homologous tails on the recipient DNAs as indicated. $Sgs1_{103\text{-}322}$ was titrated into a reaction containing the indicated ^{32}P-labeled oligo (1 nM) plus recipient oligo (1 nM) and incubated for at 37°C for 5 min. Mock (M) reactions lack protein and were incubated for 5 or 60 min. (**b**) Three SE reactions were carried out at 37°C for 5 min using the indicated concentrations of $Sgs1_{103\text{-}322}$, 1 nM of ^{32}P-labeled donor dsDNA and 20 nM of recipient oligo. +, single nucleotide.

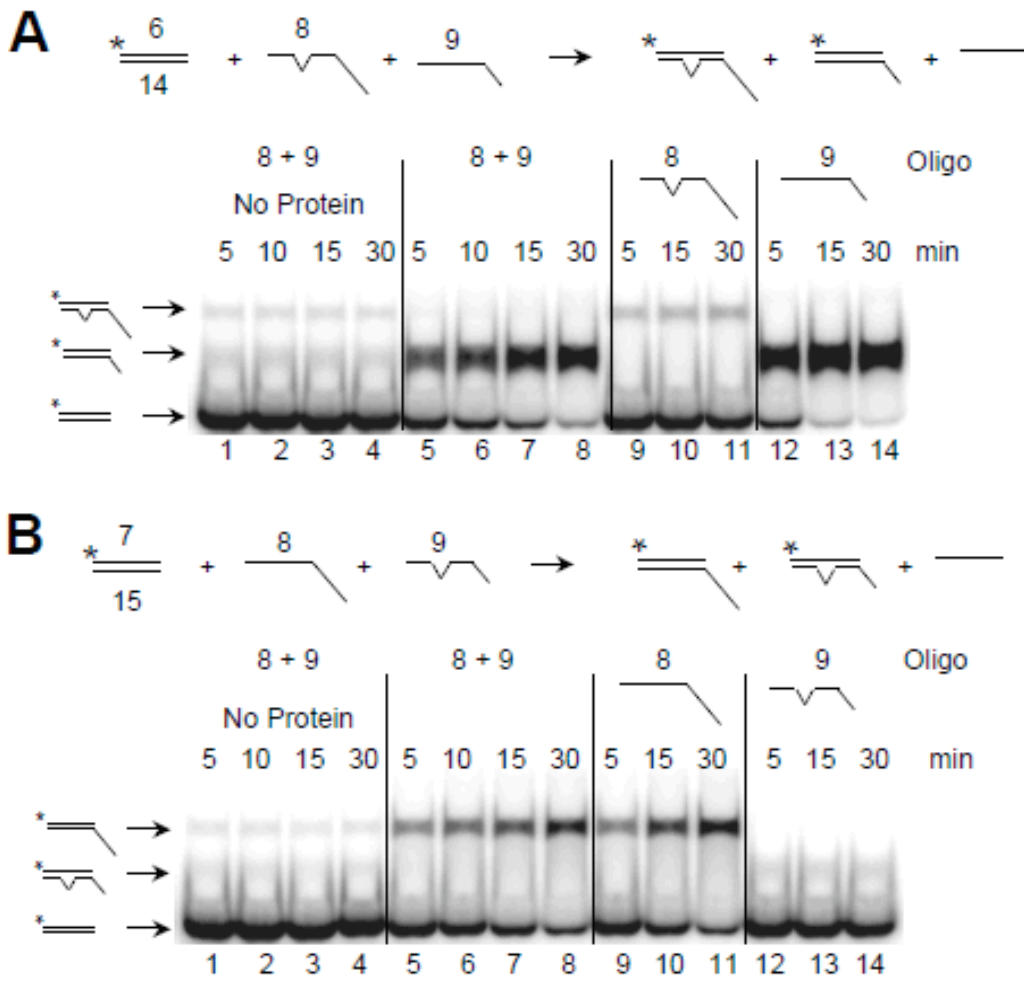

FIGURE 27. Sgs1$_{103\text{-}322}$-catalyzed SE is inhibited by a single mismatched base-pair

(**a**) The indicated SE reaction was carried out using 1 nM of a ^{32}P-labeled donor DNA with flush ends and 20 nM of either oligo 8 alone (*Lanes 9-11*), oligo 9 alone (*Lanes 12-14*), or both oligos (*Lanes 1-8*) as recipient. Sgs1$_{103\text{-}322}$ was either absent (*Lanes 1-4*) or present at 1.6 µM (*Lanes 5-14*). (**b**) The indicated SE reaction was performed as in (**a**). Note that reactions using flush donor substrates are slower than those with 3' ssDNA extensions.

Discussion

Blm/Sgs1 forms part of a multi-functional complex with both DNA helicase and DNA topoisomerase activities. The strand exchange activity we have characterized localizes to the N-terminus of Sgs1 and is a previously unidentified activity. Several results suggest that this SE activity is biologically relevant. First, SE is unusually stringent as it is inhibited on substrates containing a single mismatch. Based on this stringency, we are inclined to favor SE over SA as the bona fide *in vivo* activity. Second, SE is conserved in at least two other BLM orthologs. Third, the SE domain is required for most *in vivo* activities of *SGS1,* and in both cases that we tested the corresponding human domain was able to provide those activities. Fourth, control experiments rule out artifactual "meltase" or nuclease activities as explanations for strand transfer *in vitro*.

The SA and SE activities reported here appear to be distinct from similar activities associated with the helicase domains of BLM and other RecQ family members (Cheok, Wu et al. 2005; Muftuoglu, Kulikowicz et al. 2008). However, their relationship to similar activities identified in full-length RecQ homologs is not clear. Although the SA activity observed here is distinguished by its insensitivity to nucleotide analogs, the inhibition of SA by non-hydrolyzable analogs (Cheok, Wu et al. 2005; Machwe, Xiao et al. 2005; Sharma, Sommers et al. 2005; Muzzolini, Beuron et al. 2007; Capp, Wu et al. 2009) seems to be explained in part by the fixation of RecQ helicase on ssDNA in the presence of AMPPNP (Capp, Wu et al. 2009). Since this would affect both helicase- and non-helicase domains in the full-length protein, it is unclear whether the SA activities of all five RecQ homologs are limited to their helicase domains. In the case of SE, most RecQ family members require ATP. This includes the ability of WRN, BLM, and

RecQ5ß to catalyze coordinated ATP-dependent DNA strand exchange reactions (Machwe, Xiao et al. 2005; Machwe, Lozada et al. 2006; Weinert and Rio 2007) in addition to the reported second helicase domain of the RecQ4 N-terminus (Xu and Liu 2009). However, strand exchange by both BLM and WRN has been observed in the absence of ATP (Machwe, Xiao et al. 2005; Bugreev, Mazina et al. 2009). Therefore an important next step is to determine whether the SA and SE activities we have described can be assayed when tethered to the RecQ helicase domain and whether they are regulated by the helicase.

Several details of this work suggest that the BLM/Sgs1 strand exchange activity is linked to Top3-Rmi1 function. First, the location of the SE domain adjacent to the Top3-Rmi1 binding domain (TR) suggests that SE and Top3-Rmi1 act on the same substrate based simply on their proximity. Second, strand exchange would be expected to generate topological problems in a chromosomal context that would require topoisomerase activity. Third, removal of the TR domain uncovers an SE-dependent toxicity (Mullen, Kaliraman et al. 2000) that appears to phenocopy *top3*Δ (Wallis, Chrebet et al. 1989; Bennett and Wang 2001; Weinstein and Rothstein 2008). Although the hypermorphic phenotype of such *sgs1*-Δ*SE* alleles is suppressed by helicase-defective *SGS1* alleles, it is not known whether translocation by the helicase is actually driving this genetic instability. Since stable ssDNA binding by both BLM and RecQ4 is dependent on ATP (Weinert and Rio 2007; Capp, Wu et al. 2009), mutations that reduce the ability of Sgs1 to bind and/or hydrolyze ATP may have multiple effects. Thus, it is possible that helicase-defective *SGS1* alleles suppress the hypermorphic phenotype indirectly by inhibiting its ability to bind DNA. We suggest that the above results are most simply

explained by a model in which SE generates a substrate for Top3-Rmi1. More specifically, SE may provide the necessary directionality for strand passage or access to ssDNA that is required by DNA topoisomerase III.

In Fig. 28 we relate these ideas to two of the most likely pathways for BLM/Sgs1 function. BLM/Sgs1 is thought to play a role in dismantling D-loops given that D-loops are optimal substrates for BLM unwinding (Bachrati, Borts et al. 2006), that D-loop unwinding is an essential step in the Synthesis-Dependent Strand Annealing (SDSA) pathway for which BLM is required in *Drosophila* (Adams, McVey et al. 2003), and that the SE domain binds D-loops on its own (Figure 16b). As shown in Figure 27a, we suggest that an essential role of BLM/Sgs1 is not simply to displace the invading strand with its helicase activity but to properly restore the D-loop to its duplex state. D-loop formation should involve unwinding of the parental duplex especially in cases where the invading strand is extended significantly by DNA polymerase. Thus, in wt cells, BLM/Sgs1 could bind at the proximal end of the D-loop where the SE domain drives reannealing of the donor duplex (Figure 28a, i) and displacement of the invading strand in a simplified strand-transfer reaction (ii). Importantly, the reannealling step requires the catenating activity of Top3-Rmi1 to re-wind the donor duplex (iii). The BLM/Sgs1 3'-5' DNA helicase activity is expected to assist in the displacement of the invading strand. In this model, the genomic instability of *top3*Δ strains may arise due to displacement of the invading strand in the absence of re-winding the parental duplex. The formation of such unwound DNA, which is expected to be recombinogenic, may be exacerbated in *sgs1-*Δ*SE* strains if Top3-Rmi1 regulates SE function.

Recent models of BLM-Top3α function have noted the need for directional strand transfer (Plank and Hsieh 2009) in double HJ dissolution (Wu and Hickson 2003; Plank, Wu et al. 2006). Figure 28b illustrates how the "HJ migration" model (Plank and Hsieh 2009) of dHJ dissolution could be aided by the SE domain by promoting the transfer of a HJ strand from one (lower) duplex to its complement in the other (upper) duplex (Figure 14b, dotted arrow). Such a transfer generates multiple topological constraints such as the intertwining on the bottom duplex (i), for example. The SE domain is expected to cooperate with Top3-Rmi1 to catalyze strand passage (ii) to remove this intertwining (iii). This unwinding event on the lower duplex must be coordinated with re-winding on the top duplex which is formally the same mechanism described in Fig. 28a. The final decatenation step in this pathway provides the best example of how the SE domain provides directionality to Top3-Rmi1strand passage (Figure 28b). Active annealing of complementary strands by SE generates constraints to be relieved by Top3-Rmi1 and the directionality needed to separate the two hemicatenanes. Such forced annealing might also contribute to the sickness of *top3*Δ single mutants. Finally, the SE domain may be involved in sensing mismatches in heteroduplex, along with mismatch repair proteins, to promote gene conversion (Sugawara, Goldfarb et al. 2004; Lo, Paffett et al. 2006).

We previously reasoned that $Sgs1_{1\text{-}652}$ contained an important functional domain since it suppressed certain *sgs1*Δ phenotypes alone, and because *SGS1* alleles lacking the TR domain displayed a hypermorphic phenotype (Mullen, Kaliraman et al. 2000). Although an intact Sgs1 DNA helicase domain is necessary to observe the hypermorphic phenotype (Mullen, Kaliraman et al. 2000; Weinstein and Rothstein 2008), it cannot be the sole cause of the instability since the SE domain is also required. Similarly, although

Sgs1 DNA helicase activity plays a role in the *top3*Δ slow-growth phenotype (Gangloff, McDonald et al. 1994), the SE domain does as well (Figure 24b). Although further experiments are needed to determine exact roles of these two activities, it remains possible that the SE domain is the ultimate source of *top3*Δ instability. The ability of the SE domain to unwind and rewind DNA strands may explain why *SGS1* alleles lacking DNA helicase activity retain the capacity to promote gene conversion, suppress MMS sensitivity, suppress hyper-recombination, suppress meiotic sporulation defects, and induce slow-growth in *top3*Δ cells (Lu, Mullen et al. 1996; Miyajima, Seki et al. 2000; Mullen, Kaliraman et al. 2000; Rockmill, Fung et al. 2003; Lo, Paffett et al. 2006).

FIGURE 28. Proposed roles of SE in Sgs1-Top3-Rmi1 function

(**a**) SE-dependent D-loop unwinding in the SDSA recombination pathway. Following strand invasion and elongation, the nascent strand (red) is displaced by the combined activities of Top3, Rmi1, Sgs-SE and Sgs1 helicase (T, R, SE and H, respectively). As shown in the bracket are intermediate steps: the displaced parental strand is rewound by SE which anneals the blue parental strands (i) and displaces the red nascent strand (ii) while Top3-Rmi1 interlinks the parental strands (iii). Repeating this cycle "n" times leads to strand displacement. (**b**) SE mediates double HJ branch migration. The circular inset presents an example where the red DNA strand of the right-hand HJ is annealed back to its parental complement (in the direction of the dotted arrow). As in branch migration, this displaces the blue strand in the upper heteroduplex so that it can be re-annealled to the lower duplex (in this case by SE), however the DNA between two HJs is topologically constrained. Shown in the bracket is an example of the topological stress encountered on the bottom duplex (i) where the red strand must pass through the blue strand via Top3-Rmi1 activity (ii) yielding one unlinking of the bottom duplex (iii). Not shown is the rewinding of the lower blue strands or reciprocal reactions on the upper duplex. Repeating these cycles of SE- and Top3-Rmi1-mediated strand passage "n" times leads to displacement of the heteroduplex between the HJs and formation of a double hemi-catenane. Resolution of the hemi-catenane is promoted by the strand annealing activity of SE and catalyzed by Top3-Rmi1 to yield non-crossover products.

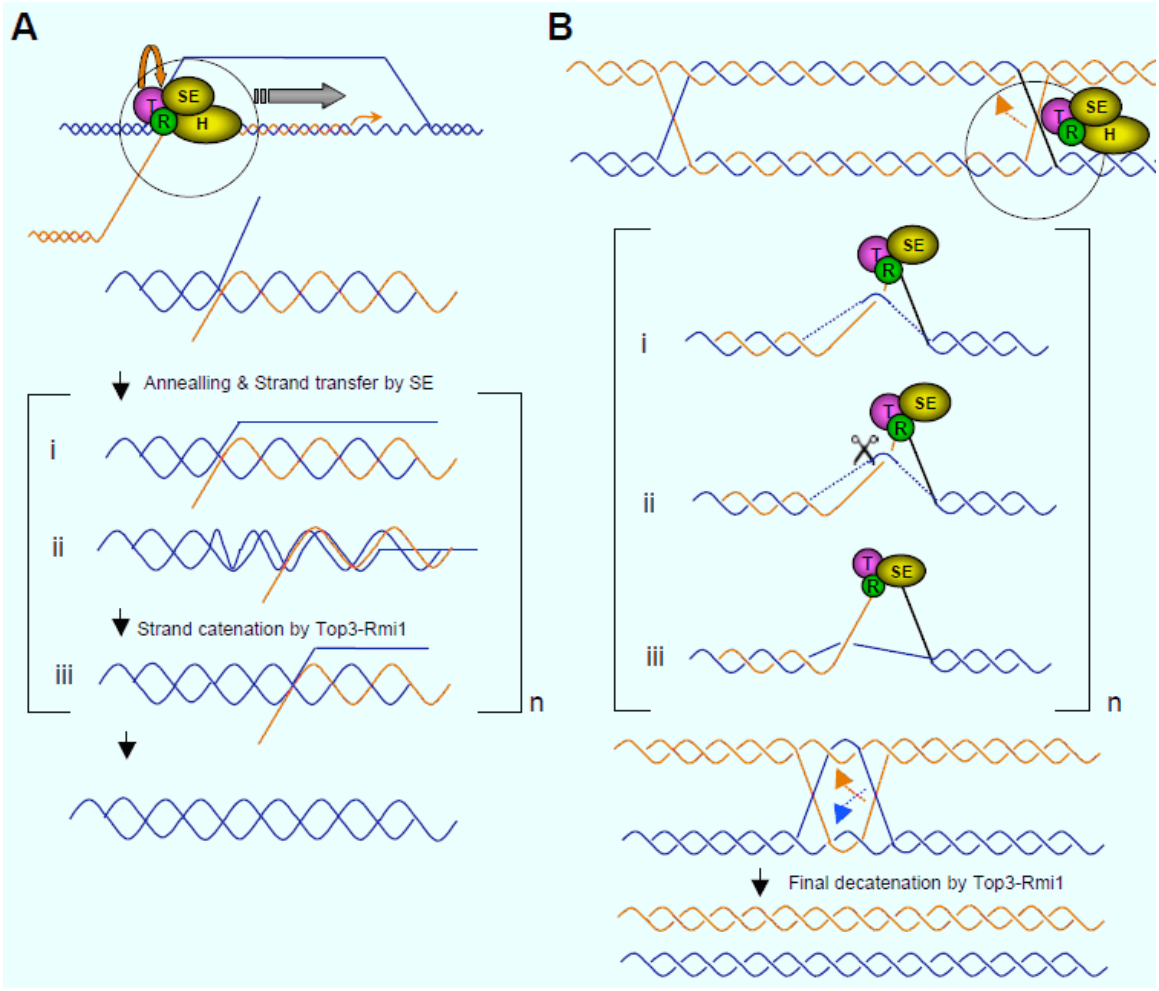
A
SE
T
R
H
Annealling & Strand transfer by SE
i
ii
Strand catenation by Top3-Rmi1
iii
n
B
SE
T
R
H
i
ii
iii
n
Final decatenation by Top3-Rmi1

Experimental Methods

Proteins and DNA substrates

All GST-fusion proteins including $Sgs1_{1-158}$, $Sgs1_{1-322}$, $Sgs1_{1-652}$, $Sgs1_{323-652}$, $Sgs1_{51-322}$, $Sgs1_{103-322}$, $Sgs1_{159-484}$, $Sgs1_{103-250}$, $hsBLM_{1-294}$, and $dmBLM_{1-380}$ were expressed and purified from *E. coli* BL21(DE3)-RIL cells as described for GST-$Sgs1_{1-158-HA}$ (Fricke, Kaliraman et al. 2001). All His6-tagged proteins including $Sgs1_{1-652}$, $Sgs1_{1-322}$, $Sgs1_{103-322}$, $hsBLM_{1-294}$ and $dmBLM_{1-380}$ were expressed and purified essentially as described for $Sgs1_{1-652}$-V5(His6) (Chen and Brill 2007). *E. coli* BL21(DE3)-RIL cells were transformed with T7 expression plasmids and colonies were pooled and grown in 1L LB media containing 0.1 mg/ml ampicillin at 37°C until OD600 = 0.4. The recombinant protein was induced by addition of 0.4 mM isopropyl-1-thio-D-galactopyranoside and the cells were grown at 16°C for 16 hours. Induced cells were pelleted and resuspended in 40 ml Buffer N (25 mM Tris-HCl (pH7.5), 0.1 mM phenylmethylsulfonyl fluoride, 0.01% Nonidet P-40, 1 mM dithiothreitol, 10 % glycerol and 500 mM NaCl) containing 10 mM imidazole and protease inhibitors as above. The cells were sonicated for 2 min with a Branson sonifer 450 microtip at setting 2 and 25% duty cycle. The lysate was centrifuged at 13,500 rpm in an SS34 rotor at 4°C for 15 min and the supernatant was filtered before loading onto a 5 ml Ni column. The column was washed with 10 CVs of Buffer N plus 10 mM imidazole and eluted with a 8 CV gradient from 10 to 500 mM imidazole in Buffer Peak fractions were pooled and dialyzed against buffer A (25 mM Tris-HCl (pH7.5), 0.1 mM phenylmethylsulfonyl fluoride, 0.01% Nonidet P-40, 1 mM dithiothreitol, 10 % glycerol and 1mM EDTA) plus 200 mM NaCl and stored at 80°C. The oligonucleotides (IDT) used in this study are shown in

Table 4. Plasmid-based D-loop used for DNA binding assay was prepared and purified as described previously (McIlwraith, Vaisman et al. 2005).

EMSA DNA binding assay

^{32}P-labeled DNA substrates were prepared and assayed by EMSA essentially as described (Mullen, Nallaseth et al. 2005). Proteins were were incubated with ^{32}P-labeled DNA substrate in a final volume of 20 µl containing 25 mM Tris (pH 7.5), 50 mM NaCl, 1 mM dithiothreitol, 1.0 mg/ml BSA, and at 25°C for 20 min. Loading dye was added to a final concentration of 8% glycerol and 0.25% bromophenol blue. Oligonucleotide binding was tested by electrophoresis at 10 volts/cm through a 10% polyacrylamide gel (29:1 acrylamide:bis) in 1X TBE at room temperature. Binding to plasmid-based DNA probes was detected on a 2.5% polyacrylamide mixed with 0.8% agarose at room temperature. The gel was fixed in 50% EtOH/10% acetic acid for 15 min, dried, and visualized by a Molecular Dynamics phosphorimager.

DNA Filter-binding assay

Reactions were performed as described in EMSA but analyzed by alkali-treated nitrocellulose paper (McEntee et al, 1981). Reactions were filtered under vacuum onto a 0.45 _m Protran nitrocellulose membrane (*Whatman*) and washed with 0.5 ml of reaction buffer twice at room temperature. Filters were dried and assayed for radioactivity by scintillation counting.

Strand annealing assay and strand exchange assay

The standard strand annealing and strand transfer reactions contained 25 mM Tris-HCl (pH 7.5), 50 mM sodium chloride, 1 mM EDTA, 10 µg/ml bovine serum albumin and 1 mM DDT in a final volume of 20 µl. The reactions were assembled on ice and initiated by shifting to 37 °C for 5 min. Reactions were stopped by treating with a final concentration of 50 mM EDTA, 1% SDS and 1 mg/ml proteinase K at 37 °C for 15 min. The STOP buffer for all strand annealing reactions included unlabeled version of the labeled oligo at a final concentration of 100 nM (oligo 1 or 6) (Machwe, Lozada et al. 2006). After addition of loading dye the samples were resolved on a 10% polyacrylamide at room temperature.

Genetic assays

Synthetic lethality, MMS sensitivity and genetic recombination were assayed as described (Mullen, Kaliraman et al. 2000). The heteroduplex rejection assay based on cell survival was performed as described previously (Goldfarb and Alani 2005).

Yeast extract preparation and immunoprecipitation

The cell pellet from 2L of culture was resuspended in 2x CE buffer [50 mM Tris-HCl (pH 7.5), 4 mM magnesium chloride, 1 mM EDTA, 20% glycerol, 5 mM DTT, 0.5 M sodium chloride] plus the following protease inhibitors (PIs): pepstatin, 10 mg/ml; leupeptin, 5 mg/ml; benzamidine, 10 mM; bacitracin, 100 mg/ml; aprotinin, 20 mg/ml; phenylmethylsulfonyl fluoride, 0.1 mM and sodium metabisulfite, 10mM. This cell suspension was frozen in liquid nitrogen and pulverized under liquid nitrogen using a SPEX 6850 freezer mill (Spex Inc., Metuchen, NJ). The sample was thawed and

centrifuged in a Ti45 rotor at 44,000 RPM for 30 min. Typical extracts contained 10 mg/ml protein which were aliquoted and stored at -80°C.

Immunoprecipitations (IPs) were performed at 4°C as follows. Two mg of total protein were incubated for one hour with 40 μl protein G-Sepharose beads conjugated to anti-FLAG mouse monoclonal antibodies (Sigma), or with 1 μl of anti-HA (Roche, 5 μg/μl) or anti-V5 (Invitrogen, 1 μg/μl) monoclonal antibodies. Thirty microliters of Protein-A sepharose beads (Amersham-Pharmacia) were added to each sample, followed by rocking for one hour. The immune complexes were then washed three times with 1 ml of RIPA buffer [150 mM NaCl, 50 mM Tris-HCl (pH 7.5), 1% (v/v) NP40, 0.5% (w/v) deoxycholate, 0.1% (w/v) SDS]. Bound proteins were resuspended in Laemmli buffer and resolved by sodium dodecylsulfate polyacrylamide gel electrophoresis (SDS-PAGE). Following SDS-PAGE the gels were transferred to nitrocellulose membranes and treated with either anti-FLAG (Sigma), anti-V5, or anti-HA as the primary antibody at a 1:10,000 dilution. Blots were then treated with anti-mouse HRP-conjugated secondary antibody (1:10,000; Gibco-BRL) and developed with chemiluminescence reagents (Pierce) prior to capturing the image on a chemiluminescence camera (Fujifilm).

Table 4. Oligonucleotides used in this study

Oligo Name	Original name	Size	DNA sequence (5'-3')
1	1253	50	TGGGTCAACGTGGGCAAAGATGTCCTAGCAATGTAATCGTCTATGACGTT
2	1254	50	TGCCGAATTCTACCAGTGCCAGTGATGGACATCTTTGCCCACGTTGACCC
3	2558	25	TGGGTCAACGTGGGCAAAGATGTCC
4	2559	25	GGACATCTTTGCCCACGTTGACCCA
5	2600	25	TCACTGGCACTGGTAGAATTCGGCA
6	2625	32	TCCTTTTGATAAGAGGTCATTTTTGCGGATGG
7	2640	32	TCCTTTTGATAAGAGCTCATTTTTGCGGATGG
8	2651	94	CTTTAGCTGCATATTTACAACATGTTGACCTACAGCACCAGATTCAGCAATTAAGCTCTAAGCCATCCGCAAAAATGAGCTCTTATCAAAAGGA
9	2655	57	CCAGATTCAGCAATTAAGCTCTATCCCATCCGCAAAAATGACCTCTTATCAAAAGGA
10	2624	57	CCATCCGCAAAAATGACCTCTTATCAAAAGGATGGACATCTTTGCCCACGTTGACCC
11	2626	94	CTTTAGCTGCATATTTACAACATGTTGACCTACAGCACCAGATTCAGCAATTAAGCTCTAAGCCATCCGCAAAAATGACCTCTTATCAAAAGGA
12	2653	34	TCTCCTTTTGATAAGAGGTCATTTTTGCGGATGG
13	2654	34	TCCTTTTGATAAGAGGTCATTTTTGCGGATGGCT
14	2639	32	CCATCCGCAAAAATGACCTCTTATCAAAAGGA
15	2641	32	CCATCCGCAAAAATGAGCTCTTATCAAAAGGA
16	2129 (Phi-X174)	50	AAAGGTCGCAAAGTAAGAGCTTCTCGAGCTGCGCAAGGATAGGTCGAATT
17	2044 (D-loop)	50	CGTTCTTCGGGGCGAAAACTCTCAAGGATCTTACCGCTGTTGAGATCCAG
18	1317 (DNA binding)	90	GATCCGAATTCTGGCTTGCTAGGACATCTTTGCCCACGTTGACCCGGGTTGGCGTTAGGAGATAGTCAGTTATAGCTGCGGCTGCTAAGG

Epilogue

This work has led to the further understanding of Sgs1-Top3-Rmi1 complex. Further biochemical characterization of Sgs1-Top3-Rmi1 will reveal how Sgs1-Top3-Rmi1 complex works on DNA repair and genome stability. Although full length Sgs1 has been purified recently, the function of Sgs1-Top3-Rmi1 is not clear. Purification of Sgs1-Top3-Rmi1 complex or individual proteins will allow us to test different biochemical assays and lead to understanding of the function of Sgs1-Top3-Rmi1 on double strand break repair.

Further characterization of N-terminus BLM, WRN and RECQ4 can elucidate what is the function of N-terminus RecQ family in human. It is interesting to know whether these N-terminus human RecQ paralogs have the same acitivity, especially for strand-exchange activity.

Sgs1-SE domain and Rad52-SE domain have an ATP- independent strand exchange activity *in vitro*. It is reasonable to compare their strand exchange activities. Purification and characterization of Rad52 should allow us to understand what is different in strand exchange activity between Sgs1-SE and Rad52-SE.

References

1. Abdel-Monem, M., H. Durwald, et al. (1976). "Enzymic unwinding of DNA. 2. Chain separation by an ATP-dependent DNA unwinding enzyme." Eur J Biochem **65**(2): 441-9.
2. Adams, M. D., M. McVey, et al. (2003). "Drosophila BLM in double-strand break repair by synthesis-dependent strand annealing." Science **299**(5604): 265-7.
3. Agrawal, V. and K. V. Kishan (2003). "OB-fold: growing bigger with functional consistency." Curr Protein Pept Sci **4**(3): 195-206.
4. Ajima, J., K. Umezu, et al. (2002). "Elevated incidence of loss of heterozygosity (LOH) in an sgs1 mutant of Saccharomyces cerevisiae: roles of yeast RecQ helicase in suppression of aneuploidy, interchromosomal rearrangement, and the simultaneous incidence of both events during mitotic growth." Mutat Res **504**(1-2): 157-72.
5. Bachrati, C. Z., R. H. Borts, et al. (2006). "Mobile D-loops are a preferred substrate for the Bloom's syndrome helicase." Nucleic Acids Res **34**(8): 2269-79.
6. Bachrati, C. Z. and I. D. Hickson (2003). "RecQ helicases: suppressors of tumorigenesis and premature aging." Biochem J **374**(Pt 3): 577-606.
7. Bahr, A., F. De Graeve, et al. (1998). "Point mutations causing Bloom's syndrome abolish ATPase and DNA helicase activities of the BLM protein." Oncogene **17**(20): 2565-71.
8. Balajee, A. S., A. Machwe, et al. (1999). "The Werner syndrome protein is involved in RNA polymerase II transcription." Mol Biol Cell **10**(8): 2655-68.
9. Bastin-Shanower, S. A., W. M. Fricke, et al. (2003). "The mechanism of Mus81-Mms4 cleavage site selection distinguishes it from the homologous endonuclease Rad1-Rad10." Mol Cell Biol **23**(10): 3487-96.
10. Bennett, R. J. and J. L. Keck (2004). "Structure and function of RecQ DNA helicases." Crit Rev Biochem Mol Biol **39**(2): 79-97.
11. Bennett, R. J., J. L. Keck, et al. (1999). "Binding specificity determines polarity of DNA unwinding by the Sgs1 protein of S. cerevisiae." J Mol Biol **289**(2): 235-48.
12. Bennett, R. J., M. F. Noirot-Gros, et al. (2000). "Interaction between yeast sgs1 helicase and DNA topoisomerase III." J Biol Chem **275**(35): 26898-905.
13. Bennett, R. J., M. F. Noirot-Gros, et al. (2000). "Interaction between yeast Sgs1 helicase and DNA topoisomerase III." J Biol Chem **275**(35): 26898-26905.
14. Bennett, R. J., J. A. Sharp, et al. (1998). "Purification and characterization of the Sgs1 DNA helicase activity of Saccharomyces cerevisiae." J Biol Chem **273**(16): 9644-50.

15. Bennett, R. J. and J. C. Wang (2001). "Association of yeast DNA topoisomerase III and Sgs1 DNA helicase: studies of fusion proteins." Proc Natl Acad Sci U S A **98**(20): 11108-13.
16. Bernstein, D. A. and J. L. Keck (2003). "Domain mapping of Escherichia coli RecQ defines the roles of conserved N- and C-terminal regions in the RecQ family." Nucleic Acids Res **31**(11): 2778-85.
17. Bernstein, D. A. and J. L. Keck (2005). "Conferring substrate specificity to DNA helicases: role of the RecQ HRDC domain." Structure **13**(8): 1173-82.
18. Bernstein, D. A., M. C. Zittel, et al. (2003). "High-resolution structure of the E.coli RecQ helicase catalytic core." EMBO J **22**(19): 4910-21.
19. Bernstein, K. A., E. Shor, et al. (2009). "Sgs1 function in the repair of DNA replication intermediates is separable from its role in homologous recombinational repair." EMBO J **28**(7): 915-25.
20. Bi, B., N. Rybalchenko, et al. (2004). "Human and yeast Rad52 proteins promote DNA strand exchange." Proc Natl Acad Sci U S A **101**(26): 9568-72.
21. Bochkarev, A. and E. Bochkareva (2004). "From RPA to BRCA2: lessons from single-stranded DNA binding by the OB-fold." Curr Opin Struct Biol **14**(1): 36-42.
22. Bochkarev, A., R. A. Pfuetzner, et al. (1997). "Structure of the single-stranded-DNA-binding domain of replication protein A bound to DNA." Nature **385**(6612): 176-81.
23. Brosh, R. M., Jr., D. K. Orren, et al. (1999). "Functional and physical interaction between WRN helicase and human replication protein A." J Biol Chem **274**(26): 18341-50.
24. Bugreev, D. V., O. M. Mazina, et al. (2009). "Bloom syndrome helicase stimulates RAD51 DNA strand exchange activity through a novel mechanism." J Biol Chem **284**(39): 26349-59.
25. Bugreev, D. V., X. Yu, et al. (2007). "Novel pro- and anti-recombination activities of the Bloom's syndrome helicase." Genes Dev **21**(23): 3085-94.
26. Bussen, W., S. Raynard, et al. (2007). "Holliday junction processing activity of the BLM-Topo IIIalpha-BLAP75 complex." J Biol Chem **282**(43): 31484-92.
27. Capp, C., J. Wu, et al. (2009). "Drosophila RecQ4 has a 3'-5' DNA helicase activity that is essential for viability." J Biol Chem **284**(45): 30845-52.
28. Capp, C., J. Wu, et al. (2009). "*Drosophila* RecQ4 has a 3'-5'DNA helicase activity that is essential for viability." J Biol Chem.
29. Caruthers, J. M. and D. B. McKay (2002). "Helicase structure and mechanism." Curr Opin Struct Biol **12**(1): 123-33.
30. Cejka, P. and S. C. Kowalczykowski "The full-length S. cerevisiae SGS1 protein is a vigorous DNA helicase that preferentially unwinds Holliday junctions." J Biol Chem.

31. Chaganti, R. S., S. Schonberg, et al. (1974). "A manyfold increase in sister chromatid exchanges in Bloom's syndrome lymphocytes." Proc Natl Acad Sci U S A **71**(11): 4508-12.
32. Chang, M., M. Bellaoui, et al. (2005). "RMI1/NCE4, a suppressor of genome instability, encodes a member of the RecQ helicase/Topo III complex." EMBO J **24**(11): 2024-33.
33. Chen, C. F. and S. J. Brill (2007). "Binding and activation of DNA topoisomerase III by the Rmi1 subunit." J Biol Chem **282**(39): 28971-9.
34. Cheok, C. F., C. Z. Bachrati, et al. (2005). "Roles of the Bloom's syndrome helicase in the maintenance of genome stability." Biochem Soc Trans **33**(Pt 6): 1456-9.
35. Cheok, C. F., L. Wu, et al. (2005). "The Bloom's syndrome helicase promotes the annealing of complementary single-stranded DNA." Nucleic Acids Res **33**(12): 3932-41.
36. Chu, W. K. and I. D. Hickson (2009). "RecQ helicases: multifunctional genome caretakers." Nat Rev Cancer **9**(9): 644-54.
37. Cohen, H. and D. A. Sinclair (2001). "Recombination-mediated lengthening of terminal telomeric repeats requires the Sgs1 DNA helicase." Proc Natl Acad Sci U S A **98**(6): 3174-9.
38. Cromie, G. A., R. W. Hyppa, et al. (2008). "The fission yeast BLM homolog Rqh1 promotes meiotic recombination." Genetics **179**(3): 1157-67.
39. Cui, S., D. Arosio, et al. (2004). "Analysis of the unwinding activity of the dimeric RECQ1 helicase in the presence of human replication protein A." Nucleic Acids Res **32**(7): 2158-70.
40. DiGate, R. J. and K. J. Marians (1988). "Identification of a potent decatenating enzyme from *Escherichia coli*." J Biol Chem **263**(26): 13366-73.
41. Doherty, K. M., J. A. Sommers, et al. (2005). "Physical and functional mapping of the replication protein a interaction domain of the werner and bloom syndrome helicases." J Biol Chem **280**(33): 29494-505.
42. Duno, M., B. Thomsen, et al. (2000). "Genetic analysis of the Saccharomyces cerevisiae Sgs1 helicase defines an essential function for the Sgs1-Top3 complex in the absence of SRS2 or TOP1." Mol Gen Genet **264**(1-2): 89-97.
43. Ellis, N. A., J. Groden, et al. (1995). "The Bloom's syndrome gene product is homologous to RecQ helicases." Cell **83**(4): 655-66.
44. Fabre, F., A. Chan, et al. (2002). "Alternate pathways involving Sgs1/Top3, Mus81/ Mms4, and Srs2 prevent formation of toxic recombination intermediates from single-stranded gaps created by DNA replication." Proc Natl Acad Sci U S A **99**(26): 16887-92.
45. Feng, Q., L. During, et al. (2007). "Rad52 and Rad59 exhibit both overlapping and distinct functions." DNA Repair (Amst) **6**(1): 27-37.

46. Frei, C. and S. M. Gasser (2000). "The yeast Sgs1p helicase acts upstream of Rad53p in the DNA replication checkpoint and colocalizes with Rad53p in S-phase-specific foci." Genes Dev **14**(1): 81-96.
47. Fricke, W. M., V. Kaliraman, et al. (2001). "Mapping the DNA topoisomerase III binding domain of the Sgs1 DNA helicase." J Biol Chem **276**(12): 8848-55.
48. Fricke, W. M., V. Kaliraman, et al. (2001). "Mapping the DNA topoisomerase III binding domain of the Sgs1 DNA helicase." J Biol Chem **276**(12): 8848-55.
49. Gangloff, S., B. de Massy, et al. (1999). "The essential role of yeast topoisomerase III in meiosis depends on recombination." EMBO J **18**(6): 1701-11.
50. Gangloff, S., J. P. McDonald, et al. (1994). "The yeast type I topoisomerase Top3 interacts with Sgs1, a DNA helicase homolog: a potential eukaryotic reverse gyrase." Mol Cell Biol **14**(12): 8391-8.
51. Gangloff, S., J. P. McDonald, et al. (1994). "The yeast type I topoisomerase Top3 interacts with Sgs1, a DNA helicase homolog: a potential eukaryotic reverse gyrase." Molecular & Cellular Biology **14**(12): 8391-8.
52. Gangloff, S., C. Soustelle, et al. (2000). "Homologous recombination is responsible for cell death in the absence of the Sgs1 and Srs2 helicases." Nat Genet **25**(2): 192-4.
53. Garcia, P. L., Y. Liu, et al. (2004). "Human RECQ5beta, a protein with DNA helicase and strand-annealing activities in a single polypeptide." EMBO J **23**(14): 2882-91.
54. German, J., R. Archibald, et al. (1965). "Chromosomal Breakage in a Rare and Probably Genetically Determined Syndrome of Man." Science **148**: 506-7.
55. German, J., M. M. Sanz, et al. (2007). "Syndrome-causing mutations of the BLM gene in persons in the Bloom's Syndrome Registry." Hum Mutat **28**(8): 743-53.
56. Gogol, E. P., S. E. Seifried, et al. (1991). "Structure and assembly of the Escherichia coli transcription termination factor rho and its interaction with RNA. I. Cryoelectron microscopic studies." J Mol Biol **221**(4): 1127-38.
57. Goldfarb, T. and E. Alani (2005). "Distinct roles for the *Saccharomyces cerevisiae* mismatch repair proteins in heteroduplex rejection, mismatch repair and nonhomologous tail removal." Genetics **169**(2): 563-74.
58. Guo, R. B., P. Rigolet, et al. (2005). "Structural and functional characterizations reveal the importance of a zinc binding domain in Bloom's syndrome helicase." Nucleic Acids Res **33**(10): 3109-24.
59. Harmon, F. G., R. J. DiGate, et al. (1999). "RecQ helicase and topoisomerase III comprise a novel DNA strand passage function: a conserved mechanism for control of DNA recombination." Mol Cell **3**(5): 611-20.

60. Harmon, F. G. and S. C. Kowalczykowski (2001). "Biochemical characterization of the DNA helicase activity of the escherichia coli RecQ helicase." J Biol Chem **276**(1): 232-43.
61. Hickman, A. B. and F. Dyda (2005). "Binding and unwinding: SF3 viral helicases." Curr Opin Struct Biol **15**(1): 77-85.
62. Hickson, I. D. (2003). "RecQ helicases: caretakers of the genome." Nat Rev Cancer **3**(3): 169-78.
63. Hook, G. J., E. Kwok, et al. (1984). "Sensitivity of Bloom syndrome fibroblasts to mitomycin C." Mutat Res **131**(5-6): 223-30.
64. Hu, J. S., H. Feng, et al. (2005). "Solution structure of a multifunctional DNA- and protein-binding motif of human Werner syndrome protein." Proc Natl Acad Sci U S A **102**(51): 18379-84.
65. Hu, Y., X. Lu, et al. (2005). "Recql5 and Blm RecQ DNA helicases have nonredundant roles in suppressing crossovers." Mol Cell Biol **25**(9): 3431-42.
66. Huang, P., F. E. Pryde, et al. (2001). "SGS1 is required for telomere elongation in the absence of telomerase." Curr Biol **11**(2): 125-9.
67. Ii, M. and S. J. Brill (2005). "Roles of SGS1, MUS81, and RAD51 in the repair of lagging-strand replication defects in Saccharomyces cerevisiae." Curr Genet **48**(4): 213-25.
68. Ii, T., J. Fung, et al. (2007). "The yeast Slx5-Slx8 DNA integrity complex displays ubiquitin ligase activity." Cell Cycle **6**(22): 2800-9.
69. Ii, T., J. R. Mullen, et al. (2007). "Stimulation of in vitro sumoylation by Slx5-Slx8: evidence for a functional interaction with the SUMO pathway." DNA Repair (Amst) **6**(11): 1679-91.
70. Ilyina, T. V., A. E. Gorbalenya, et al. (1992). "Organization and evolution of bacterial and bacteriophage primase-helicase systems." J Mol Evol **34**(4): 351-7.
71. Ira, G., A. Malkova, et al. (2003). "Srs2 and Sgs1-Top3 suppress crossovers during double-strand break repair in yeast." Cell **115**(4): 401-11.
72. Johnson, F. B., R. A. Marciniak, et al. (2001). "The Saccharomyces cerevisiae WRN homolog Sgs1p participates in telomere maintenance in cells lacking telomerase." EMBO J **20**(4): 905-13.
73. Kaliraman, V., J. R. Mullen, et al. (2001). "Functional overlap between Sgs1-Top3 and the Mms4-Mus81 endonuclease." Genes Dev **15**(20): 2730-40.
74. Karow, J. K., R. K. Chakraverty, et al. (1997). "The Bloom's syndrome gene product is a 3'-5' DNA helicase." J Biol Chem **272**(49): 30611-4.
75. Karow, J. K., A. Constantinou, et al. (2000). "The Bloom's syndrome gene product promotes branch migration of holliday junctions." Proc Natl Acad Sci U S A **97**(12): 6504-8.

76. Killoran, M. P. and J. L. Keck (2006). "Three HRDC domains differentially modulate Deinococcus radiodurans RecQ DNA helicase biochemical activity." J Biol Chem **281**(18): 12849-57.
77. Kim, R. A. and J. C. Wang (1992). "Identification of the yeast *TOP3* gene product as a single strand-specific DNA topoisomerase." J. Biol. Chem. **267**(24): 17178-85.
78. Kim, R. A. and J. C. Wang (1992). "Identification of the yeast TOP3 gene product as a single strand-specific DNA topoisomerase." J Biol Chem **267**(24): 17178-85.
79. Koonin, E. V. and A. E. Gorbalenya (1992). "The superfamily of UvrA-related ATPases includes three more subunits of putative ATP-dependent nucleases." Protein Seq Data Anal **5**(1): 43-5.
80. Korolev, S., J. Hsieh, et al. (1997). "Major domain swiveling revealed by the crystal structures of complexes of E. coli Rep helicase bound to single-stranded DNA and ADP." Cell **90**(4): 635-47.
81. Krepinsky, A. B., J. A. Heddle, et al. (1979). "Sensitivity of Bloom's syndrome lymphocytes to ethyl methanesulfonate." Hum Genet **50**(2): 151-6.
82. Laursen, L. V., E. Ampatzidou, et al. (2003). "Role for the fission yeast RecQ helicase in DNA repair in G2." Mol Cell Biol **23**(10): 3692-705.
83. Lee, J. W., J. Harrigan, et al. (2005). "Pathways and functions of the Werner syndrome protein." Mech Ageing Dev **126**(1): 79-86.
84. Lee, J. W., R. Kusumoto, et al. (2005). "Modulation of Werner syndrome protein function by a single mutation in the conserved RecQ domain." J Biol Chem **280**(47): 39627-36.
85. Lei, M., E. R. Podell, et al. (2003). "DNA self-recognition in the structure of Pot1 bound to telomeric single-stranded DNA." Nature **426**(6963): 198-203.
86. LeRoy, G., R. Carroll, et al. (2005). "Identification of RecQL1 as a Holliday junction processing enzyme in human cell lines." Nucleic Acids Res **33**(19): 6251-7.
87. Lindsley, J. E. (1999). "Overexpression and purification of Saccharomyces cerevisiae DNA topoisomerase II from yeast." Methods Mol Biol **94**: 187-97.
88. Liu, J. L., P. Rigolet, et al. (2004). "The zinc finger motif of Escherichia coli RecQ is implicated in both DNA binding and protein folding." J Biol Chem **279**(41): 42794-802.
89. Liu, Z., M. J. Macias, et al. (1999). "The three-dimensional structure of the HRDC domain and implications for the Werner and Bloom syndrome proteins." Structure **7**(12): 1557-66.
90. Lo, Y. C., K. S. Paffett, et al. (2006). "Sgs1 regulates gene conversion tract lengths and crossovers independently of its helicase activity." Mol Cell Biol **26**(11): 4086-94.

91. Lu, C. Y., C. H. Tsai, et al. "Sumoylation of the BLM ortholog, Sgs1, promotes telomere-telomere recombination in budding yeast." Nucleic Acids Res **38**(2): 488-98.
92. Lu, J., J. R. Mullen, et al. (1996). "Human homologs of yeast DNA helicase." Nature **383**: 678-9.
93. Lu, J., J. R. Mullen, et al. (1996). "Human homologues of yeast helicase." Nature **383**(6602): 678-9.
94. Lundblad, V. (2002). "Telomere maintenance without telomerase." Oncogene **21**(4): 522-31.
95. Machwe, A., E. M. Lozada, et al. (2006). "Competition between the DNA unwinding and strand pairing activities of the Werner and Bloom syndrome proteins." BMC Mol Biol **7**: 1.
96. Machwe, A., L. Xiao, et al. (2005). "RecQ family members combine strand pairing and unwinding activities to catalyze strand exchange." J Biol Chem **280**(24): 23397-407.
97. Macris, M. A., L. Krejci, et al. (2006). "Biochemical characterization of the RECQ4 protein, mutated in Rothmund-Thomson syndrome." DNA Repair (Amst) **5**(2): 172-80.
98. Maftahi, M., C. S. Han, et al. (1999). "The top3(+) gene is essential in Schizosaccharomyces pombe and the lethality associated with its loss is caused by Rad12 helicase activity." Nucleic Acids Res **27**(24): 4715-24.
99. Maftahi, M., J. C. Hope, et al. (2002). "The severe slow growth of Deltasrs2 Deltarqh1 in Schizosaccharomyces pombe is suppressed by loss of recombination and checkpoint genes." Nucleic Acids Res **30**(21): 4781-92.
100. Mankouri, H. W., T. J. Craig, et al. (2002). "SGS1 is a multicopy suppressor of srs2: functional overlap between DNA helicases." Nucleic Acids Res **30**(5): 1103-13.
101. Mankouri, H. W. and A. Morgan (2001). "The DNA helicase activity of yeast Sgs1p is essential for normal lifespan but not for resistance to topoisomerase inhibitors." Mech Ageing Dev **122**(11): 1107-20.
102. McIlwraith, M. J., A. Vaisman, et al. (2005). "Human DNA polymerase eta promotes DNA synthesis from strand invasion intermediates of homologous recombination." Mol Cell **20**(5): 783-92.
103. McVey, M., M. Kaeberlein, et al. (2001). "The short life span of Saccharomyces cerevisiae sgs1 and srs2 mutants is a composite of normal aging processes and mitotic arrest due to defective recombination." Genetics **157**(4): 1531-42.
104. Mimitou, E. P. and L. S. Symington (2008). "Sae2, Exo1 and Sgs1 collaborate in DNA double-strand break processing." Nature **455**(7214): 770-4.
105. Miyajima, A., M. Seki, et al. (2000). "Different domains of Sgs1 are required for mitotic and meiotic functions." Genes Genet Syst **75**(6): 319-26.

106. Miyajima, A., M. Seki, et al. (2000). "Different domains of Sgs1 are required for mitotic and meiotic functions." Genes Genet Syst **75**(6): 319-26.
107. Mortensen, U. H., C. Bendixen, et al. (1996). "DNA strand annealing is promoted by the yeast Rad52 protein." Proc Natl Acad Sci U S A **93**(20): 10729-34.
108. Moser, M. J., J. Oshima, et al. (1999). "WRN mutations in Werner syndrome." Hum Mutat **13**(4): 271-9.
109. Muftuoglu, M., T. Kulikowicz, et al. (2008). "Intrinsic ssDNA annealing activity in the C-terminal region of WRN." Biochemistry **47**(39): 10247-54.
110. Mullen, J. R., V. Kaliraman, et al. (2000). "Bipartite structure of the *SGS1* DNA helicase in *Saccharomyces cerevisiae*." Genetics **154**: 1101-14.
111. Mullen, J. R., V. Kaliraman, et al. (2000). "Bipartite structure of the SGS1 DNA helicase in Saccharomyces cerevisiae." Genetics **154**(3): 1101-14.
112. Mullen, J. R., V. Kaliraman, et al. (2001). "Requirement for three novel protein complexes in the absence of the Sgs1 DNA helicase in *Saccharomyces cerevisiae*." Genetics **157**(1): 103-18.
113. Mullen, J. R., V. Kaliraman, et al. (2001). "Requirement for three novel protein complexes in the absence of the Sgs1 DNA helicase in Saccharomyces cerevisiae." Genetics **157**(1): 103-18.
114. Mullen, J. R., F. S. Nallaseth, et al. (2005). "Yeast Rmi1/Nce4 controls genome stability as a subunit of the Sgs1-Top3 complex." Mol Cell Biol **25**(11): 4476-87.
115. Murray, J. M., H. D. Lindsay, et al. (1997). "Role of Schizosaccharomyces pombe RecQ homolog, recombination, and checkpoint genes in UV damage tolerance." Mol Cell Biol **17**(12): 6868-75.
116. Murzin, A. G. (1993). "OB(oligonucleotide/oligosaccharide binding)-fold: common structural and functional solution for non-homologous sequences." EMBO J **12**(3): 861-7.
117. Muzzolini, L., F. Beuron, et al. (2007). "Different quaternary structures of human RECQ1 are associated with its dual enzymatic activity." PLoS Biol **5**(2): e20.
118. Myung, K., A. Datta, et al. (2001). "SGS1, the Saccharomyces cerevisiae homologue of BLM and WRN, suppresses genome instability and homeologous recombination." Nat Genet **27**(1): 113-6.
119. Nakayama, H., K. Nakayama, et al. (1984). "Isolation and genetic characterization of a thymineless death-resistant mutant of Escherichia coli K12: identification of a new mutation (recQ1) that blocks the RecF recombination pathway." Mol Gen Genet **195**(3): 474-80.
120. Neff, N. F., N. A. Ellis, et al. (1999). "The DNA helicase activity of BLM is necessary for the correction of the genomic instability of bloom syndrome cells." Mol Biol Cell **10**(3): 665-76.

121. Nimonkar, A. V., A. Z. Ozsoy, et al. (2008). "Human exonuclease 1 and BLM helicase interact to resect DNA and initiate DNA repair." Proc Natl Acad Sci U S A **105**(44): 16906-11.
122. Oakley, T. J. and I. D. Hickson (2002). "Defending genome integrity during S-phase: putative roles for RecQ helicases and topoisomerase III." DNA Repair (Amst) **1**(3): 175-207.
123. Onoda, F., M. Seki, et al. (2000). "Elevation of sister chromatid exchange in Saccharomyces cerevisiae sgs1 disruptants and the relevance of the disruptants as a system to evaluate mutations in Bloom's syndrome gene." Mutat Res **459**(3): 203-9.
124. Onoda, F., M. Seki, et al. (2001). "Involvement of SGS1 in DNA damage-induced heteroallelic recombination that requires RAD52 in Saccharomyces cerevisiae." Mol Gen Genet **264**(5): 702-8.
125. Onodera, R., M. Seki, et al. (2002). "Functional and physical interaction between Sgs1 and Top3 and Sgs1-independent function of Top3 in DNA recombination repair." Genes Genet Syst **77**(1): 11-21.
126. Ooi, S. L., D. D. Shoemaker, et al. (2003). "DNA helicase gene interaction network defined using synthetic lethality analyzed by microarray." Nat Genet **35**(3): 277-86.
127. Orren, D. K., R. M. Brosh, Jr., et al. (1999). "Enzymatic and DNA binding properties of purified WRN protein: high affinity binding to single-stranded DNA but not to DNA damage induced by 4NQO." Nucleic Acids Res **27**(17): 3557-66.
128. Philipova, D., J. R. Mullen, et al. (1996). "A hierarchy of SSB protomers in replication protein A." Genes Dev **10**(17): 2222-33.
129. Plank, J. and T. S. Hsieh (2009). "Helicase-appended topoisomerases: new insight into the mechanism of directional strand transfer." J Biol Chem **284**(45): 30737-41.
130. Plank, J. L., S. H. Chu, et al. (2005). "Drosophila melanogaster topoisomerase IIIalpha preferentially relaxes a positively or negatively supercoiled bubble substrate and is essential during development." J Biol Chem **280**(5): 3564-73.
131. Plank, J. L. and T. S. Hsieh (2006). "A novel, topologically constrained DNA molecule containing a double Holliday junction: design, synthesis, and initial biochemical characterization." J Biol Chem **281**(25): 17510-6.
132. Plank, J. L., J. Wu, et al. (2006). "Topoisomerase IIIalpha and Bloom's helicase can resolve a mobile double Holliday junction substrate through convergent branch migration." Proc Natl Acad Sci U S A **103**(30): 11118-23.
133. Ralf, C., I. D. Hickson, et al. (2006). "The Bloom's syndrome helicase can promote the regression of a model replication fork." J Biol Chem **281**(32): 22839-46.

134. Raynard, S., W. Bussen, et al. (2006). "A double Holliday junction dissolvasome comprising BLM, topoisomerase IIIalpha, and BLAP75." J Biol Chem **281**(20): 13861-4.
135. Raynard, S., W. Zhao, et al. (2008). "Functional role of BLAP75 in BLM-topoisomerase IIIalpha-dependent holliday junction processing." J Biol Chem **283**(23): 15701-8.
136. Rockmill, B., J. C. Fung, et al. (2003). "The Sgs1 helicase regulates chromosome synapsis and meiotic crossing over." Curr Biol **13**(22): 1954-62.
137. Rose, M. D., F. Winston, et al. (1990). *Methods in Yeast Genetics*. Cold Spring Harbor, NY, Cold Spring Harbor Laboratory Press.
138. Saffi, J., V. R. Pereira, et al. (2000). "Importance of the Sgs1 helicase activity in DNA repair of Saccharomyces cerevisiae." Curr Genet **37**(2): 75-8.
139. Sharma, S., J. A. Sommers, et al. (2005). "Biochemical analysis of the DNA unwinding and strand annealing activities catalyzed by human RECQ1." J Biol Chem **280**(30): 28072-84.
140. Shiraishi, Y., T. H. Yosida, et al. (1985). "Inhibition of bromodeoxyuridine-associated sister chromatid exchanges in Bloom's syndrome cells with cycloheximide." Cancer Genet Cytogenet **17**(1): 43-54.
141. Shor, E., S. Gangloff, et al. (2002). "Mutations in homologous recombination genes rescue top3 slow growth in Saccharomyces cerevisiae." Genetics **162**(2): 647-62.
142. Siitonen, H. A., O. Kopra, et al. (2003). "Molecular defect of RAPADILINO syndrome expands the phenotype spectrum of RECQL diseases." Hum Mol Genet **12**(21): 2837-44.
143. Sinclair, D. A., K. Mills, et al. (1997). "Accelerated aging and nucleolar fragmentation in yeast sgs1 mutants." Science **277**(5330): 1313-6.
144. Singh, T. R., A. M. Ali, et al. (2008). "BLAP18/RMI2, a novel OB-fold-containing protein, is an essential component of the Bloom helicase-double Holliday junction dissolvasome." Genes Dev **22**(20): 2856-68.
145. Singleton, M. R., M. S. Dillingham, et al. (2007). "Structure and mechanism of helicases and nucleic acid translocases." Annu Rev Biochem **76**: 23-50.
146. Singleton, M. R. and D. B. Wigley (2002). "Modularity and specialization in superfamily 1 and 2 helicases." J Bacteriol **184**(7): 1819-26.
147. Skordalakes, E. and J. M. Berger (2003). "Structure of the Rho transcription terminator: mechanism of mRNA recognition and helicase loading." Cell **114**(1): 135-46.
148. Srivenugopal, K. S., D. Lockshon, et al. (1984). "Escherichia coli DNA topoisomerase III: purification and characterization of a new type I enzyme." Biochemistry **23**(9): 1899-906.

149. Sugawara, N., T. Goldfarb, et al. (2004). "Heteroduplex rejection during single-strand annealing requires Sgs1 helicase and mismatch repair proteins Msh2 and Msh6 but not Pms1." Proc Natl Acad Sci U S A **101**(25): 9315-20.
150. Sun, H., J. K. Karow, et al. (1998). "The Bloom's syndrome helicase unwinds G4 DNA." J Biol Chem **273**(42): 27587-92.
151. Sung, P. and H. Klein (2006). "Mechanism of homologous recombination: mediators and helicases take on regulatory functions." Nat Rev Mol Cell Biol **7**(10): 739-50.
152. Theobald, D. L., R. M. Mitton-Fry, et al. (2003). "Nucleic acid recognition by OB-fold proteins." Annu Rev Biophys Biomol Struct **32**: 115-33.
153. Thomas, B. J. and R. Rothstein (1989). "The genetic control of direct-repeat recombination in Saccharomyces: the effect of rad52 and rad1 on mitotic recombination at GAL10, a transcriptionally regulated gene." Genetics **123**(4): 725-38.
154. Tong, A. H., M. Evangelista, et al. (2001). "Systematic genetic analysis with ordered arrays of yeast deletion mutants." Science **294**(5550): 2364-8.
155. Tsai, H. J., W. H. Huang, et al. (2006). "Involvement of topoisomerase III in telomere-telomere recombination." J Biol Chem **281**(19): 13717-23.
156. Ui, A., Y. Satoh, et al. (2001). "The N-terminal region of Sgs1, which interacts with Top3, is required for complementation of MMS sensitivity and suppression of hyper-recombination in sgs1 disruptants." Mol Genet Genomics **265**(5): 837-50.
157. Ui, A., M. Seki, et al. (2005). "The ability of Sgs1 to interact with DNA topoisomerase III is essential for damage-induced recombination." DNA Repair (Amst) **4**(2): 191-201.
158. Van Maldergem, L., H. A. Siitonen, et al. (2006). "Revisiting the craniosynostosis-radial ray hypoplasia association: Baller-Gerold syndrome caused by mutations in the RECQL4 gene." J Med Genet **43**(2): 148-52.
159. Velankar, S. S., P. Soultanas, et al. (1999). "Crystal structures of complexes of PcrA DNA helicase with a DNA substrate indicate an inchworm mechanism." Cell **97**(1): 75-84.
160. von Kobbe, C., N. H. Thoma, et al. (2003). "Werner syndrome protein contains three structure-specific DNA binding domains." J Biol Chem **278**(52): 52997-3006.
161. Walker, J. E., M. Saraste, et al. (1982). "Distantly related sequences in the alpha- and beta-subunits of ATP synthase, myosin, kinases and other ATP-requiring enzymes and a common nucleotide binding fold." EMBO J **1**(8): 945-51.
162. Wallis, J. W., G. Chrebet, et al. (1989). "A hyper-recombination mutation in S. cerevisiae identifies a novel eukaryotic topoisomerase." Cell **58**(2): 409-19.

163. Wang, W., M. Seki, et al. (2003). "Functional relation among RecQ family helicases RecQL1, RecQL5, and BLM in cell growth and sister chromatid exchange formation." Mol Cell Biol **23**(10): 3527-35.
164. Watt, P. M., I. D. Hickson, et al. (1996). "SGS1, a homologue of the Bloom's and Werner's syndrome genes, is required for maintenance of genome stability in Saccharomyces cerevisiae." Genetics **144**(3): 935-45.
165. Watt, P. M., E. J. Louis, et al. (1995). "Sgs1: a eukaryotic homolog of E. coli RecQ that interacts with topoisomerase II in vivo and is required for faithful chromosome segregation." Cell **81**(2): 253-60.
166. Weinert, B. T. and D. C. Rio (2007). "DNA strand displacement, strand annealing and strand swapping by the *Drosophila* Bloom's syndrome helicase." Nucleic Acids Res **35**(4): 1367-76.
167. Weinstein, J. and R. Rothstein (2008). "The genetic consequences of ablating helicase activity and the Top3 interaction domain of Sgs1." DNA Repair (Amst) **7**(4): 558-71.
168. Whitby, M. C. and J. Dixon (1998). "Substrate specificity of the SpCCE1 holliday junction resolvase of Schizosaccharomyces pombe." J Biol Chem **273**(52): 35063-73.
169. Wilson, T. M., A. D. Chen, et al. (2000). "Cloning and characterization of Drosophila topoisomerase IIIbeta. Relaxation of hypernegatively supercoiled DNA." J Biol Chem **275**(3): 1533-40.
170. Wu, L., C. Z. Bachrati, et al. (2006). "BLAP75/RMI1 promotes the BLM-dependent dissolution of homologous recombination intermediates." Proc Natl Acad Sci U S A **103**(11): 4068-73.
171. Wu, L., C. Z. Bachrati, et al. (2006). "BLAP75/RMI1 promotes the BLM-dependent dissolution of homologous recombination intermediates." Proc Natl Acad Sci USA **103**(11): 4068-73.
172. Wu, L., K. L. Chan, et al. (2005). "The HRDC domain of BLM is required for the dissolution of double Holliday junctions." Embo J **24**(14): 2679-87.
173. Wu, L., S. L. Davies, et al. (2000). "Roles of RecQ family helicases in the maintenance of genome stability." Cold Spring Harb Symp Quant Biol **65**: 573-81.
174. Wu, L., S. L. Davies, et al. (2001). "Potential role for the BLM helicase in recombinational repair via a conserved interaction with RAD51." J Biol Chem **276**(22): 19375-81.
175. Wu, L., S. L. Davies, et al. (2001). "Potential role for the BLM Helicase in recombinational repair via a conserved interaction with RAD51." J Biol Chem **276**(22): 19375-81.
176. Wu, L. and I. D. Hickson (2003). "The Bloom's syndrome helicase suppresses crossing over during homologous recombination." Nature **426**(6968): 870-4.

177. Wu, Y. and R. M. Brosh, Jr. "Distinct roles of RECQ1 in the maintenance of genomic stability." DNA Repair (Amst) **9**(3): 315-24.
178. Wu, Y., J. S. Siino, et al. (2006). "The DNA binding preference of RAD52 and RAD59 proteins: implications for RAD52 and RAD59 protein function in homologous recombination." J Biol Chem **281**(52): 40001-9.
179. Wu, Y., T. Sugiyama, et al. (2006). "DNA annealing mediated by Rad52 and Rad59 proteins." J Biol Chem **281**(22): 15441-9.
180. Xu, D., R. Guo, et al. (2008). "RMI, a new OB-fold complex essential for Bloom syndrome protein to maintain genome stability." Genes Dev **22**(20): 2843-55.
181. Xu, X. and Y. Liu (2009). "Dual DNA unwinding activities of the Rothmund-Thomson syndrome protein, RECQ4." EMBO J **28**(5): 568-77.
182. Yamagata, K., J. Kato, et al. (1998). "Bloom's and Werner's syndrome genes suppress hyperrecombination in yeast sgs1 mutant: implication for genomic instability in human diseases." Proc Natl Acad Sci U S A **95**(15): 8733-8.
183. Yang, H., P. D. Jeffrey, et al. (2002). "BRCA2 function in DNA binding and recombination from a BRCA2-DSS1-ssDNA structure." Science **297**(5588): 1837-48.
184. Yin, J., A. Sobeck, et al. (2005). "BLAP75, an essential component of Bloom's syndrome protein complexes that maintain genome integrity." Embo J **24**(7): 1465-76.
185. Zhu, Z., W. H. Chung, et al. (2008). "Sgs1 helicase and two nucleases Dna2 and Exo1 resect DNA double-strand break ends." Cell **134**(6): 981-94.
186. Zittel, M. C. and J. L. Keck (2005). "Coupling DNA-binding and ATP hydrolysis in Escherichia coli RecQ: role of a highly conserved aromatic-rich sequence." Nucleic Acids Res **33**(22): 6982-91.

Curriculum Vita

Chi-Fu Chen

Education

1998-2000 M.S., Department of Agricultural Chemistry, National Taiwan University, Taiwan

1994-1998 B.S., Department of Agricultural Chemistry, National Taiwan University, Taiwan

Publications

1. Sims, R. J. 3rd., Chen, C. F., Santos-Rosa, H., Kouzarides, T., Patel, S. S., Reinberg, D. (2005) Human but not yeast CHD1 binds directly and selectively to histone H3 methylated at lysine 4 via its tandem chromodomains. *J Biol Chem*. 280, 41789-41792.
2. Hsieh, C. W., Liu, L. K., Yeh, S. H., Chen, C. F., Lin, H. I., Sung, H. Y., Wang, A.Y. (2006) Molecular cloning and functional identification of invertase isozymes from green bamboo Bambusa oldhamii. *J Agric Food Chem*. 54, 3101-3107.
3. Chen, C. F., Brill, S. J. (2007) Binding and activation of DNA topoisomerase III by the Rmi1 subunit. *J Biol Chem*. 282, 28971-28979.
4. Sims, R. J. 3rd., Millhouse, S., Chen, C. F., Lewis, B. A., Erdjument-Bromage, H., Tempst, P., Manley, J. L., Reinberg, D. (2007) Recognition of trimethylated histone H3 lysine 4 facilitates the recruitment of transcription postinitiation factors and pre-mRNA splicing. *Mol Cell*. 28, 665-676.
5. Chen, C. F., Brill, S. J. An essential DNA strand-exchange activity is conserved in the divergent N-termini of BLM orthologs. *EMBO J.* (In Press).
6. Mullen, J. R., Chen, C. F., Brill, S. J. Wss1 is a SUMO-dependent isopeptidase that interacts genetically with Sgs1 and the Slx5-Slx8 SUMO-dependent Ub ligase. *Mol Cell Biol.* (Revision).